

# **Cooperative Traffic Control Framework for Mixed Vehicular Flows**

Mohammad Karimi

A Thesis

In the Department

of

Building, Civil, and Environmental Engineering

Presented in Partial Fulfillment of the Requirements

For the Degree of

Doctor of Philosophy (Civil Engineering) at

Concordia University

Montreal, Quebec, Canada

November 2019

© Mohammad Karimi, 2019

**CONCORDIA UNIVERSITY**  
**SCHOOL OF GRADUATE STUDIES**

This is to certify that the thesis prepared

By:                    Mohammad Karimi

Entitled:            Cooperative Traffic Control Framework for Mixed Vehicular Flows

and submitted in partial fulfillment of the requirements for the degree of

Doctor Of Philosophy (Civil Engineering)

complies with the regulations of the University and meets the accepted standards with respect to originality and quality.

Signed by the final examining committee:

\_\_\_\_\_Chair  
Dr. Anjali Awasthi

\_\_\_\_\_External Examiner  
Dr. Luis F Miranda-Moreno

\_\_\_\_\_External to Program  
Dr. Ali Dolatabadi

\_\_\_\_\_Examiner  
Dr. Samuel Li

\_\_\_\_\_Examiner  
Dr. Attila Zsaki

\_\_\_\_\_Thesis Supervisor  
Dr. Ciprian Alecsandru

Approved by \_\_\_\_\_  
Dr. Michelle Nokken, Graduate Program Director

January 22, 2020

\_\_\_\_\_  
Dr. Amir Asif, Dean  
Gina Cody School of Engineering & Computer Science

# ABSTRACT

## Cooperative Traffic Control Framework for Mixed Vehicular Flows

**Mohammad Karimi, Ph.D.**

**Concordia University, 2019**

A prompt revolution is foreseen in the transportation sector, when the current conventional human-driven vehicles will be replaced by fully connected and automated vehicles. As a result, there will be a transition period where both types will coexist until the later type is fully adopted in the traffic networks. This new mix of traffic flow on the existing transportation network will require developing a new ecosystem able to accommodate both types of vehicles in traffic network environments of the future. A major challenging issue related to the emerging mixed transportation ecosystem is the lack of an adequate model and control framework. This is especially important for modeling traffic safety and operations at network bottlenecks such as highway merging areas. Therefore, the main goal of this thesis is to develop a microscopic modeling and hierarchical cooperative control framework specifically for mixed traffic at highway on-ramps. In this thesis, a two-level hierarchical traffic control framework is proposed for mixed traffic at highway merging areas. In this regard, for the lower level of the proposed framework, this thesis establishes a set of fundamental trajectory-based cooperative control algorithms for different merging scenarios under mixed traffic conditions. We identify six scenarios, consisting of triplets of vehicles, defined based on the different combinations of CAVs and conventional vehicles. For each triplet, different consecutive movement phases along with corresponding desired distance and velocity set-points are defined. Via the movement phases, the CAVs engaged in each triplet cooperate to calculate their optimal-smooth trajectories aiming at facilitating the merging maneuver while complying with the realistic constraints related to the safety and comfort of vehicle occupants. The vehicles in each triplet are modeled by a distinct system, and a Model Predictive Control scheme is employed to calculate the cooperative optimal control inputs (acceleration values) for CAVs, accounting for conventional vehicles' uncertainties.

In the next step of the thesis, for the higher level of the proposed framework, a merging sequence determination and triplets' formation methodology is developed based on predicting the

arrival time of vehicles into the merging area and according to the priority in choosing different triplet types. To model the merging maneuvers when two consecutive triplets share a vehicle, the interactions between triplets of vehicles are also investigated. In order to develop a microscopic traffic simulator, we analytically formulate different vehicles' driving behaviors under cooperative (i.e., the proposed traffic control framework) and non-cooperative (i.e., normal) operation modes and discuss the switching conditions between these driving modes.

To evaluate the effectiveness of the proposed framework, first, each triplet is simulated in MATLAB and evaluated for different sets of system initial values. Without a need for readjusting the algorithm for different initial values, the simulation results show that the proposed cooperative merging algorithms ensure smooth merging maneuvers while satisfying all the prescribed constraints, e.g., speed limits, safe distances, and comfortable acceleration and jerk values. Moreover, a simulator is developed in MATLAB for the entire framework (including both the higher and lower level of the framework) to evaluate the impact of all the triplets on continuous mixed traffic flow. Different penetration rates of CAVs under different traffic flow conditions are evaluated through the developed simulator. The simulation results show that the proposed cooperative methodology, comparing to the non-cooperative operation, can improve the average travel time of merging vehicles without disturbing the mainstream flow, provide safer merging maneuvers by avoiding the merging vehicles to stop at the end of the acceleration lane, and guarantee smooth motion trajectories for CAVs (i.e., derivable position and speed along with limited changes in acceleration values).

Generally, the results emphasize that the proposed cooperative traffic control framework can improve the mixed traffic conditions in terms of both traffic safety and operations. Moreover, the simulator provides a tool for the transportation community to evaluate their existing infrastructures under different penetration rates of CAVs and examine different traffic control plans for a mixed traffic environment. As the merging maneuver is only one application of gap-acceptance models, other types of maneuvers (e.g., lane changing, vehicle turning, etc.) can be similarly modelled. Thus, we can extend the proposed framework to the multi-lane highways, roundabouts, and urban area intersections. Furthermore, the arrival time prediction of the vehicles can be improved to elevate the performance of the proposed framework during the very congested traffic conditions.

## ACKNOWLEDGMENT

I would like to express my great appreciation to my supportive supervisor *Dr. Ciprian Alecsandru* for his valuable and constructive suggestions and training during the planning and development of this research work. I would also like to greatly thank *Dr. Roncoli Claudio* and *Dr. Markos Papageorgiou* for their advice in developing this thesis and willingness to give generously of their time.

I would also like to thank the members of my committee *Dr. Luis Miranda-Moreno*, *Dr. Ali Dolatabadi*, *Dr. S. Samuel Li*, and *Dr. Attila Michael Zsaki*.

I dedicate this dissertation to my amazing wife. This would not have been possible without her love, support, and patience. Also, I would like to convey my appreciation to my parents for their endless love and support throughout my life.

This research has been supported by NSERC, FRQNT (Fonds de Recherche du Québec – Nature et technologies), and Ministry of Transport, Bourse Alain Lamoureux, and I would like to extend my sincere gratitude for their generosity.

# CONTENTS

<b>List of Figures .....</b>	<b>vii</b>
<b>List of Tables .....</b>	<b>x</b>
<b>List of Acronyms and Notations .....</b>	<b>xi</b>
<b>Chapter 1: Introduction.....</b>	<b>1</b>
1.1 Thesis Motivation .....	2
1.2 Literature Review.....	2
1.3 Thesis Objectives .....	9
1.4 Thesis Scope and Tasks .....	9
1.5 Thesis Layout.....	10
<b>Chapter 2: Background .....</b>	<b>11</b>
2.1 Car-Following Model.....	11
2.2 Free-Flow Model .....	13
2.3 Merging Model .....	13
2.4 Merging Sequence .....	15
2.5 Model-Based Predictive Control Scheme .....	17
2.6 Concluding Remarks.....	18
<b>Chapter 3: Cooperative Optimal Merging Algorithms.....</b>	<b>19</b>
3.1 The Characteristics of Merging Triplets .....	21
3.2 Model Predictive Control Design .....	43
3.3 Simulations for Different Triplets of Vehicles.....	47
3.4 Concluding remarks .....	58
<b>Chapter 4: Merging Under Continuous Traffic Flow .....</b>	<b>60</b>
4.1 Merging Sequence and Triplets Formation Algorithm .....	60
4.2 Triplets' Interactions .....	62
4.3 Normally and Cooperatively Operated Traffic Conditions.....	66
4.4 Simulations for Continuous Mixed-Traffic Flow .....	72
4.5 Concluding Remarks.....	85
<b>Chapter 5: Conclusions And The Future Direction .....</b>	<b>87</b>
5.1 Summary .....	87
5.2 Research Contributions .....	88
5.3 Future Work.....	88
<b>Chapter 6: Appendices.....</b>	<b>90</b>
6.1 Appendix I .....	90
6.2 Appendix II .....	91
6.3 Appendix III.....	93
<b>Chapter 7: References.....</b>	<b>95</b>

## LIST OF FIGURES

Figure 2-1-MPC general form [95].....	17
Figure 3-1.The two-level hierarchical traffic control framework .....	20
Figure 3-2- A single lane merging area containing conventional (in white) and CAVs (in red).....	21
Figure 3-3. Sketch of triplet type I.....	24
Figure 3-4. Movement phases of triplet type I.....	25
Figure 3-5. Sketch of triplet type II.....	29
Figure 3-6. Movement phases of triplet type II.....	30
Figure 3-7. Sketch of triplet type III .....	32
Figure 3-8. Movement phases of triplet type III .....	32
Figure 3-9. Sketch of triplet type IV .....	34
Figure 3-10. Movement phases of triplet type IV .....	35
Figure 3-11. Sketch of triplet type V .....	38
Figure 3-12. Movement phases of triplet type V .....	39
Figure 3-13. Sketch of triplet type VI.....	41
Figure 3-14. Movement phases of triplet type VI.....	42
Figure 3-15. The result of merging scenario related to triplet type I .....	50
Figure 3-16. The result of merging scenario related to triplet type II.....	51
Figure 3-17. The result of merging scenario related to triplet type III.....	52
Figure 3-18. The result of merging scenario related to triplet type IV .....	53
Figure 3-19. The result of merging scenario related to triplet type V.....	54
Figure 3-20. The result of merging scenario related to triplet type VI .....	55
Figure 3-21. The result of merging scenario related to triplet type II, assuming smaller headways .....	57
Figure 3-22. The hypothetical location of V2 with respect to V1 and V3 .....	57
Figure 3-23. 25,000 samples of initial conditions of vehicles locations to test the merging algorithms ....	58
Figure 4-1. The higher level of control framework.....	61
Figure 4-2. The light traffic leads to independency between triplets.....	62
Figure 4-3. A shared conventional vehicle between two consecutive triplets .....	63
Figure 4-4. A shared CAV between two consecutive triplets.....	63
Figure 4-5. Sketch of two interacting triplets when the following one is type I.....	65
Figure 4-6. Sketch of two interacting triplets when the upstream triplet is type V .....	65
Figure 4-7. Sketch of two interacting triplets when the upstream one is type III .....	66

Figure 4-8. Sketch of two interacting triplets when the following one is type VII.....	66
Figure 4-9. Flowchart for driving behaviors of vehicles under normal operation condition .....	69
Figure 4-10. Flowchart for driving behaviors of CAVs able to cooperate for merging .....	71
Figure 4-11. Developed simulator in MATLAB.....	72
Figure 4-12. Effectiveness of the proposed framework in the light traffic flow of 1,000 veh/h with 50% CAVs and 50% ramp flow ratio.....	78
Figure 4-13. Effectiveness of the proposed framework in moderate traffic flow of 1,500 veh/h with 50% CAVs and 50% ramp flow ratio.....	79
Figure 4-14. Effectiveness of the proposed framework in the moderate traffic flow of 1,500 veh/h with 10% CAVs and 50% ramp flow ratio. ....	80
Figure 4-15. The effectiveness of the proposed framework to improve the traffic safety and operation assuming a total traffic demand of 1,500 veh/h. ....	81
Figure 4-16. Effectiveness of the proposed framework in the moderate traffic flow of 2,000 veh/h with 50% CAVs and 20% ramp flow ratio. ....	83
Figure 4-17. The effectiveness of the proposed framework to improve the traffic safety and operation assuming a total traffic demand of 2,000 veh/h. ....	85



## LIST OF TABLES

Table 3-1- One-way transition conditions in each phase of movement.....	23
Table 3-2- List of constraints.....	49
Table 4-1- The symbolic layouts of different triplets of vehicles;.....	64
Table 4-2- Results of 450 different scenarios for cooperative (shown by “Coop.”) and non-cooperative (shown by “Non-Coop.”) traffic conditions.....	75

## LIST OF ACRONYMS AND NOTATIONS

Acronym	Description
CAV	Connected and Automated Vehicle
MPC	Model Predictive Control
V2V communication	Vehicle to Vehicle Communication
V2I communication	Vehicle to Infrastructure Communication
QP	Quadratic Programing

Symbol	Description	Unit
$a_i$	Acceleration of vehicle $i$	$m/s^2$
$v_i$	Speed of vehicle $i$	$m/s$
$x_i$	Position of vehicle $i$	$m$
$\Delta v_{n,k}$	Relative speed between vehicles $n$ and $k$	$m/s$
$\Delta x_{n,k}$	Gap between vehicles $n$ and $k$	$m$
$\tau_i$	Reaction time of conventional vehicle $i$	$s$
$X$	System state-space vector	-
$U$	System control input vector	$m/s^2$
$Y_i^d$	The desired system output in phase $i$	-
$\hat{Y}_j$	Vector of predicted outputs	-
$\hat{U}_j$	Vector of predicted control inputs	-
$\hat{X}_j^{k_3}$	Memory vector	-
$J$	Cost function	-
$v_{main}^d$	Desired speed of mainstream vehicles	$m/s$
$v_i^d$	Desired speed of vehicle $i$	$m/s$
$g_{d,lead}$	Desired acceptable lead gap	$m$
$g_{d,lag}$	Desired acceptable lag gap	$m$
$g_{n,k}$	Desired steady-state distance headway between vehicles $n$ and $k$	$m$
$\Phi_i$	Movement phase number $i$	-

## Chapter 1: INTRODUCTION

A new paradigm of roadway vehicles, the connected and automated vehicles (CAVs), is emerging rapidly. The main goal of these technologies is to enhance the safety and comfort while reducing fuel consumption, emissions, and traffic congestions [1]. It has been suggested that the automated vehicles will transport people within cities in 10 to 15 years ahead, and between the cities in 20 to 30 years ahead [2]. Moreover, recently, most major car companies (e.g., GM, Ford, Tesla, Honda, and BMW) has been massively spending on research and technology for automated vehicles. Thus, a revolution is foreseen in the transportation sector, which is to shift from the conventional vehicles to the fully automated vehicles [3]–[5]. However, more testing and experience with deploying automated vehicles is needed to increase the levels of trust and acceptance [6]. Additionally, the economic factors (e.g., reaching affordable prices to allow mass-marketing) and policy factors (e.g., establishing new policies to address, for example, liability issues that AVs could raise) require more investigation [7]. As a result, there will be a long and critical transition period where both types will coexist until the later type is fully adopted for a given road network.

Whether the automated vehicles will have negative or positive impacts on our daily lives highly depends on how prepared we are for this mixed traffic network. Most of the current transportation facilities and infrastructures, traffic control systems, and safety-related treatments are designed and built assuming the conventional vehicles as the only users. Accordingly, the impact of CAVs on the efficiency of the mixed traffic environment is uncertain [1], [8], and overlooking the unanticipated problems caused by automated vehicles may lead the transportation networks to lose the level of services and safety in the near future. Therefore, without an effective modeling and control framework, it is not possible to accurately evaluate and predict the effectiveness of CAVs in the mixed traffic networks [9]. Although fully automated transportation system models are common research topics, traffic modeling and control frameworks have not been yet thoroughly investigated for a mixed traffic environment (with different penetration rates of CAVs), particularly in the merging areas of the freeways. In the following subsections, we discuss the motivation for our research, as well as review the literature to shed some lights on the unaddressed gaps. Then, the objectives of the thesis is discussed to outline the scope and tasks of the proposed methodologies.

## **1.1 Thesis Motivation**

Emerging the automated and connected vehicles can cause abundant unexpected transportation-related and environmental issues, especially in the freeways bottleneck (e.g., merging areas). Merging areas are among the most critical freeway structures with respect to traffic performance and safety as well as the stability of traffic flow operations [10]–[12]. In this regard, an interesting issue is the merging maneuver of a vehicle into the mainstream lane [13]. Developing an efficient and realistic merging algorithm in the mixed traffic environment can reduce the activation of the bottlenecks corresponding the merging areas. Proposing a comprehensive modelling and control framework for the mixed traffic networks in the merging areas enables us to evaluate the mixed traffic networks and reach an optimal control strategy considering different penetration rates of CAV under different traffic flow conditions. By doing so, we can anticipate the possible negative impacts of CAV on the current network while achieving the greatest output of the works in terms of the level of performance, safety, and comfort.

## **1.2 Literature Review**

Based on National Highway Traffic Safety Administration (NHTSA) definition, the autonomy levels of the vehicles are categorized in five levels [6], [14]. In level zero, the driver has the full control of the vehicle (e.g., brake, steering, and throttle). In level one, there are one or two automated functions (e.g., electronic stability control and pre-charged braking system). Level two involves automation of at least two primary control functions to help the driver in controlling the vehicle (e.g., adaptive cruise control and lane centering systems). Level three is a limited self-driving automation condition, where the vehicle can have the full control of the vehicle under certain traffic and environmental conditions (e.g., Google self-driving car [15]). In level four, as a full self-driving automation level, the vehicle can undertake full control of the safety-critical driving functions while monitoring the roadway conditions for the entire trip. In this regard, main expectations of these technologies include enhancing safety and comfort while reducing fuel consumption, emissions, and traffic congestions [1]. For instance, the integration into a highway system of automated vehicles along with the proper control, communication, and computing technologies can significantly elevate the road safety and capacity without the need to building new lanes [16]. Moreover, an in-car advisory system controlled by a traffic management center can provide optimal lane distribution, reduce the capacity drop and spillbacks in highways [17]. Furthermore, the traffic flow optimization can be achieved in multi-lane motorways with a

sufficient penetration rate of vehicles equipped with Vehicle Automation and Communication Systems [18].

Various models, simulation platform, and control strategies are developed for the traffic networks containing only CAV (e.g., [1], [19]–[21]). The mixed traffic of conventional vehicles and “semiautomated” CAVs was also partially studied and addressed. For example, Bose and Ioannou [22] investigated the effects of “semiautomated” vehicles (ACC/CACC) on traffic flow characteristic and the environment in a mixed traffic network. It was illustrated that these vehicles filter out the response of rapidly accelerating conventional lead vehicles, which leads to a smooth traffic flow. It was also proved that the fuel consumption and consequently the level of pollutants of the following vehicles decrease due to the fact that “semiautomated” vehicles are able to track accurately the desired speed and to respond smoothly – to accommodate the passengers’ comfort. Yuan et al. [23] investigated the traffic flow characteristics of the mixed traffic by using a hybrid model that comprises cellular automaton (for conventional vehicles) and car-following (for ACC vehicles) modeling approaches. Ngoduy [24] proposed a macroscopic model framework for mixed traffic of regular human-driven vehicles and adaptive cruise control (ACC) vehicles using an improved multiclass gas-kinetic theory. In order to develop the autonomous vehicles longitudinal acceleration model, Talebpour and Mahmassani [9] utilized the sensors characteristics to obtain the safe distance in the linear car-following model of CACC presented in [25].

Among all types of freeway structures, merging areas are the most critical ones with respect to both traffic safety and stability of traffic flow operations [10]–[12]. One of the early stage studies to achieve smooth merging is presented in [26]. The authors generated a virtual vehicle by mapping an existing vehicle from a given lane onto the adjacent lane to control the longitudinal distance between the vehicle on different lanes (i.e., ramp and main lane). They also developed a data transmission algorithm for intra-platoon and inter-platoon communications. A distributed control algorithm for both merging and yielding vehicles was developed by Antoniotti et al. [27] in the context of automated highway systems (AHS). The authors evaluate the impact of the algorithm on safety and congestion considering different demand scenarios. The study concluded that the suggested algorithm is feasible only for low level of demand values. The interface problem between AHS and the conventional roadways was also investigated in [28]. The authors proposed a microscopic model for the case of automated merging maneuvers. It was shown that the

minimum ramp lengths are related to the speed of the merging and mainstream vehicles as well as the acceleration rate of the merging vehicles. An extended version of the virtual vehicle concept in AHS was implemented in [29] through a virtual platooning paradigm, in order to assure safe and effective merging maneuver executions. The authors suggested that the virtual platoon should be formed before reaching the merging point. Also, they determined that the merging vehicles should move with a certain safe distance and from/at the same speed and acceleration values as the platooned vehicles in the mainstream. Yet another study [30] used virtual platooning concept to develop a longitudinal control of automated vehicles for merging maneuvers in AHS. The proposed algorithm was adaptive and suitable for the real-time application purpose.

Generally, control strategies to facilitate the merging maneuvers can be applied separately either on mainstream vehicles [31], [32], on-ramp vehicles [33], [34], or on all the vehicles on the mainstream and on-ramp [35], [36]. In this regard, vehicles on the mainstream can manage to create larger gaps between vehicles for merging vehicles. Moreover, the vehicles on the merging lane should use efficient acceleration trajectories for merging maneuvers into the adjacent lane. In [31], an enhanced Intelligent Driving Model was proposed to facilitate the merging maneuver by creating larger gaps between vehicles on the main approach of the merging area. Using vehicle-to-vehicle and vehicle-to-infrastructure communications, a lane changing advisory algorithm was developed with a variable gap size concept. It was shown that the proposed methodology leads to a higher average speed in the freeway lanes within a merge area and reduce the emissions. The drawback of the proposed model is that the algorithm works efficiently at a very high driver compliance rate (90% or higher). In another study, Sivaraman et al. [33] integrate measurements from multiple sensors of the automated vehicles a model named Dynamic Probabilistic Drivability Map (DPDM). The merging maneuver was formulated as a dynamic programming problem over the DPDM to minimize the merging costs. A driver assistance system was developed to recommend the drivers how, when, and which acceleration values to use for merging maneuvers into the adjacent lane. In [35], a cooperative automated control algorithm was developed based on the Internet of vehicles to avoid the collision on the freeways merging areas. The authors compared the scenario where a platoon of vehicles merges between two vehicles in the main lane with the scenario where individual vehicles consecutively merge between the vehicles in the main lane. It was shown that the former scenario disrupts the main lane traffic flow more severely than the latter one. Wei et al. [37] proposed a prediction-based and cost function-based algorithm (PCB) to

provide robust driving in autonomous vehicles. Three modules of driving were designed (distance keeper, lane selector, and merge planner). Each autonomous vehicle used a human-understandable and representative cost function library to evaluate the predicted scenario that it will face. Then, the decision with the lower cost are selected to be executed. This study did not cover the cooperative merging behavior among autonomous vehicles.

In the automated highway merging control systems, the main goal of some studies was to avoid stop-and-go driving behavior while accommodating the safe and efficient merging maneuvers. For example, the study in [38] was an early stage work in this category that assumed a given merging sequence. Therefore, the speed errors between each consecutive pairs of vehicles were minimized to minimize the impact on the desired headway of a single string of vehicles. More recently, the authors in [36] attempted to determine the optimal merging sequence of the vehicles to reduce the merging time for the vehicles closer to the merging area. In [39], an optimal coordinating method for CAV was proposed at the merging areas to capture a smooth traffic flow and avoid stop-and-go driving behavior.

Wang et al. [40] attempted to optimize the highway throughput near the ramps by proposing proactive algorithms for merging different streams of vehicles into a single stream. All the vehicles were assumed to be equipped with some sensors capable of detecting distance from neighboring vehicles. The sensor-enabled vehicles utilized the position, speed, and acceleration information of the other vehicles to make a merging decision before actually reaching the merging point. It was shown that this algorithm outperforms the conventional priority-based merging algorithm (where vehicles do not adjust their speed before reaching the merging area). Awal [36] extended the proactive algorithm concept by optimizing the merging time at on-ramps at the cost of increasing by small amounts the average travel time for vehicles on the main approach. In both studies, only a one-lane main road was assumed which limits the advantage of the cooperative behavior between vehicles.

Scarinci et al. [41] presented a cooperative merging assistant (CMA) strategy to reduce congestion at the motorway junctions. CMA collects the distributed spaces between main carriageway vehicles to estimate the adequate gaps for merging vehicles, and accordingly, it facilitates the merging maneuvers. CMA was implemented using a microscopic simulation framework and it was shown that CMA can lead to the reduction of late-merging vehicles and

improvement in congestion. Another study by Scarinci et al. [42] proposed a method in which using intelligent vehicles equipped with communication technologies, proper gaps between platoons of vehicles in the mainstream lane were provided for the platoons released by ramp meter. It was assumed that all the vehicles can communicate and stay in platoons of vehicles. The authors in [43] proposed a method for producing the longitudinal trajectories for the ego vehicle (merging vehicle) and putative leader on the mainstream. It was assumed that time-headways and vehicle speeds at the end of the maneuver (merging point) are pre-specified. The problem was formulated as a finite-horizon optimal control problem and was solved analytically to minimize the acceleration (which affects fuel consumption) and its first and second derivatives (which affect passengers comfort) during the merging maneuver. In some studies, the control problem of the centralized or decentralized modeling framework was solved using a Model Predictive Control (MPC) scheme. Generally, by predicting the future values of state variables in a specific prediction horizon, MPC chooses the optimal control action for the current time to minimize a cost function [44]. For example, to solve a decentralized problem in [45], MPC were employed to cope with the real-time and uncertain nature of the information exchanging between vehicles. Kim and Kumar [46] also employed MPC to solve a local optimization problem.

In [47], a longitudinal freeway merging control algorithm for connected and automated vehicles was proposed to maximize the total average travel speed. Applying the optimized trajectories to the automated vehicles showed a significant improvement in comparison to the case when only conventional vehicles exist. However, the study does not offer any solution for mixed traffic network. In [48] and the extended version in [39], an optimal coordination of CAVs at merging roadways was presented. Using Hamiltonian analysis, a closed-form solution was developed to minimize the travel time and fuel consumption in presence of longitudinal collision constraints. In [49], a microsimulation framework was developed to compare the efficiency of a network with a 100% CAV with a network with 100% conventional vehicle in the merging roadways. The Gipps car-following model [50] and an optimal control scheme were utilized to model the behavior of the conventional vehicles and CAV, respectively. The practical constraints on lateral and longitudinal distances, speed, and acceleration of the CAV were considered and a Hamiltonian analysis was applied to obtain the optimal solution (i.e., the optimal control input, speed, and position). Based on the results under average and high congestion scenario, the network with 100% CAV was shown to significantly reduce the fuel consumption and travel time.



Although the impact of CAVs on on-ramp bottlenecks is investigated in the studies mentioned above, they all consider scenarios where all vehicles are CAVs, often comparing results with fully manual driven vehicles scenarios, leaving uncertain how such systems may work in the case of mixed traffic of conventional vehicles and CAVs. Therefore, they do not account for the impact of human-driven vehicles on CAVs effectiveness.

The following studies address the merging maneuvers in the mixed traffic of ACC/Cooperative ACC (CACC)-equipped vehicles and conventional vehicles. Davis [51] investigated the impact of the automated vehicles equipped with ACC on mixed traffic flow near the on-ramp. In proposed a cooperative merging of ACC vehicles to enhance the throughput and the travel time of the network. The proposed ACC system was able to communicate with more than one vehicle ahead or behind. In this methodology, the ACC vehicles could adjust their speed to provide a safe gap for the merging vehicles. It was shown that the large demand limited the throughput by the downstream capacity (which could be calculated by headway time and speed limit).

Pueboobpaphan et al. [52] proposed a decentralized merging assistant to enhance the traffic stability by minimizing the conflict and limiting the changes in speed in the mixed traffic network of manual and Cooperative Adaptive Cruise Control (CACC) vehicles. The authors assumed that the mainstream contains mixed vehicular traffic, while the merging lane contains only conventional vehicles. Using preemptive and smooth deceleration, the vehicles upstream of the merging area in the mainstream created proper gaps for on-ramp vehicles. It is worth mentioning that CACC is an extension of ACC to enable the vehicles to follow its leader at closer distances via a vehicle-to-vehicle communication infrastructure. The impact of CACC on traffic flow characteristics was also investigated in [25].

Zhou et al. [53] modified the intelligent driver model (IDM [54]) to add the cooperation characteristic to the sensor-enabled ACC vehicles. The controller of the new model (Cooperative IDM—CIDM) calculated the acceleration rate of vehicle based on the actions of the surrounding vehicles to improve the road capacity and string stability. It was found that CIDM was able to eliminate or alleviate the freeway oscillation (stop-and-go) caused by the vehicles merging from the ramps. Kerner [8] investigated the impact of different penetration rates of the ACC-equipped vehicles on traffic breakdown. Kerner-Klenov microscopic stochastic three-phase traffic flow model and classical ACC model were utilized to simulate the conventional and the automated

vehicles, respectively. By simulating a single lane road with an on-ramp bottleneck, it was concluded that depending on different model parameters and penetration rates of the automated vehicles in the mixed traffic network, the probability of traffic breakdown at network bottlenecks (ramps) is uncertain.

The optimally coordinated CAV in a single lane roundabout (rather than an on-ramp) was investigated in [55] to achieve a smooth traffic flow. The optimal solution for each CAV was calculated without violating the constraints (i.e., speed and acceleration limits). By investigating the network containing different penetration rate of CAV, it was concluded that model cannot accommodate relatively small reductions in the CAV rates. For example, the mixed traffic networks with 80% CAV were shown to be significantly less effective in comparison to the network with 100% CAV, for both travel time and fuel saving criteria. The reason that this study [55] was not able to improve the performance of the mixed traffic network was that the uncertainty in the dynamics of the conventional vehicles was not considered in calculating the control inputs.

In conclusion, the review of the available literature shows that the automated vehicles concept can be categorized into three types: (a) fully automated vehicles, (b) vehicles equipped with CACC/ACC, and (c) vehicles with an onboard advisory display [56]. The fully automated vehicles need an advance centralized control framework to work in a fully automated network, while the vehicles with CACC/ACC can keep a safe distance from other vehicles given prescribed constraints. Moreover, the vehicles with an onboard advisory display can only receive advice (like the advanced-driving assistant system—ADAS). In most of the reviewed studies, e.g., [8], [51]–[53], only partially automated vehicles (ACC/CACC) were considered in the mixed traffic at the merging areas, rather than fully automated vehicles capable of cooperation, and creating optimal motion trajectories according to human-driven vehicles' uncertainties. Whereas models integrating fully automated vehicles have been studied only as purely automated networks, for which there are no human-driven vehicles. The main conclusion of the investigation of the literature is that in a mixed traffic environment, merging maneuvers require more sophisticated algorithms in order to calculate the optimal trajectories for CAVs while capturing the uncertainties of surrounding human-driven vehicles.

### **1.3 Thesis Objectives**

Based on the review of the literature, merging algorithms development for mixed traffic of conventional and CAVs has not been thoroughly investigated. Since the merging areas can highly degrade the performance of current highways and are associated with more frequent safety issues, a reliable modeling and cooperative merging control framework can be of great importance. Therefore, developing an efficient merging behavior in the mixed traffic environment can reduce the activation of the bottlenecks corresponding the merging areas. Moreover, most of the maneuvers such as lane changing, passing, and right/left turning are the special cases of merging maneuver. In other words, the merging maneuver is expandable to other driving scenarios [52]. Accordingly, defining a comprehensive merging algorithm will lead to developing more steps towards modelling additional vehicle interactions.

The main objective of this thesis is to develop a modeling and cooperative traffic control framework for the mixed traffic network of conventional vehicles and CAVs for uninterrupted traffic flow facilities (i.e. freeways, highways, etc.) while capturing the interactions between the human-driven vehicles and CAVs in the system models. The control goal is to facilitate merging maneuvers by providing smooth motion trajectories for CAVs while complying with the existing constraints. By doing so, the proposed algorithms facilitate the merging maneuvers and avoid stopping of the merging vehicle at the end of the acceleration lane, which would entail idling and waiting for another sufficient gap to merge and would thereby cause increase of delays, fuel consumption and air pollution. Facilitating the merging maneuver also prevents the merging vehicle from unsafely merging in front of a vehicle that moves at a higher speed causing its deceleration.

### **1.4 Thesis Scope and Tasks**

In this thesis, a two-level hierarchical control framework is developed to facilitate the merging maneuvers in mixed traffic environment. The higher level of the traffic control framework has access to the information of all vehicles within the control zone and is responsible for determining the merging sequence, namely, determines that each merging vehicle will engage with which pair of the vehicles on the mainstream lane to accomplish a merging maneuver. In this regard, a merging sequence determination method is developed for the higher level of traffic control framework. For the lower level of the traffic control framework, different cooperative merging

algorithms are developed for different combinations of CAVs and conventional vehicles (i.e., triplets of vehicles). For each triplet of vehicles engaged in the merging maneuver, a system model is developed such that the impact of conventional vehicles on CAV is captured, and a cooperative merging algorithms are defined in consecutive optimal multi-phase movements using corresponding desired control targets (i.e., desired distances and velocities). In each movement phase, to achieve the control goals, a model predictive control (MPC) scheme is employed to cope with uncertainties and delays in the system, while obtaining the optimal acceleration trajectories for CAVs.

To show the effectiveness of the proposed hierarchical traffic control framework, different simulations are conducted in MATLAB for both levels of the framework under different traffic conditions.

## **1.5 Thesis Layout**

The report is structured as follows: in chapter 2, the models of driving behavior for conventional vehicles, i.e., car-following, free-flow, and gap acceptance merging, as well as MPC scheme are investigated; moreover, the literature of determining merging sequence is reviewed. Adequate driving behavior models to be integrated into the proposed mixed traffic model as well as appropriate indicators for merging sequence determination are highlighted. In chapter 3, the proposed traffic control framework is presented and cooperative merging algorithms along with simulation results are developed for different triplets of vehicles. In chapter 4, the proposed method for triplets' formation by the higher level of traffic control framework is presented. The interactions between triplets, as well as the driving modes are discussed under cooperative and non-cooperative driving conditions. Furthermore, a simulator is developed in MATLAB to evaluate the proposed framework under different conditions. In chapter 5, the concluding remarks are presented while the future direction of the research is specified.

## Chapter 2: **BACKGROUND**

The goal of this thesis is to establish a traffic control framework for mixed traffic of conventional and CAVs in the merging areas. Therefore, it is required to review the existing models related to the conventional vehicles driving behaviors. Conventional vehicles refer to the regular vehicles with no communication and automated driving control capability. Moreover, we investigate the existing merging sequence determination methodologies to establish a method appropriate for the higher level of the traffic control in the mixed traffic. Furthermore, before employing MPC scheme for cooperating driving control in the next chapter, we introduce this controller and shed some lights on its characteristics.

### **2.1 Car-Following Model**

Since the proposed traffic control framework will be utilized in real-time, the computational time of the controllers will be of great importance. In this regard, among the conventional vehicles' models, we are interested in those that impose less computation efforts on the controllers—i.e. linear models, as the gradient values are available for the optimizer. Moreover, the models should be able to properly address the uncertainties related to the human-driven vehicles. Therefore, the linear models capable to address the model uncertainties are of great interest. In this subsection, the conventional models—particularly, the relevant linear models—are reviewed to determine the best fit options in our framework.

A conventional vehicle moving within a roadway network is oftentimes modeled using the car-following paradigm. That is, the driving behavior of a subject vehicle is controlled through a car-following model if it is close enough to an upstream vehicle (i.e. the leader vehicle) [57]. Significant literature exists on various car-following models. Some of these models are based on a stimulus-response framework. For example, the GM model [58], [59] assumes that the rate of change of speed of the subject vehicle depends on its relative speed with respect to the leader. The main deficiency of these early models was their lack of sensitivity to the relative distance between the vehicles. Several extensions of GM model were developed such as acceleration and deceleration asymmetry [60], memory function [61], and multiple car-following [62]. However, Koutsopoulos [63] found out that the idea of “drivers accelerate when their speed difference is positive or decelerate when the speed difference is negative” is not valid. In [64], an acceleration model, capable of avoiding the crashes, was proposed based on identifying the behavioral

mechanism using the prospect theory in [65]. Moreover, a model was presented in [66] based on the relationship of acceleration with the combination of the space and relative speed between the leader and follower. The spacing model was proposed in [67], where the speed of the follower depends on the space headway from the leader. This model was somewhat similar to the derivative form of GM model.

The non-linear intelligent driver model (IDM) [54] and optimal speed models [68], [69] proposed deterministic acceleration-based models. However, the proposed models are sensitive to the reaction time and might produce unrealistically high acceleration values in certain situations. Therefore, IDM is mainly suitable for the connected vehicles, where the driver is aware of the vehicles in its close proximity, and accordingly, the reaction time is very low [9].

All in all, among the aforementioned car-following models, this thesis focuses on linear models that are able to capture the desired headway distance, and mainly because these models require less computational effort. In this regard, Helly's model [70] as a direct measures model (or linear model) considers the desired space headway that the follower would like to follow. In this model, the follower acceleration is modeled as follows:

$$a_n(t) = \alpha_1 \Delta V_n(t - \tau_n) + \alpha_2 [\Delta X_n(t - \tau_n) - D_n(t - \tau_n)] \quad 2-1$$

where  $D_n$  represents the desired headway,  $\Delta V_n$  and  $\Delta X_n$  are the relative speed and space-headway between the leader and follower, respectively, while  $\tau_n$  represents the reaction time of the driver. The desired headway is modeled as follows:

$$D_n(t - \tau_n) = \beta_1 + \beta_2 V_n(t - \tau_n) + \beta_3 a_n(t - \tau_n) \quad 2-2$$

In some studies [70], [71], the desired headway is simplified as:

$$D_n(t - \tau_n) = L_{n-1} + T V_n(t - \tau_n) \quad 2-3$$

where  $L_{n-1}$  is the length of the leader and  $T$  represents the desired time-headway. This model mostly is attributed to a linear model. The main difficulty with these models is that they need two times calibration and most of the parameters are unobservable in the real world, which makes their estimation more challenging. Many attempts have been done for calibrating the model. In [72], Helly tried to estimate other parameters, where the result of calibration is as follows:

$$a = 0.5\Delta v(t - 0.5) + 0.125(\Delta x(t - 0.5) - D_n(t)),$$

$$D_n(t) = 20 + v(t - 0.5)$$
2-4

## 2.2 Free-Flow Model

A subject vehicle that is far (i.e., it exceeds the space headway threshold) from the leading vehicle will not follow it, as is not modeled using the car-following model, instead it can be model by a free-flow driving model. In this regard, general acceleration models (e.g., [73]–[75]) are able to capture the free-flow driving conditions. The first general acceleration model was developed by Gipps [76], where the maximum acceleration values are determined such that the desired speed is not exceeded and safe headway is maintained. In some of general acceleration models (e.g., [74]), the acceleration value is modeled based on different conditions that the vehicle may face (e.g. car-following, free-flow, lane drops, and engaging in courtesy yielding). As is suggested by Ahmed in [57], the free-flow behavior can be also shown separately by a linear model as follows:

$$a_n(t) = \lambda[DV_n(t - \tau_n) - V_n(t - \tau_n)] + \varepsilon_n(t)$$
2-5

where  $\lambda$  is a constant sensitivity term,  $\varepsilon_n(t)$  as a normally distributed error represents the uncertainty of the model. The desired speed is shown by  $DV_n$ , which is a function of explanatory variables affected by the vehicle type, density and flow rate, the speed limit, roadway, geometry, and weather condition.

## 2.3 Merging Model

Suppose that a conventional vehicle is approaching the merging area on the merging section with the permitted speed. It looks for a proper gap to merge while it is driving in the acceleration lane next to the mainstream lane. In the case of light traffic conditions, the driver can find enough gap before the end of the acceleration lane. While in the congested traffic conditions, it may fail to find a desired gap, and accordingly, it has to stop at the end of acceleration lane and wait for the proper desired gap to merge.

Merging into the mainstream is a special case of lane changing (MLC) [77]. Therefore, most of the lane changing models can be applied to capture the merging maneuver (e.g., utility theory based models [78], [79], cellular automata based models [80], [81], and Markov process based models [82], [83]). A lane changing maneuver includes four steps: decision to consider a LC, choice of the target lane, and search for an acceptable gap, and executing the lane change. While,

in the case of merging maneuver, the vehicle has to merge and only looks for a sufficient gap to execute the maneuver. Usually the difference between different lane changing models are incorporate in the decision process (first and second steps). For example, [75] modeled the lane changing process using a probability function, while [84] utilized a deterministic model. Therefore, we will focus only on the gap acceptance procedure to model the merging maneuver. In this model, if there is an enough gap between the putative leader (i.e., the leader in the target lane) and putative follower (i.e., the follower in the target lane), the merging vehicle will decide to merge. The gap acceptance model is formulated as a binary choice procedure as follows:

$$\gamma_n(t) = \begin{cases} 1 & \text{if } G_n(t) \geq G_n^{cr}(t) \\ 0 & \text{if } G_n(t) < G_n^{cr}(t) \end{cases} \quad 2-6$$

where  $\gamma_n(t)$  is the choice indicator,  $G_n^{cr}(t)$  represents the critical gap, and  $G_n(t)$  is the available gap. Critical gap is the minimum acceptable gap for executing the merging maneuver. Various studies attempted to model the critical gap as a random variable such as an exponential distribution [85], a normal distribution [86], or a log-normal distribution [87]. Ahmed in [57] proposed a model in which the lead and lag gaps were estimated separately. The lead gap is the space between the front of the merging vehicle and the rear of the leader in the target lane. The lag gap is the space between the rear of the merging vehicle and the front of the follower in the target lane. In this model the critical gap for driver  $n$  at time  $t$  is captured by the following equation:

$$G_n^{cr,g}(t) = \exp(X_n^g(t)\beta^g + \alpha^g v_n + \varepsilon_n^g(t)) \quad 2-7$$

where,  $g \in \{lead, lag\}$ ,  $X_n^g(t)$  is the vector of explanatory variables,  $v_n$  is a normally distributed individual specific random term that captures the correlations among lead and lag critical gaps for a driver, and  $\varepsilon_n^g$  is a normally distributed generic random term. A conservative driver tends to have higher value of  $v_n$  than that of an aggressive driver. Ahmed calibrated the model as follows:

$$G_n^{cr,lead}(t) = \exp(0.508 - 0.420 \min(0, \Delta v_n^{lead}) + \varepsilon_n^{lead}(t)) \quad 2-8$$

$$G_n^{cr,lag}(t) = \exp(2.02 + 0.153 \min(0, \Delta v_n^{lag}) + 0.188 \max(0, \Delta v_n^{lag}) + \varepsilon_n^{lag}(t)) \quad 2-9$$

where

$$\begin{aligned} \Delta v_n^{lead} &= \text{lead vehicle speed} - \text{subject speed}, \\ \Delta v_n^{lag} &= \text{lag vehicle speed} - \text{subject speed}, \\ \text{and } \varepsilon_n^{lead}(t) &\sim \mathcal{N}(0, 0.488^2) \text{—a normally distributed noise.} \end{aligned}$$



After the merging vehicle accomplishes the merging maneuver, it will face two conditions of either car-following or free-flowing modes. This process can be simulated by a simple deterministic speed model such as [88]:

$$\hat{v} = \min(v^+, v + \Delta v_r) \quad 2-10$$

where  $\hat{v}$  is the merging's speed,  $v^+$  represents the speed of the putative leader, and  $\Delta v_r$  describes the maximum possible increase in speed. This model is a simple version of the car-following models. Therefore, we prefer to utilize the more advanced linear models discussed in the previous section.

However, if the merging vehicle cannot find a proper gap to merge, it has to stop before the end of the acceleration lane. Thereafter, it has to wait to find a sufficient gap and abruptly accelerate to merge. In this study, we attempt to provide the merging conditions prior to reaching the merging area to ensure that the merging vehicle will find enough gap to merge.

#### 2.4 Merging Sequence

Generally, in traffic networks comprising only conventional vehicles, the sequence of merging is determined by giving the priority to the mainstream vehicles. While, in the congested traffic condition, the merging vehicles may avoid obeying the priority rule and merge regardless of existing an available gap. Sarvi and Kuwahara [89] modeled this type of behavior using zip merging concept to show that vehicles merge one by one under congested traffic. A fixed merging ratio also was proposed by Cassidy Ahn [90] to model the congested traffic condition.

Many efforts are done to show that CAVs can improve the traffic conditions using different sequencing strategies. Wang et al. [40] presented a series of proactive merging algorithms for the communication- and sensor-enabled vehicles to separate the decision point and actual merging point. The general merging algorithm could switch between different proactive merging strategies (i.e., distance-based, speed-based, and platoon-speed-based) that was the best fit for the existing traffic condition. Moreover, the authors utilized a sliding decision point concept to modify the decision point under different road conditions. In an extended study, based on the concept of time geography, Wang et al. [91] presented a robust proactive merging algorithm to overcome the uncertainties related to the sensors.

In [36], a proactive optimal merging strategy was proposed to determine the merging order of two streams of communication- and sensor-enabled vehicles. By separating the decision-making point from the actual merging point, the methodology searches different feasible and prospective orders of the vehicles for merging beforehand. Based on the estimated times to arrive at the merging point, the methodology chooses the optimal sequence of merging. It was found that this strategy beats the conventional mainstream priority merging as well as platoon-speed-based algorithm presented in [40] in terms of merging time and rate, waiting time, energy consumption, flow, and average speed.

Li et al. [92] treated the closure of one lane of a highway section similar to the merging scenario. In this regard, the scheduling tree was developed to take all the combinations of merging sequences and lane-changing options into account. Depending on the objective (e.g., the average travel time of merging), the algorithm chose one of the combinations.

Ntousakis et al. [93] considered a fully connected network and defined a cooperation area in which the vehicles can communicate for merging maneuver. Two different algorithms were proposed to determine the merging sequence. In the first algorithm, vehicles merged according to the order of entering the cooperation area. In the second algorithm, by assuming a fixed merging point, the sequence of vehicles depended on the needed time to arrive at the merging point. It was shown that both algorithms have very similar performance in providing smooth merging trajectories.

In all of the aforementioned studies, all the vehicles on the mainstream and the merging lane were CAV rather than a mixed traffic of conventional vehicles and CAVs. However, Pueboobpaphan et al. [52] presented a merging assistant problem for the mixed traffic network, where the merging vehicles were conventional and the vehicles on the mainstream were mixed of conventional and CACC-equipped vehicles. By roughly predicting the arrival time of merging vehicles on the mainstream, the sequence of merging was determined. Accordingly, the corresponding CACC-equipped vehicle on the mainstream would decelerate (if necessary) to provide a safe gap for the merging vehicle. It was shown that depending on different traffic conditions, the performance of the merging assistant can be different and some unnecessary large gaps were generated under some conditions.

Through investigating the literature, we conclude that a more sophisticated algorithm for the merging sequence determination is required to work efficiently in a mixed traffic on both merging and mainstream lanes.

## 2.5 Model-Based Predictive Control Scheme

Model-based Predictive Control (MPC) has been utilized in the process industries since 1980. Some abilities of MPC (e.g., ability in handling multi-variable systems in presence of the constraints and uncertainties) have made it an interesting tools to be employed in other fields such as automation, aerospace, energy, food processing, robotics, etc. [94] [95]. Generally, MPC works based on the steps below [94]:

- 1- Predicting the output at a time horizon using the explicit form of the model
- 2- Obtaining the control sequence to minimize an objective function
- 3- Receding strategy: at each instant, the prediction horizon applied toward the future, and the first control input of the sequence calculated at each step determined and used to update the actual control law.

In other words, in MPC, an objective function should be defined to formulate the control goal from the current time until the finite prediction horizon. Afterward, at each instant, a sequence of control inputs will be obtained to minimize the objective function over the defined prediction horizon. Only the control input corresponding to the current time among the calculated optimal control sequence will be utilized to apply to the actual system. This procedure should be undertaken in each instant to find the control input. Note that the objective function can be defined based on different control goal (e.g., regulation and tracing the desired output) [94]. The basic structure of the MPC is shown in Figure 2-1.

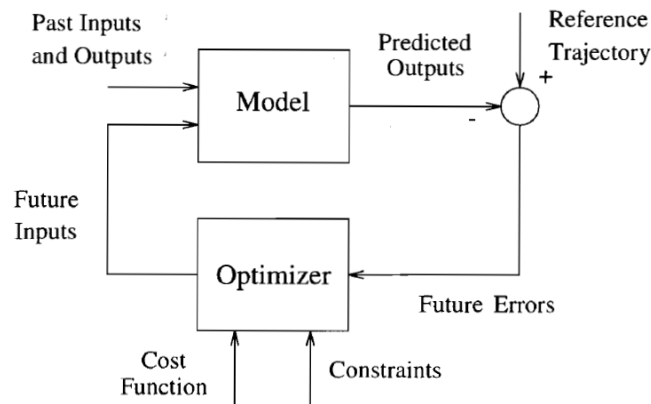


Figure 2-1-MPC general form [95]

MPC estimates the predicted outputs and compares to the reference trajectory (i.e., the desired output to be followed by the model) to obtain the future error. Then the optimizer uses this error to minimize the cost function with respect to the constraints by choosing the control input sequences. Some advantages of MPC are as bellow [95]:

- 1- The concept is very intuitive and easy to understand
- 2- It is applicable to most of the process (dynamics with delay and disturbance)
- 3- It can easily handle the multivariable systems
- 4- It is efficient in the cases that the future references are known.

However, MPC could be a time-consuming process, especially when the system has many constraints to be satisfied. Moreover, since MPC works based on the system model, it needs an accurate system identification process to find an accurate system model.

## **2.6 Concluding Remarks**

All in all, in this study, we use Helly's linear model [70] for the car-following behavior of the conventional vehicles. Moreover, Ahmed's linear model, presented in [57], will be used for the free-flow driving behavior of the conventional vehicles as it is able to capture most of the uncertainties. To consider both lead and lag gaps in the gap acceptance merging model, we will employ Ahmed's model [57]. Through reviewing the literature, it is concluded that prediction the arrival time of the vehicles based on their current motion conditions can be considered as one indicator in developing the novel merging sequence determination methodology for the traffic control framework. In the next chapter, we will discuss the proposed traffic control framework to model and control the merging areas in a mixed traffic network.

### Chapter 3: COOPERATIVE OPTIMAL MERGING ALGORITHMS

In this chapter, a modelling and cooperative control framework is developed for the mixed traffic flow comprising CAVs and conventional vehicles in the merging area. We envision that cooperative merging for the case of mixed traffic is implemented via a two-level hierarchical control framework shown in Figure 3-1, is required. The higher level has access to the information of all vehicles in the merging area using various methods (e.g., vehicle to vehicle (V2V) communication, vehicle to infrastructure (V2I) communication, video surveillance, etc.). Moreover, the higher level of the framework determines the merging sequence, namely assigns, for each vehicle on the on-ramp (i.e., the merging vehicle), the pair of mainstream vehicles that will become leader (i.e., the lead vehicle) and follower (i.e., the lag vehicle) of the merging vehicle after the merging maneuver is completed. We denote as *triplet* the set of these three vehicles, i.e., a merging vehicle, a lead vehicle, and a lag vehicle, that interact with each other during the merging maneuver, according to their types (i.e., conventional or CAV) and initial conditions prior to triplet formation. A control zone is defined, where V2V and V2I communication methods are provided. As a merging vehicle enters the control zone, the higher level of traffic control assigns it to a triplet of vehicles, i.e., forms a triplet, based on certain rules (i.e., prediction of the arrival time of the vehicles, types of triplets which can be formed, etc.). Note that in case of low traffic demand on the mainstream or on the ramp, the higher level of control can assume a hypothetical conventional lead or lag vehicles far from the merging area to form the triplets. However, if the merging vehicle faces no vehicle on the mainstream, forming a triplet is not required. In this chapter, we assume that triplets' formation is decided by the higher level of traffic control, and we focus only on the lower level of traffic control framework, which is related to developing merging algorithms for different types of triplets. However, in the next chapter, the higher level of framework is elaborated.

The lower level of the framework aims at optimizing the movements of CAVs within each triplet of vehicles. Our assumption is that, for each triplet, the optimal control inputs (i.e., acceleration values for CAVs) are calculated by an individual entity, i.e., either a CAV within the triplet or a device in the infrastructure, and such information is delivered to all other CAVs (if existing) within the triplet via V2I/V2V communication.

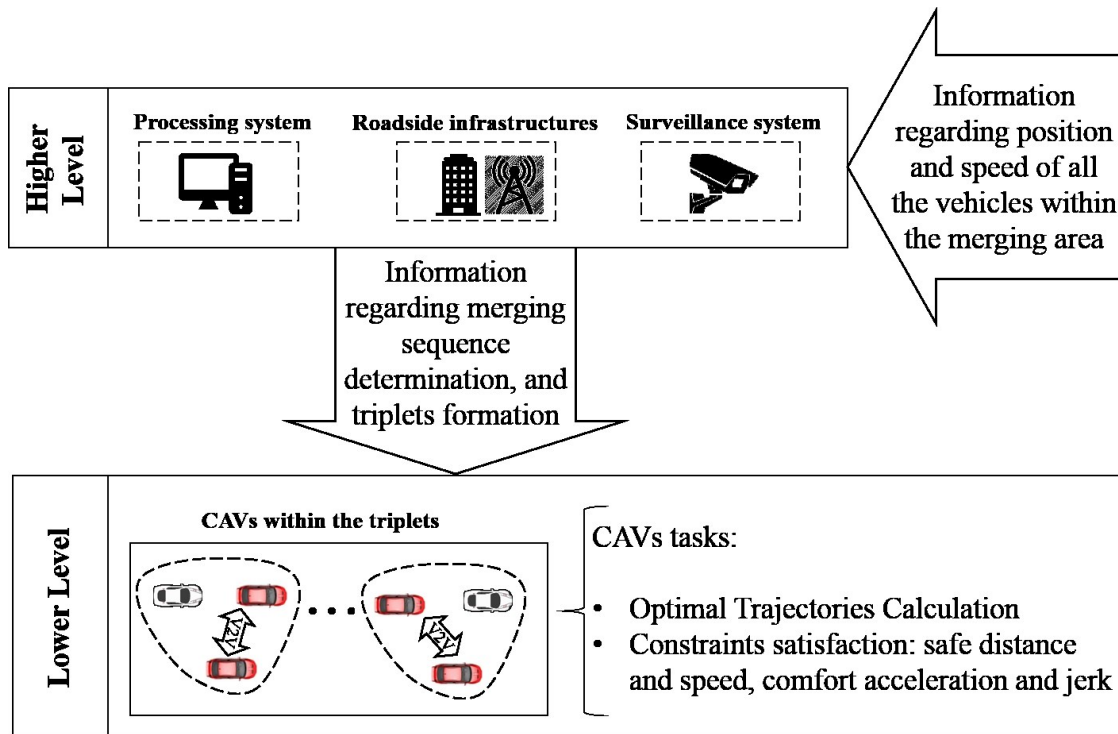


Figure 3-1. The two-level hierarchical traffic control framework

Moreover, the necessary information related to all vehicles is collected and communicated through V2V/V2I. These assumptions enable the proposed methodology to be used in real-time and to reduce the computation needs in the higher level of the framework (i.e., a central coordinator). This study is focused on mixed traffic merging situations, hence only six types of triplets that consist of both CAV and conventional vehicle are considered. Specifically, we do not investigate the triplet composed of three CAVs, as this has been thoroughly investigated in previous studies [35], [37]–[39], [43]; nor the triplet of only conventional vehicles where no external control is required. Like in most previous studies, we focus mainly on the cooperative gap control and longitudinal vehicle movement without lane changing, hence a single mainstream lane of a freeway is considered, along with the adjacent single lane of a merging on-ramp (Figure 3-2).

For the lower level of the framework, a distinct Multi-Input Multi-Output (MIMO) system model for each type of triplets is developed such that interactions between conventional vehicles and CAVs engaged in the merging maneuver are captured. For each type of triplets, different consecutive phases of movements, with different desired control targets, are proposed. For each movement phase, the control goal is to track the desired speed and gaps to provide the conditions to start the next movement phase. By doing so, the proposed algorithms facilitate the merging

maneuvers and avoid stopping of the merging vehicle at the end of the acceleration lane, which would entail idling and waiting for another sufficient gap to merge and would thereby cause increase of delays, fuel consumption and air pollution. Facilitating the merging maneuver also prevents the merging vehicle from unsafely merging in front of a vehicle that moves at a higher speed causing its deceleration.

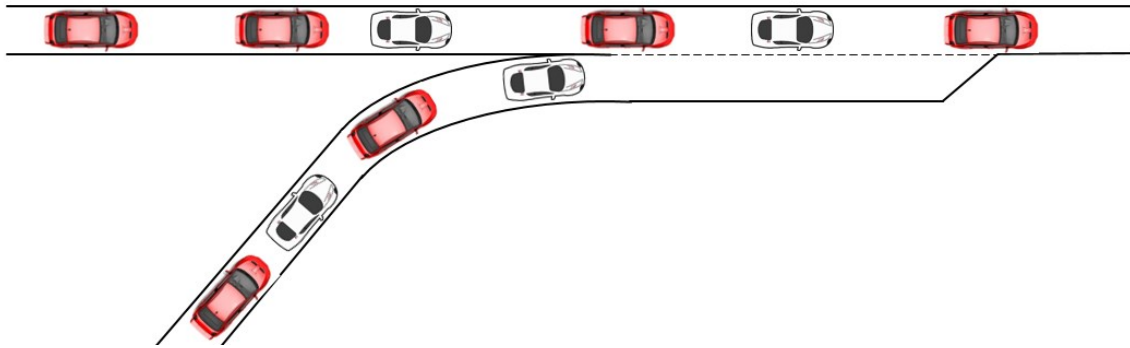


Figure 3-2- A single lane merging area containing conventional (in white) and CAVs (in red).

A model predictive control (MPC) scheme is employed to cope with the uncertainties and delays in the system model (caused by conventional vehicles) and to optimize the defined cost functions by calculating the optimal control inputs for CAVs. Moreover, the controller complies with the existing constraints related to vehicles safety (e.g., rear-end accidents) and occupants’ comfort (e.g., adequate acceleration and jerk values—i.e., the first derivative of acceleration). The latter one also mitigates the consequences of switching between different phases of movement (e.g., sharp acceleration changes). Note that, by “acceleration”, we mean both positive and negative values of the first derivative of speed.

In the following section, the six different types of triplets are discussed to develop merging algorithms.

### 3.1 The Characteristics of Merging Triplets

In this section, for each type of triplets, a corresponding consecutive multi-phase movement algorithm is analytically developed to control the merging maneuvers. Note that the last phase of the movement is considered to simulate the vehicles after merging under the normal operation condition, i.e., when triplets disjoint. The models of individual vehicles in each triplet are combined in a state-space MIMO system model. For simplicity, we model each CAV by second-order dynamics, while two modes of movement are considered for conventional vehicles, i.e., car-

following and free-flow. Since the proposed framework is developed for real-time implementation, linear models for conventional vehicles are used in order to maintain low computational efforts for the controllers. Therefore, among the conventional vehicle models, such as [54], [58]–[61] etc., we utilize the linear car-following Helly’s model [70] and a linear free-flow model [57]. These models are able to capture most aspects of the uncertainties related to human-driven vehicles, such as reaction time and uncertainty in following the desired free-flow speed. Moreover, we model only longitudinal movements, i.e., we do not account for steering angle and lateral movements.

Generally, merging maneuvers of conventional vehicles at on-ramps are described in three steps: first, the driver monitors the target lane, evaluates, and determines when a proper gap occurs in order to merge safely; second, the driver adjusts the vehicle to align with the targeted gap and mainstream vehicles speed; and finally, the driver accomplishes the merging maneuver [43]. Let us introduce the definitions of lead gap as the space between the front of the merging vehicle and the rear of the lead vehicle in the target lane; and lag gap as the space between the rear of the merging vehicle and the front of the lag vehicle in the target lane [57]. We assume that, if a conventional merging vehicle faces sufficient acceptable lead and lag gaps, it will merge between the lead and lag vehicles. In addition, if the merging vehicle travels at the same speed as the mainstream vehicles, it can accept a smaller gap to merge [57]. Therefore, in addition to sufficient lead and lag gaps availability, we also account for moving at the same speed to allow for merging accomplishment. Additionally, we assume that a lag conventional vehicle will cooperate with the merging vehicle (by providing sufficient lag gap) if they move at the same speed while the merger is located on the acceleration lane between the lead and lag vehicles (We proved this idea in Appendix I).

We illustrate all six types of triplets in Figure 3-3 to Figure 3-14, where vehicles shown in red are of the CAV type, vehicles shown in white are of conventional type, and the vehicles shown in gray can be of either type. The conditions of one-way transition to the next movement phase for all types of triplets are summarized in Table 3-1, which will be elaborated in this section. Point *A* and *B* are defined as the beginning and the end of acceleration lane respectively, along which merging is allowed and has to be completed. A control zone is defined, in which I2V communication is provided (as is shown by two large dashed parentheses in Figure 3-3 to Figure 3-14).



**Table 3-1- One-way transition conditions in each phase of movement**

Triplet types	Conditions to be satisfied in each phase for transition to the next phase	
	Phase 1	Phase 2
<b>Type I</b>	If V2 is downstream of point <i>A</i> and V2 is located between V3 and V1 on the acceleration lane, at the same speed of V3 (with acceptable $\pm 5\%$ tolerance), V3 will agree to cooperate, and the second phase will start.	V2 is on the acceleration lane between points <i>A</i> and <i>B</i> . If desired acceptable lead and lag gaps are provided for V2, it will merge, and phase 3 will start.
<b>Type II</b>	V2 and V3 cooperate to create desired acceptable lead and lag gaps before they reach point <i>A</i> . Therefore, after passing point <i>A</i> , if V2 faces acceptable lead and lag gaps, it will merge, and phase 2 will start.	
<b>Type III</b>	V1 and V3 cooperate to create the acceptable lead and lag gaps for V2 before reaching point <i>A</i> . After V2 passes point <i>A</i> , if it perceives the available gaps, it will merge, and phase 2 will start.	
<b>Type IV</b>	V3 follows V1, keeping the distance of desired acceptable <i>lead + lag</i> gaps. If V2 has 100 meters left to reach point <i>A</i> , phase 2 will start.	V2 passes point <i>A</i> . If desired acceptable lead (by speed difference between V1 and V2) and lag (by V3) gaps are provided, V2 will merge, and phase 3 will start.
<b>Type V</b>	V1 travels such that when V2 reaches point <i>A</i> , it locates between V1 and V3 on the acceleration lane at the same speed (with acceptable $\pm 5\%$ tolerance). Therefore, after V2 passed point <i>A</i> , if it locates between V1 and V3 at the same speed, V3 will agree to cooperate, and phase 2 will start.	V2 is on the acceleration lane between points <i>A</i> and <i>B</i> . If desired acceptable lead (by V1) and lag (by V3) gaps are provided, V2 will merge, and phase 3 will start.
<b>Type VI</b>	V2 travels such that it locates between V1 and V3, when reaches point <i>A</i> . Therefore, after V2 passes point <i>A</i> , if it locates within between V1 and V3 on the acceleration lane at the same speed (with acceptable $\pm 5\%$ tolerance), V3 will agree to cooperate, and phase 2 will start.	V2 is on the acceleration lane between points <i>A</i> and <i>B</i> . If desired acceptable lead (by V2) and lag (by V3) gaps are provided, V2 will merge, and phase 3 will start.

The remaining of this chapter provides more details on different movement phases of each triplet type. To facilitate an intuitive reference to various triplet types, we use the types of lead (V1), merging (V2), and lag (V3) vehicles as V1-V2-V3, respectively. In addition, in this chapter, the merging algorithms are elaborated and the state-space models of each scenario are developed.

### 3.1.1 Type I: CAV-CAV-Conventional

In this scenario, the lead (V1) and the merging vehicles (V2) are both CAVs, while the lag vehicle (V3) is a conventional vehicle (Figure 3-3). In this case, behavior of V3 is modeled using a combination of a car-following model and a free-flow model, depending on its distance from V1. VL1 and VL2 (the immediate vehicles ahead of V1 and V2, respectively) are also considered as a disturbance to the system to guarantee compliancy with a safe distance from them. Note that, V1 and V2 can be either CAV or conventional vehicle; however, their dynamic models are not required in the triplet model.

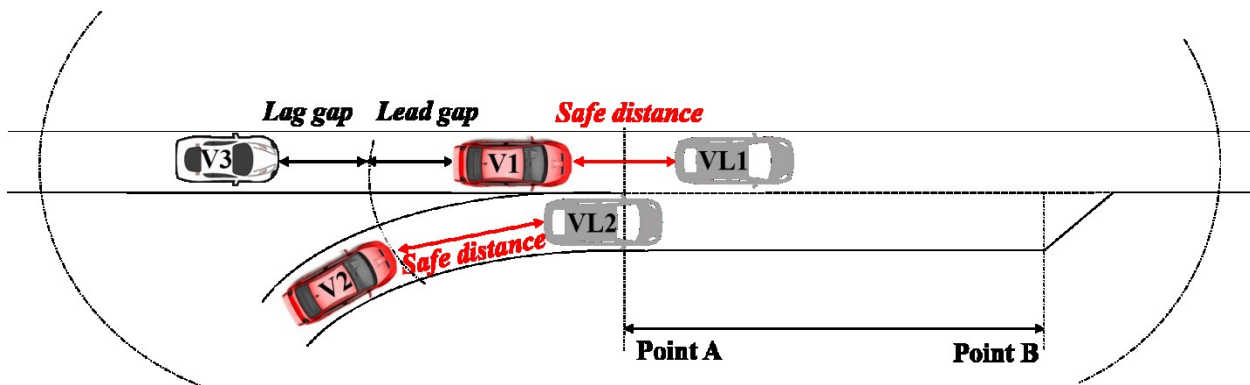


Figure 3-3. Sketch of triplet type I

If V3 is far from V1 (i.e., more than the threshold distance required to activate a car-following behavior), V3 moves at its own desired free-flow speed independently of V1. Consequently, V2 will have enough gap to merge between V1 and V3. On the other hand, if V3 follows V1, the small distance between them will not allow V2 to merge easily. Accordingly, we will discuss the latter condition as a worst-case scenario. In this scenario, three main movement phases are considered to describe the merging strategy (Figure 3-4).

#### 3.1.1.1 Phase 1 (merging vehicle approaches the acceleration lane)

The vehicles enters the control zone and V3 is following V1. In this case, V2 will merge only if V1 and V3 can provide enough lead and lag gaps respectively, while V2 is in the acceleration lane (between point A and B shown in Figure 3-4). Since V3 is a conventional vehicle, it cannot be controlled, rather it is modeled through a stochastic car-following/free-flow algorithm. This merging methodology proposes a mechanism to provide the conditions to gain the cooperation of V3—the conventional vehicle, in order to create the acceptable lag gap for V2—the CAV merging

vehicle. In this regard, as mentioned in previous section, it is assumed that if V2 moves at the same speed as mainstream vehicles (V1 and V3) and V2 is located between them, V3 (as a conventional vehicle) will cooperate with V2 to provide enough lag gap for merging. Therefore, V2 moves such that it reaches the point *A* between V3 and V1 at the same speed as V3. Accordingly, when V3 perceives V2 at the beginning of the acceleration lane, it cooperates with it to merge by providing the acceptable lag gap. In this phase, the control goal is that V2 follows V1 with half the distance (or less) between V1 and V3. At the same time, V1 has to maintain the desired speed of the mainstream. To model this phase, the linear Helly's model [70] is considered as a conventional car-following model. Therefore, for V3, we have

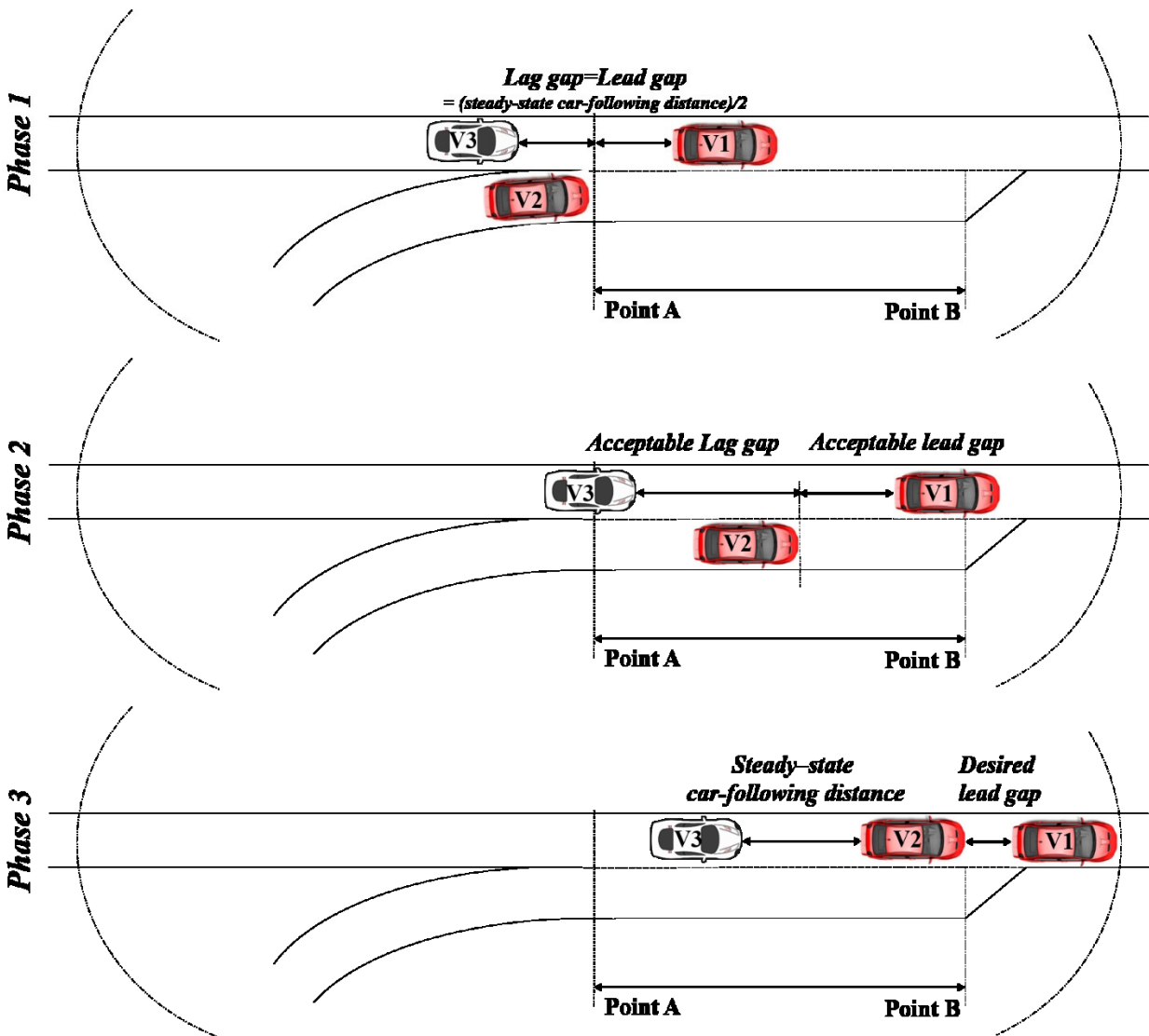


Figure 3-4. Movement phases of triplet type I

$$a_3(t) = \alpha_1 \Delta v_{1,3}(t - \tau_3) + \alpha_2 [\Delta x_{1,3}(t - \tau_3) - g_{s3}(t - \tau_3)] \quad 3-1$$

where  $g_{s3}$  represents the desired distance headway,  $\Delta v_{1,3} = v_1 - v_3$  and  $\Delta x_{1,3} = x_1 - x_3$  are the relative speed and space headway between V1 and V3, respectively. The model coefficients,  $\alpha_i$ s, can be calibrated using real data. Moreover,  $a_3$  represents the acceleration of V3, and  $\tau_3$  the reaction time of V3. The desired distance headway is modeled as follows [70], [71]

$$g_{s3}(t - \tau_3) = \beta_1 + \beta_2 v_3(t - \tau_3) \quad 3-2$$

By substituting  $g_{s3}$  in  $a_3$ , we have

$$a_3(t) = \gamma_1 v_3(t - \tau_3) + \gamma_2 v_1(t - \tau_3) + \gamma_3 \Delta x_{1,3}(t - \tau_3) + \gamma_4 \quad 3-3$$

where  $\gamma_i$ s can be defined as:

$$\gamma_1 = -\alpha_1 - \alpha_2 \beta_2, \gamma_2 = \alpha_1, \gamma_3 = \alpha_2, \gamma_4 = -\alpha_2 \beta_1 \quad 3-4$$

By substituting  $\Delta x_{1,3}(t - \tau_3) = \Delta x_{1,2}(t - \tau_3) + \Delta x_{2,3}(t - \tau_3)$  in (3), we have

$$a_3(t) = \gamma_1 v_3(t - \tau_3) + \gamma_2 v_1(t - \tau_3) + \gamma_3 \Delta x_{1,2}(t - \tau_3) + \gamma_3 \Delta x_{2,3}(t - \tau_3) + \gamma_4 \quad 3-5$$

In this phase, V1 and V2 should also keep a safe distance from their leaders (if exist), hence, we need to take  $\Delta \dot{x}_{L1,1}(t) = v_{L1}(t) - v_1(t)$  and  $\Delta \dot{x}_{L2,2}(t) = v_{L2}(t) - v_2(t)$  into account in the system model, where  $\Delta x_{L1,1}(t)$  and  $\Delta x_{L2,2}(t)$  are the distances of V1 and V2 from their leaders, and  $v_{L1}(t)$  and  $v_{L2}(t)$  are the speeds of VL1 and VL2, respectively.

### 3.1.1.2 Phase 2 (merging vehicle on the acceleration lane)

It is assumed that V3 agrees to cooperate when it perceives V2 (i.e., when V2 has reached point A) in phase 1. As a result, in phase2, V3 changes its leader from V1 to V2 and starts following V2 with the car-following prescribed distance (acceptable lag gap). Accordingly, the acceleration of V3 changes to

$$a_3(t) = \gamma_1' v_3(t - \tau_3) + \gamma_2' v_2(t - \tau_3) + \gamma_3' \Delta x_{2,3}(t - \tau_3) + \gamma_4' \quad 3-6$$

The coefficients of equation 3-6 are modified to provide a lag gap larger than the steady-state car-following gap (equal to acceptable lag gap). In this phase, as the control goal, V1 and V2 cooperate such that the distance between them reaches the desired acceptable lead gap and the speed of vehicles reaches the desired speed of the mainstream. When the desired acceptable lead and lag gaps are provided for V2, V2 will merge between V1 and V3 and the system enters the

third phase. Furthermore, V1 and V2 must always keep a safe distance from their leaders if there is any (the leader of V2 might merge anytime in the mainstream lane).

Note that V3's perception of a merging vehicle depends on many factors such as the geometry of the ramp, weather conditions, the type and size of both vehicles, the driver characteristics, vehicles current speeds, and the most important one, the distance between them [96]. In this study, it is assumed that when the merging vehicle (i.e., V2) reaches point  $A$ , it is perceivable by the lag vehicle (i.e., V3) if they are longitudinally closer than the car following threshold.

### 3.1.1.3 Phase 3 (merging vehicle completes the maneuver)

After completing the merging maneuver, V3 follows V2 using a conventional car-following model; V2 keeps a distance (smaller than the desired acceptable lead gap) from its leader (V1); V1 will move at its desired mainstream speed while keeping desired safe distance from the downstream vehicle in front. In this phase, the acceleration of V3 can be modeled as follows:

$$a_3(t) = \gamma_1 v_3(t - \tau_3) + \gamma_2 v_2(t - \tau_3) + \gamma_3 \Delta x_{2,3}(t - \tau_3) + \gamma_4 \quad 3-7$$

### 3.1.1.4 The general model and control targets of triplet type I

The general model for all the phases is as follows:

$$\begin{aligned} \Delta \dot{x}_{1,2}(t) &= v_1(t) - v_2(t) \\ \Delta \dot{x}_{2,3}(t) &= v_2(t) - v_3(t) \\ \Delta \dot{x}_{L1,1}(t) &= v_{L1}(t) - v_1(t) \\ \Delta \dot{x}_{L2,2}(t) &= v_{L2}(t) - v_2(t) \\ \dot{v}_1(t) &= a_1(t) \\ \dot{v}_2(t) &= a_2(t) \end{aligned} \quad 3-8$$

$$\dot{v}_3(t) = \begin{cases} \gamma_1 v_3(t - \tau_3) + \gamma_2 v_1(t - \tau_3) + \gamma_3 \Delta x_{1,2}(t - \tau_3) + \gamma_4 & \Phi = 1 \\ \gamma_1' v_3(t - \tau_3) + \gamma_2' v_2(t - \tau_3) + \gamma_3' \Delta x_{2,3}(t - \tau_3) + \gamma_4' & \Phi = 2 \\ \gamma_1 v_3(t - \tau_3) + \gamma_2 v_2(t - \tau_3) + \gamma_3 \Delta x_{2,3}(t - \tau_3) + \gamma_4 & \Phi = 3 \end{cases}$$

where  $\Phi$  indicates the movement phase number.

Considering  $X(t) = [\Delta x_{1,2}(t) \ \Delta x_{2,3}(t) \ v_1(t) \ v_2(t) \ v_3(t) \ \Delta x_{L1,1}(t) \ \Delta x_{L2,2}(t)]^T$  as the state-space vector,  $U(t) = [a_1(t) \ a_2(t)]^T$  as the input vector, and  $Y(t) = [\Delta x_{1,2}(t) \ v_1(t)]^T$  as the system output, the state-space system model is

$$\begin{aligned} \dot{X}(t) &= AX(t) + A_i^\tau X(t - \tau_3) + BU(t) + D_i, \quad i = \Phi \in \{1,2,3\} \\ Y(t) &= CX(t) \end{aligned} \quad 3-9$$

where  $A_i^\tau$  and  $D_i$  are the coefficient matrices for phase  $i$ , and

$$\begin{aligned} A &= \begin{bmatrix} 0 & 0 & 1 & -1 & 0 & 0 & 0 \\ 0 & 0 & 0 & 1 & -1 & 0 & 0 \\ 0 & 0 & 0 & 0 & 0 & 0 & 0 \\ 0 & 0 & 0 & 0 & 0 & 0 & 0 \\ 0 & 0 & 0 & 0 & 0 & 0 & 0 \\ 0 & 0 & -1 & 0 & 0 & 0 & 0 \\ 0 & 0 & 0 & -1 & 0 & 0 & 0 \end{bmatrix}, B = \begin{bmatrix} 0 & 0 \\ 0 & 0 \\ 1 & 0 \\ 0 & 1 \\ 0 & 0 \\ 0 & 0 \\ 0 & 0 \end{bmatrix}, C = \begin{bmatrix} 1 & 0 & 0 & 0 & 0 & 0 & 0 \\ 0 & 0 & 1 & 0 & 0 & 0 & 0 \end{bmatrix}, \\ A_1^\tau &= \begin{bmatrix} 0 & 0 & 0 & 0 & 0 & 0 & 0 \\ 0 & 0 & 0 & 0 & 0 & 0 & 0 \\ 0 & 0 & 0 & 0 & 0 & 0 & 0 \\ 0 & 0 & 0 & 0 & 0 & 0 & 0 \\ \gamma_3 & \gamma_3 & \gamma_2 & 0 & \gamma_1 & 0 & 0 \\ 0 & 0 & 0 & 0 & 0 & 0 & 0 \\ 0 & 0 & 0 & 0 & 0 & 0 & 0 \end{bmatrix}, A_2^\tau = \begin{bmatrix} 0 & 0 & 0 & 0 & 0 & 0 & 0 \\ 0 & 0 & 0 & 0 & 0 & 0 & 0 \\ 0 & 0 & 0 & 0 & 0 & 0 & 0 \\ 0 & \gamma_3' & 0 & \gamma_2' & \gamma_1' & 0 & 0 \\ 0 & 0 & 0 & 0 & 0 & 0 & 0 \\ 0 & 0 & 0 & 0 & 0 & 0 & 0 \\ 0 & 0 & 0 & 0 & 0 & 0 & 0 \end{bmatrix}, \\ A_3^\tau &= \begin{bmatrix} 0 & 0 & 0 & 0 & 0 & 0 & 0 \\ 0 & 0 & 0 & 0 & 0 & 0 & 0 \\ 0 & 0 & 0 & 0 & 0 & 0 & 0 \\ 0 & 0 & 0 & 0 & 0 & 0 & 0 \\ 0 & \gamma_3 & 0 & \gamma_2 & \gamma_1 & 0 & 0 \\ 0 & 0 & 0 & 0 & 0 & 0 & 0 \\ 0 & 0 & 0 & 0 & 0 & 0 & 0 \end{bmatrix}, D_1 = \begin{bmatrix} 0 \\ 0 \\ 0 \\ 0 \\ \gamma_4 \\ v_{L1}(t) \\ v_{L2}(t) \end{bmatrix}, D_2 = \begin{bmatrix} 0 \\ 0 \\ 0 \\ 0 \\ \gamma_4' \\ v_{L1}(t) \\ v_{L2}(t) \end{bmatrix}, D_3 = \begin{bmatrix} 0 \\ 0 \\ 0 \\ 0 \\ \gamma_4 \\ v_{L1}(t) \\ v_{L2}(t) \end{bmatrix}. \end{aligned} \quad 3-10$$

In phase 1, V2 should reach the merging area between the vehicles on the mainstream at the same speed. Therefore, the control goal is that the output tracks the vector defined by equation 3-11.

$$Y_1^d(t) = \begin{bmatrix} \Delta x_{1,3}(t)/2 \\ v_{main}^d \end{bmatrix} \quad 3-11$$

where  $v_{main}^d$  is the desired mainstream speed. Note that since V2 and V1 are CAVs, V2 can accept even smaller lead gap, and accordingly, we can consider a smaller value instead of  $\Delta x_{1,3}(j)/2$  in the desired output vector. In phase 2, the distance between V1 and V2 should reach the desired acceptable lead gap. Therefore, the control goal is that the output tracks

$$Y_2^d = \begin{bmatrix} g_{d,lead} \\ v_{main}^d \end{bmatrix} \quad 3-12$$

where  $g_{d,lead}$  represents the desired acceptable lead gap. In phase 3, the control goal is to follow

$$Y_3^d = \begin{bmatrix} g_{s1,2} \\ v_{main}^d \end{bmatrix} \quad 3-13$$

where  $g_{s1,2}$  is the desired steady-state distance headway value between automated vehicles (i.e., V1 and V2).

### 3.1.2 Type II: Conventional-CAV-CAV

In this scenario, V2 and V3 as the merging vehicle and lag vehicle are CAVs. V1 as a conventional vehicle moves at free-flow speed or follows its leader using a car-following model (Figure 3-5). In either of the conditions, the dynamics of V1 is not affected by the sub-system model as it can be considered as a real-time disturbance. Similarly, the distance of V2 from VL2 (the immediate vehicle ahead of V2) is considered as a real-time disturbance to guarantee a safe distance. Therefore, we can model the system using only CAVs models (i.e., a second order dynamics). This maneuvering scenario is described in two movement phases (Figure 3-6).

#### 3.1.2.1 Phase 1 (before merging)

This phase begins by entering the vehicles to the control zone. In order to facilitate the merging maneuver, V2 and V3 cooperate such that V2 keeps its desired acceptable lead gap from V1 and its desired acceptable lag gap from V2. CAVs must gain these desired values before reaching point A. When V2 reach point A, it will merge between V1 and V3, as it faces the desired acceptable lead and lag gaps.

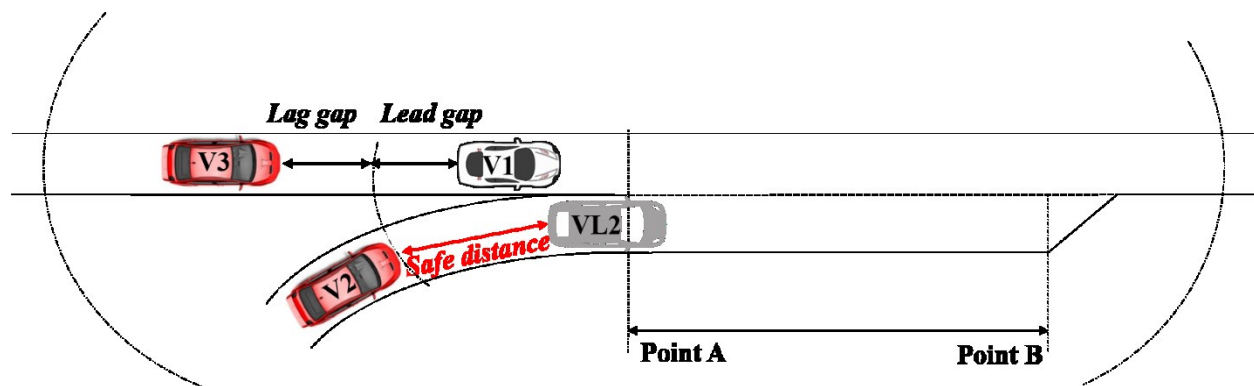


Figure 3-5. Sketch of triplet type II

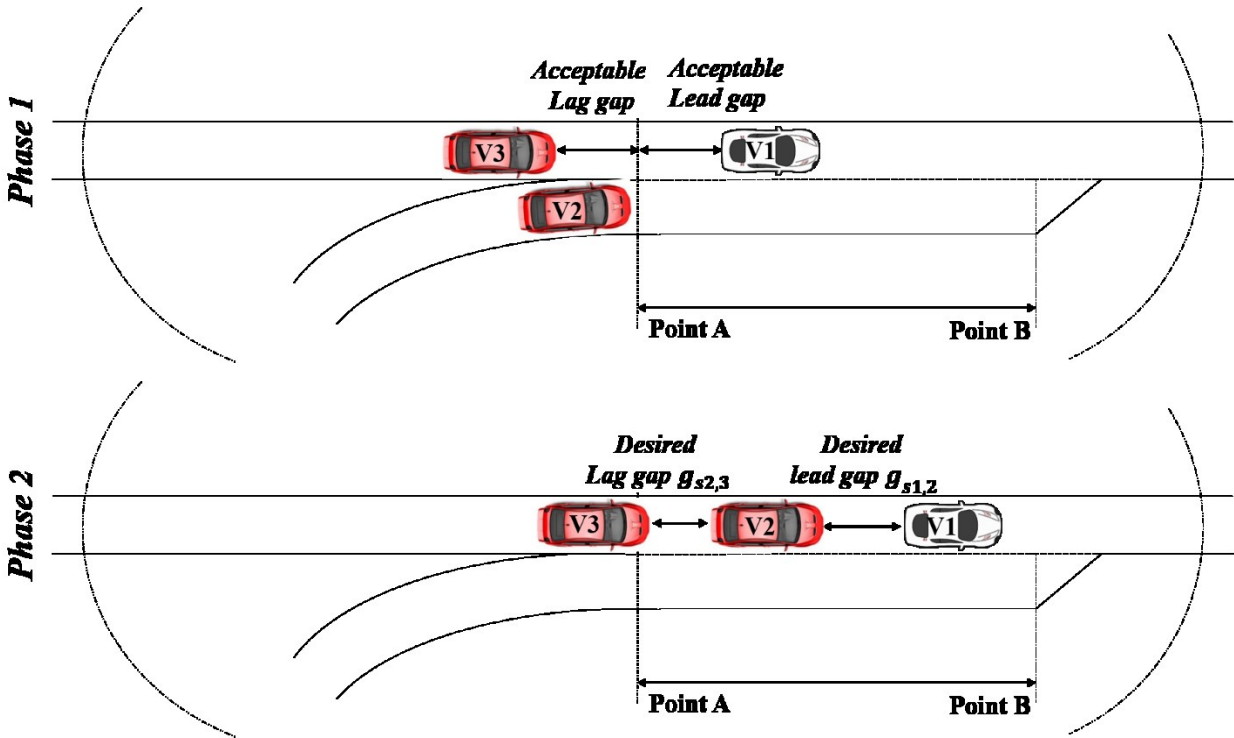


Figure 3-6. Movement phases of triplet type II

### 3.1.2.2 Phase 2 (after merging)

After V2 merged and located between V1 and V3, the desired distance between V1-V2 and V2-V3 will change to the distances smaller than before. Note that V2 and V3 regulate their speeds to track the speed of V1 while maintaining constant distances.

### 3.1.2.3 The general model and control targets of triplet type II

Note that the system model is similar for both motion phases, however, the control goal will be different in each phase. Considering  $X = [\Delta x_{1,2}(t) \Delta x_{2,3}(t) v_2(t) v_3(t) \Delta x_{L2,2}(t)]^T$  as the state-space vector,  $D(t)$  as a deterministic disturbance related to the speed of V1 and VL2,  $U(t) = [a_2(t) a_3(t)]^T$  as the control law sequence, and  $Y(t) = [\Delta x_{1,2}(t) \Delta x_{2,3}(t)]^T$  as the system output, the system model (for all the phases of the merging maneuver) is defined below

$$\dot{X}(t) = AX(t) + BU(t) + D(t)$$

$$Y(t) = CX(t)$$

3-14

where



$$A = \begin{bmatrix} 0 & 0 & -1 & 0 & 0 \\ 0 & 0 & 0 & -1 & 0 \\ 0 & 0 & 0 & 0 & 0 \\ 0 & 0 & 0 & 0 & 0 \\ 0 & 0 & -1 & 0 & 0 \end{bmatrix}, B = \begin{bmatrix} 0 & 0 \\ 1 & 0 \\ 0 & 1 \\ 0 & 0 \end{bmatrix}, D(t) = \begin{bmatrix} v_1(t) \\ 0 \\ 0 \\ 0 \\ v_{L2}(t) \end{bmatrix}, \text{ and } C = \begin{bmatrix} 1 & 0 & 0 & 0 & 0 \\ 0 & 1 & 0 & 0 & 0 \end{bmatrix}. \quad 3-15$$

For this triplet type, the control target is to provide desired acceptable lead and lag gaps in phase 1 to allow V2 to merge. Therefore, system output should follow

$$Y_1^d = \begin{bmatrix} g_{d,lead} \\ g_{d,lag} \end{bmatrix} \quad 3-16$$

where  $g_{d,lead}$  and  $g_{d,lag}$  represent the desired acceptable lead and lag gaps, respectively. The lead and lag gaps are related to a conventional vehicle and CAVs, respectively. Due to the fact that CAVs can operate with smaller distance headways, the value assigned to  $g_{d,lag}$  can be smaller than the values of  $g_{d,lead}$ . In phase 2, the target is to achieve the desired steady-state distance between the vehicles after the merging maneuver. Therefore, the vehicles only need the desired steady-state distances, which leads to the following system output target

$$Y_2^d = \begin{bmatrix} g_{s1,2} \\ g_{s2,3} \end{bmatrix} \quad 3-17$$

Note that  $g_{s1,2}$  is the desired steady-state distance between a conventional vehicle and a CAV, while  $g_{s2,3}$  is between two CAVs. Therefore,  $g_{s2,3}$  can have a smaller value than  $g_{s1,2}$ .

### 3.1.3 Type III: CAV-Conventional-CAV

In this scenario, the two vehicles on the mainstream (V1 and V3) are CAVs and the merging vehicle (V2) is a conventional (Figure 3-7). Since V1 should always keep a safe distance from the immediate vehicle ahead (VL1), we will consider it as a real-time disturbance in the triplet model. In this case, a two-phase movement is considered as below (Figure 3-8).

#### 3.1.3.1 Phase 1 (before merging)

Vehicles enter the control zone. As V1 and V3 are able to detect the location of the merging vehicle (V2), they adjust their longitudinal distance from V2 to maintain desired acceptable lead and lag gaps when they reach point *A*. Keeping a constant distance from V2 requires having the same speed as V2. By providing these goals, V2 merges when it reaches point *A*. V2's movement, before merging, can be simulated by the car-following model (similar to equation 3-1) or the free-flow

model [57] shown by equation 3-18. In this movement phase, we assumed that V2 moves by the free-flow model, however, by modifying  $A_1^c$  and  $D_1(t)$  in the general model shown in equation 3-19, it is possible to also take the car-following behavior into account.

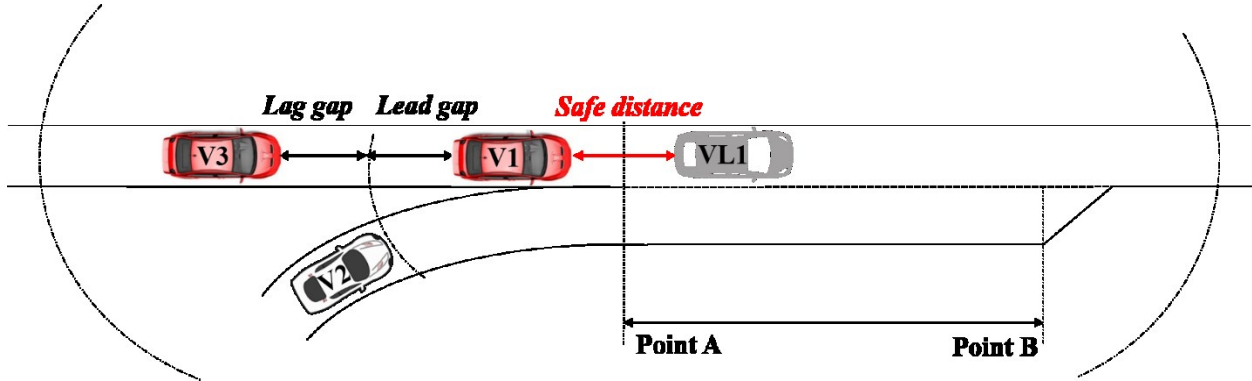


Figure 3-7. Sketch of triplet type III

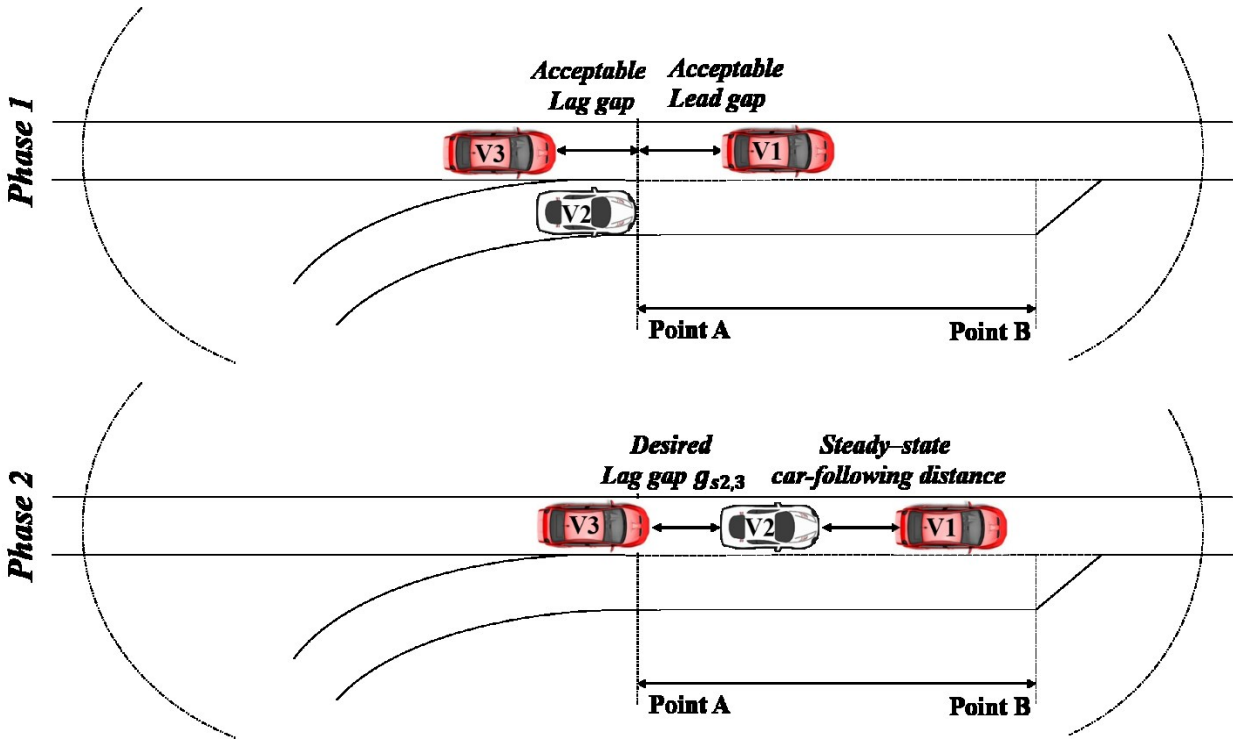


Figure 3-8. Movement phases of triplet type III

$$\dot{v}_2(t) = \lambda [v_2^d - v_2(t - \tau_2)] + \varepsilon_2(t) \quad 3-18$$

where  $\varepsilon_2(t) = \mathcal{N}(0, \sigma_2)$  is a zero-mean normally distributed error with the variance of  $\sigma_2$  and  $v_2^d$  is the desired speed of the conventional vehicles on the merging lane.

### 3.1.3.2 Phase 2 (after merging)

After V2 merges between the mainstream vehicles, its behavior changes and starts following its new leader (V1). Accordingly, the conventional car-following model (similar to equation 3-1) is employed to simulate its behavior. At the same time, V1 maintains the desired speed of the mainstream while V3 follows V2 with a certain distance (smaller than the desired acceptable lag gap).

### 3.1.3.3 The general model and control targets of triplet type III

Considering  $X(t) = [\Delta x_{1,2}(t) \ \Delta x_{2,3}(t) \ v_1(t) \ v_2(t) \ v_3(t) \ \Delta x_{L1,1}(t)]^T$  as the state-space vector,  $U(t) = [a_1(t) \ a_3(t)]^T$  as the input vector, and  $Y(t) = [\Delta x_{1,2}(t) \ \Delta x_{2,3}(t) \ v_1(t)]^T$  (for the first phase) and  $Y(t) = [\Delta x_{2,3}(t) \ v_1(t)]^T$  (for the second phase) as the system outputs, the system model is

$$\begin{aligned} \dot{X}(t) &= AX(t) + A_i^\tau X(t - \tau_2) + BU(t) + D_i(t), \quad i = \Phi \in \{1,2\} \\ Y(t) &= C_i X(t) \end{aligned} \quad 3-19$$

where

$$\begin{aligned} A &= \begin{bmatrix} 0 & 0 & 1 & -1 & 0 & 0 \\ 0 & 0 & 0 & 1 & -1 & 0 \\ 0 & 0 & 0 & 0 & 0 & 0 \\ 0 & 0 & 0 & 0 & 0 & 0 \\ 0 & 0 & 0 & 0 & 0 & 0 \\ 0 & 0 & -1 & 0 & 0 & 0 \end{bmatrix}, \quad A_1^\tau = \begin{bmatrix} 0 & 0 & 0 & 0 & 0 & 0 \\ 0 & 0 & 0 & 0 & 0 & 0 \\ 0 & 0 & 0 & 0 & 0 & 0 \\ 0 & 0 & 0 & -\lambda & 0 & 0 \\ 0 & 0 & 0 & 0 & 0 & 0 \\ 0 & 0 & 0 & 0 & 0 & 0 \end{bmatrix}, \\ A_2^\tau &= \begin{bmatrix} 0 & 0 & 0 & 0 & 0 & 0 \\ 0 & 0 & 0 & 0 & 0 & 0 \\ 0 & 0 & 0 & 0 & 0 & 0 \\ \gamma_3 & 0 & \gamma_2 & \gamma_1 & 0 & 0 \\ 0 & 0 & 0 & 0 & 0 & 0 \\ 0 & 0 & 0 & 0 & 0 & 0 \end{bmatrix}, \quad B = \begin{bmatrix} 0 & 0 \\ 0 & 0 \\ 1 & 0 \\ 0 & 0 \\ 0 & 1 \\ 0 & 0 \end{bmatrix}, \quad D_1(t) = \begin{bmatrix} 0 \\ 0 \\ 0 \\ \lambda v_2^d + \varepsilon_2(t) \\ 0 \\ v_{L1}(t) \end{bmatrix}, \\ D_2(t) &= \begin{bmatrix} 0 \\ 0 \\ 0 \\ \gamma_4 \\ 0 \\ v_{L1}(t) \end{bmatrix}, \quad C_1 = \begin{bmatrix} 1 & 0 & 0 & 0 & 0 & 0 \\ 0 & 1 & 0 & 0 & 0 & 0 \\ 0 & 0 & 1 & 0 & 0 & 0 \end{bmatrix}, \quad C_2 = \begin{bmatrix} 0 & 1 & 0 & 0 & 0 & 0 \\ 0 & 0 & 1 & 0 & 0 & 0 \end{bmatrix}. \end{aligned} \quad 3-20$$

To facilitate the merging maneuver of V2, the control target in phase 1 is defined to provide desired acceptable lead and lag gaps for V2 while vehicles on the mainstream move at the same speed as V2. Therefore, we have

$$Y_1^d(t) = \begin{bmatrix} g_{d,lead} \\ g_{d,lag} \\ v_2(t) \end{bmatrix} \quad 3-21$$

In phase 2,  $\Delta x_{1,2}(t)$  is not controllable, as V2, a conventional vehicle, follows V1. Accordingly, the control goal is that V3 follows V2 with in a closer distance while V1 travels at the mainstream free-flow speed. Therefore, we have

$$Y_2^d = \begin{bmatrix} g_{s2,3} \\ v_{main}^d \end{bmatrix} \quad 3-22$$

### 3.1.4 Type IV: Conventional-Conventional-CAV

In this scenario (Figure 3-9), all the vehicles are conventional except the follower (V3) which is a CAV. It is assumed that V2 reaches point A after V1 (it can be predicted by a higher level of hierarchical traffic control framework). Otherwise, we will face another scenario—a triplet with all conventional vehicles or all conventional except the leader (i.e., triplet type V).

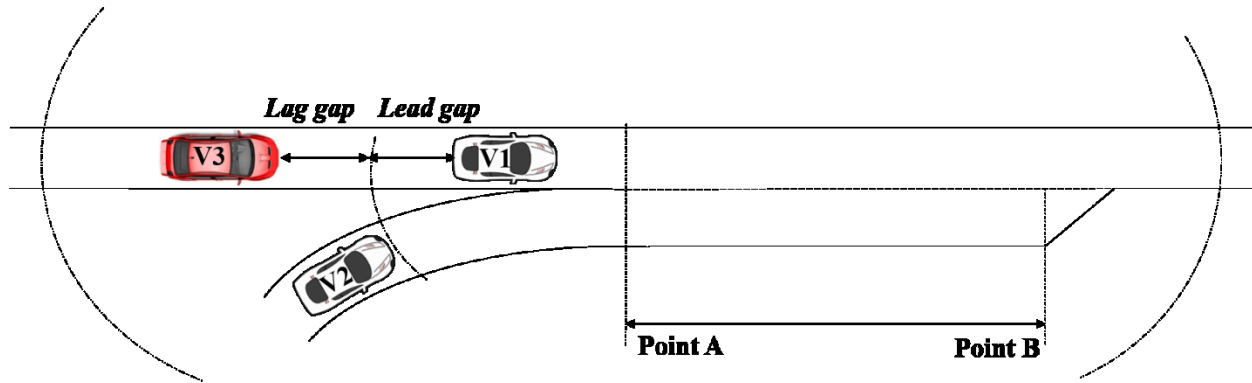


Figure 3-9. Sketch of triplet type IV

A three-phase control algorithm is proposed to facilitate the merging maneuver (Figure 3-10).

#### 3.1.4.1 Phase 1 (providing the proper distance before merging)

In this phase, vehicles are far from the merging area. To ensure that there will be enough gap between V1 and V3, V3 follows V1 at the same speed as V1 while keeping the distance of desired acceptable *lead + lag gaps* from V1. Having the same speed of desired mainstream speed helps to not disturb the mainstream flow at the beginning.

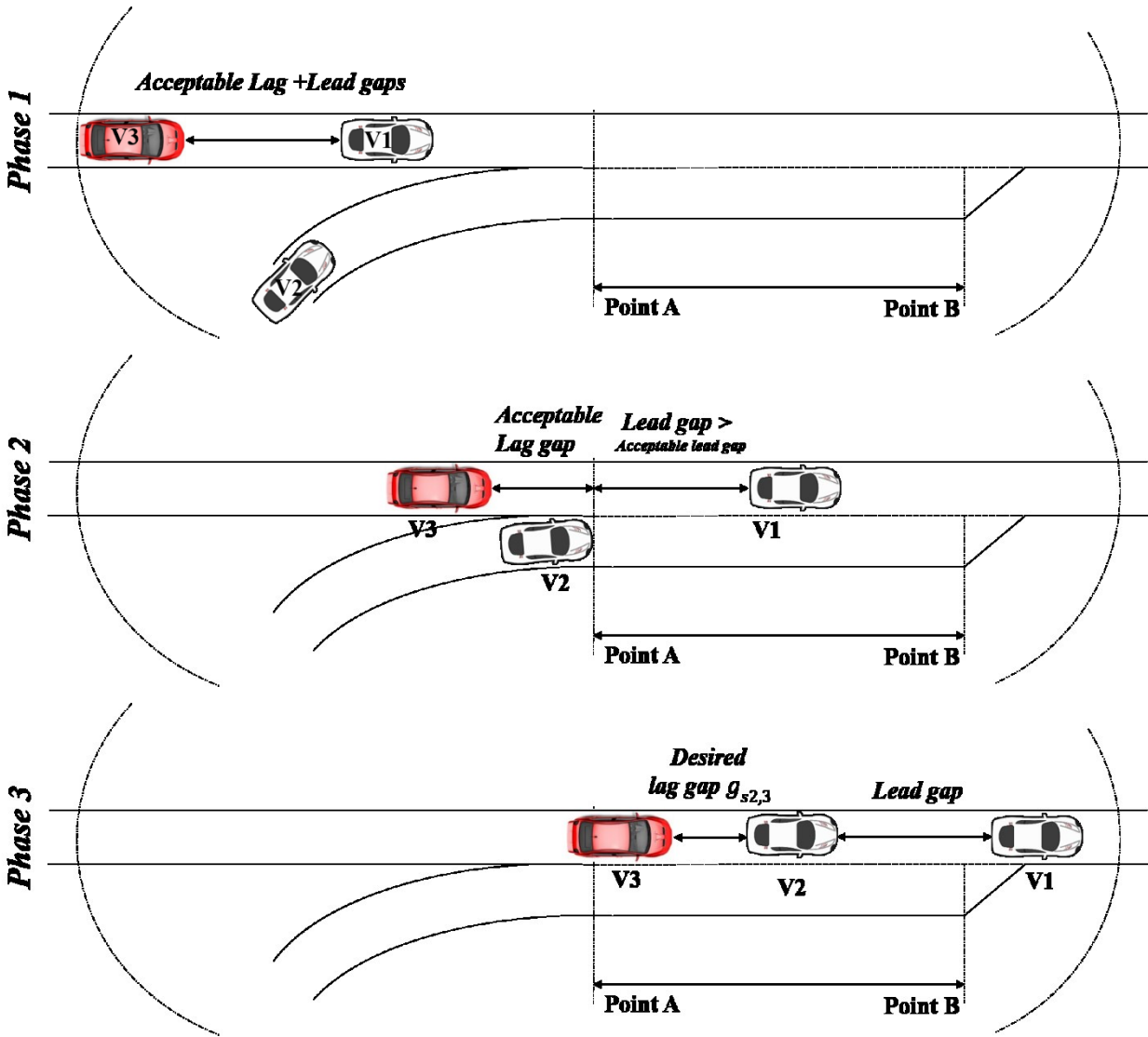


Figure 3-10. Movement phases of triplet type IV

### 3.1.4.2 Phase 2 (preparing the speed before merging)

This phase starts when all the vehicles are close to the merging area (e.g., V2 has 100 meters left to reach the point A). In this phase, V3 starts tracing the speed of V2 while keeping the desired acceptable lag gap from it. When V2 reaches point A, it will have enough lead gap (due to the fact that V1 moves faster than V2 and the desired acceptable lead gap was provided in phase 1) and enough lag gap to merge (if not it will wait for enough lag gap to be provided). Therefore, after both desired gaps are provided and V3 reached the speed of V2, the merging maneuver will take place.

In the first and second phases, both V1 and V2 move at their desired free-flow speed. Therefore, for both vehicles, a linear free-flow model [57] (similar to equation 3-18) is used.

$$\dot{v}_1(t) = \lambda [v_1^d - v_1(t - \tau_1)] + \varepsilon_1(t) \quad 3-23$$

$$\dot{v}_2(t) = \lambda [v_2^d - v_2(t - \tau_2)] + \varepsilon_2(t) \quad 3-24$$

where  $\varepsilon_{1 \text{ or } 2}(t) = \mathcal{N}(0, \sigma_{1 \text{ or } 2})$  is a zero-mean normally distributed error with the variance of  $\sigma_{1 \text{ or } 2}$  and  $v_1^d$  and  $v_2^d$  are the desired speed of the mainstream and the merging lanes, respectively.

#### 3.1.4.3 Phase 3 (after merging)

After merging, if V2 is close enough to V1, V2 will follow V1 based on a car-following model. Otherwise, V2 will move with the free-flow speed. Moreover, V3 follows V2 with a constant distance smaller than the desired acceptable lag gap. For phase 3, we have

$$\dot{v}_1(t) = \lambda [v_1^d - v_1(t - \tau_1)] + \varepsilon_1(t) \quad 3-25$$

$$\dot{v}_2(t) = \gamma_1 v_2(t - \tau_2) + \gamma_2 v_1(t - \tau_2) + \gamma_3 \Delta x_{1,2}(t - \tau_2) + \gamma_4 \quad 3-26$$

where  $\gamma_i$ s can be obtained similar to equation 3-4.

#### 3.1.4.4 The general model and control targets of triplet type IV

The general model for all the phases are as follows:

$$\Delta \dot{x}_{1,3}(t) = v_1(t) - v_3(t)$$

$$\Delta \dot{x}_{2,3}(t) = v_2(t) - v_3(t)$$

$$\dot{v}_1(t) = \lambda [v_1^d - v_1(t - \tau_1)] + \varepsilon_1(t)$$

$$\dot{v}_2(t) = \begin{cases} \lambda [v_2^d - v_2(t - \tau_2)] + \varepsilon_2(t) & , \Phi = 1 \text{ or } 2 \\ \gamma_1 v_2(t - \tau_2) + \gamma_2 v_1(t - \tau_2) + \gamma_3 \Delta x_{1,2}(t - \tau_2) + \gamma_4 & , \Phi = 3 \end{cases} \quad 3-27$$

$$\dot{v}_3(t) = a_3(t)$$

Note that in preparation for the execution of the merging maneuver (i.e., phases 1 and 2), the control goals are related to the distance between V1-V3 and V1-V2. As a result, it is more reasonable to consider  $\Delta x_{1,3}(t)$  and  $\Delta x_{2,3}(t)$  in the state-space vector. Therefore, considering  $U(t) = a_3(t)$  as the control input,  $X = [\Delta x_{1,3}(t) \Delta x_{2,3}(t) v_1(t) v_2(t) v_3(t)]^T$  as the state-space

vector,  $Y(t) = [\Delta x_{1,3}(t) \ v_3(t)]^T$  as the system output (for the first phase) and  $Y(t) = [\Delta x_{2,3}(t) \ v_3(t)]^T$  as the system outputs (for the second phase), the system model becomes:

$$\begin{aligned} \dot{X}(t) &= AX(t) + A_i^T X(t - \tau_2) + BU(t) + D_i(t), \quad i = \Phi \in \{1,2,3\} \\ Y(t) &= C_i X(t) \end{aligned} \quad 3-28$$

where

$$\begin{aligned} A &= \begin{bmatrix} 0 & 0 & 1 & 0 & -1 \\ 0 & 0 & 0 & 1 & -1 \\ 0 & 0 & 0 & 0 & 0 \\ 0 & 0 & 0 & 0 & 0 \\ 0 & 0 & 0 & 0 & 0 \end{bmatrix}, B = \begin{bmatrix} 0 \\ 0 \\ 0 \\ 0 \\ 1 \end{bmatrix}, A_1^T = A_2^T = \begin{bmatrix} 0 & 0 & 0 & 0 & 0 \\ 0 & 0 & 0 & 0 & 0 \\ 0 & 0 & -\lambda & 0 & 0 \\ 0 & 0 & 0 & -\lambda & 0 \\ 0 & 0 & 0 & 0 & 0 \end{bmatrix}, \\ A_3^T &= \begin{bmatrix} 0 & 0 & 0 & 0 & 0 \\ 0 & 0 & 0 & 0 & 0 \\ 0 & 0 & -\lambda & 0 & 0 \\ \gamma_3 & -\gamma_3 & \gamma_2 & \gamma_1 & 0 \\ 0 & 0 & 0 & 0 & 0 \end{bmatrix}, D_1(t) = D_2(t) = \begin{bmatrix} 0 \\ 0 \\ \lambda v_1^d + \varepsilon_2(t) \\ \lambda v_2^d + \varepsilon_2(t) \\ 0 \end{bmatrix}, \\ D_3(t) &= \begin{bmatrix} 0 \\ 0 \\ \lambda v_1^d + \varepsilon_2(t) \\ \gamma_4 \\ 0 \end{bmatrix}, C_1 = \begin{bmatrix} 1 & 0 & 0 & 0 & 0 \\ 0 & 0 & 0 & 0 & 1 \end{bmatrix}, \text{ and } C_2 = C_3 = \begin{bmatrix} 0 & 1 & 0 & 0 & 0 \\ 0 & 0 & 0 & 0 & 1 \end{bmatrix}. \end{aligned} \quad 3-29$$

For simplicity, in developing the controller, we can overlook the dynamics of V1 after merging, due to the fact that the dynamic of V3 is independent of V1.

In phase 1, V3 follows V1 at the same speed to ensure enough lead and lag gaps and avoid disturbing the mainstream flow. Accordingly, the desired control output is

$$Y_1^d(t) = \begin{bmatrix} g_{d,lag} + g_{d,lead} \\ v_1(t) \end{bmatrix} \quad 3-30$$

In phase 2, V3 follows V2 at the same speed with acceptable lag gap. The control target is

$$Y_2^d(t) = \begin{bmatrix} g_{d,lag} \\ v_2(t) \end{bmatrix} \quad 3-31$$

In the third phase, the target is that V3 follows V2 with a desired steady-state distance and at the same speed. Therefore, we have

$$Y_3^d(t) = \begin{bmatrix} g_{s2,3} \\ v_2(t) \end{bmatrix}$$

3-32

### 3.1.5 Type V: CAV-Conventional-Conventional

In this scenario, V2 and V3 are conventional vehicles and V1 is CAV (Figure 3-11). Similar to triplet type I, we assume that V3 follows V1 at the beginning. As V1 must always keep a safe distance from the immediate vehicle in front of it (VL1), it is considered as a real-time disturbance in the triplet modeling. To facilitate the merging maneuver, a three-phase movement is considered (Figure 3-12).

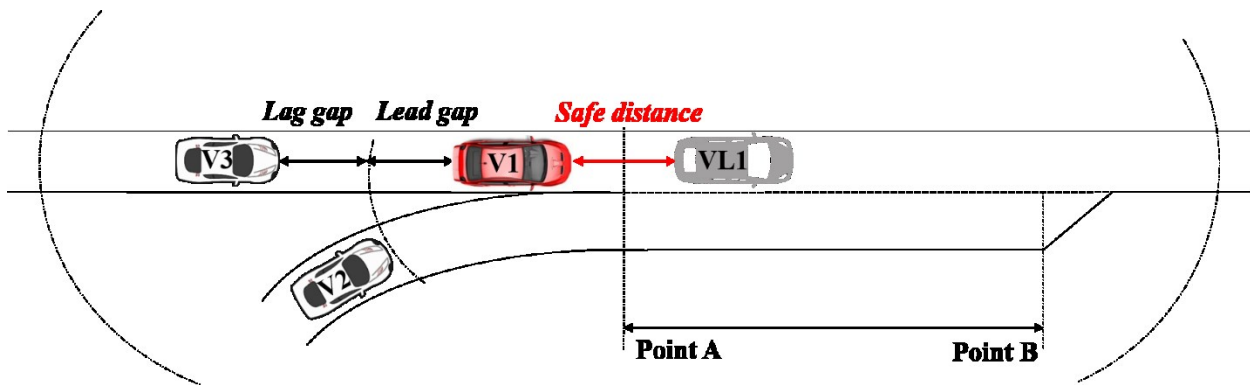


Figure 3-11. Sketch of triplet type V

#### 3.1.5.1 Phase 1 (merging vehicle approaches the acceleration lane)

In this phase, V1 keeps a certain longitudinal distance (lower than steady-state following distance between V3 and V1) from V2 to ensure that V2 reaches point A between V1 and V3. By doing so, all the vehicles will move at the same speed (i.e. the speed of V2), when V2 reaches point A in front of V3. Accordingly, V2 can be perceived by V3 and gain its cooperation for merging. In this study, we assume that if V2 moves further than V3 on the acceleration lane at the same speed, V3 will cooperate to allow V2 to merge in front of it. Moreover, in this phase, the car-following model (similar to equation 3-1) is used to simulate V3 and the free-flow model (similar to equation 3-18) is applied to simulate V2.



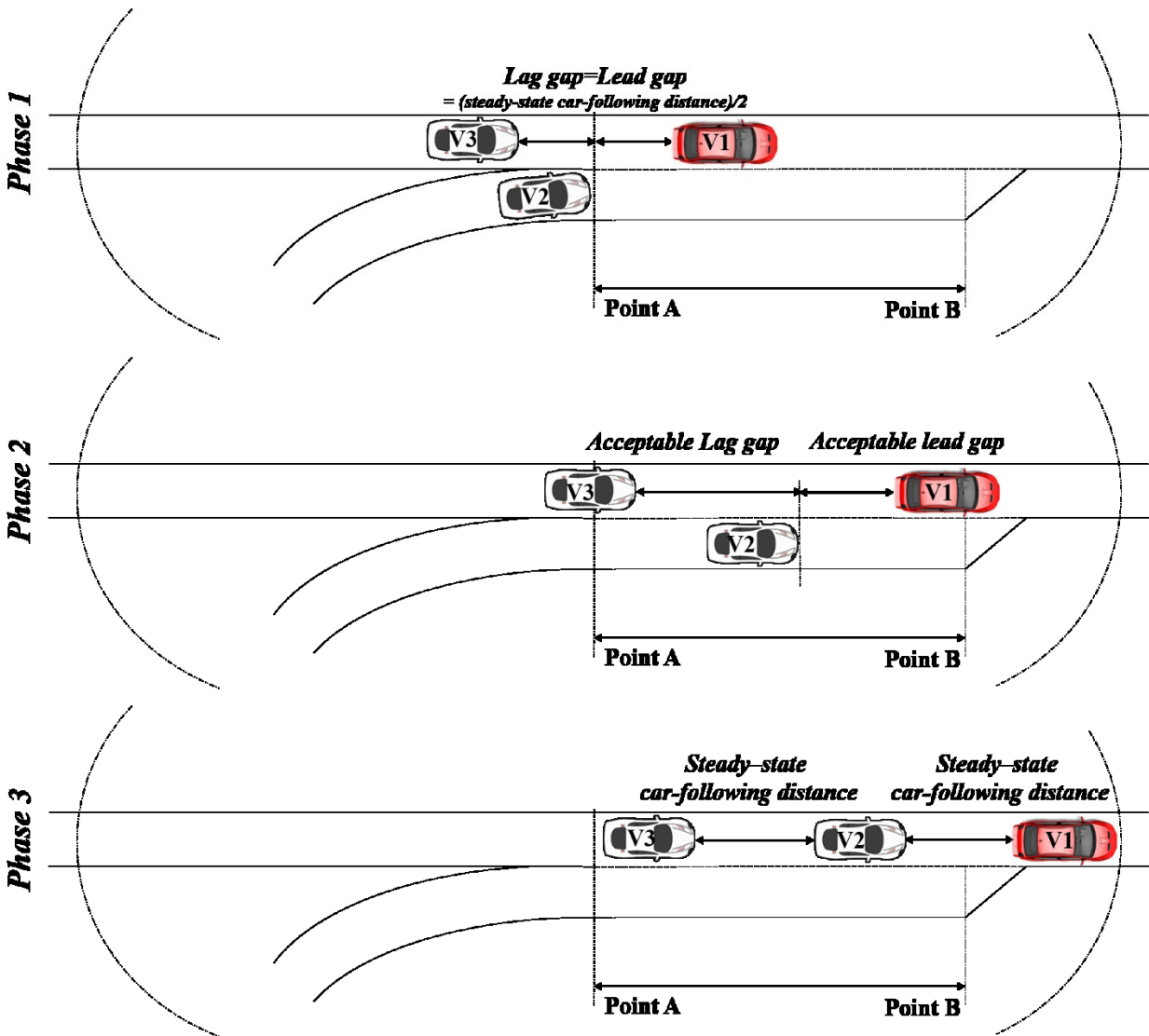


Figure 3-12. Movement phases of triplet type V

### 3.1.5.2 Phase 2 (merging vehicle on the acceleration lane)

In this phase, to cooperate for providing an acceptable lag gap for V2, V3 takes V2 as a new leader and starts following it by maintaining a certain headway distance (i.e., desired acceptable lag gap). To simulate V3, the car-following model similar to the one defined by equation 3-1), but with different model parameters is used. Meanwhile, the control goal of V1 is to provide the desired acceptable lead gap. At the same time, V2 moves at the desired free-flow speed of merging lane while waiting for the acceptable lead and lag gaps to merge. The motion of V2 is modeled using the free-flow model (similar to equation 3-18). V2 will continue moving on the acceleration lane and will merge if V3 and V1 provide enough lag and lead gaps, respectively.

### 3.1.5.3 Phase 3 (merging vehicle completes the maneuver)

After undertaking the merging maneuver, V2 will follow V1 using conventional car-following model and V1 will increase its speed to reach the desired speed of the mainstream. Moreover, V3 follows V2 with a closer distance than the desired acceptable lag gap.

### 3.1.5.4 The general model and control targets of triplet type V

Considering  $X = [\Delta x_{1,2}(t) \ \Delta x_{2,3}(t) \ v_1(t) \ v_2(t) \ v_3(t) \ \Delta x_{L1,1}(t)]^T$  as the state-space vector,  $U(t) = a_1(t)$  as the input vector, and  $Y(t) = [\Delta x_{1,2}(t) \ v_1(t)]^T$  (in the first and second phases) and  $Y(t) = [v_1(t)]^T$  (in the third phase) as the system outputs, the system model will be

$$\begin{aligned} \dot{X}(t) &= AX(t) + A_i^\tau X(t - \tau) + BU(t) + D_i(t), \quad i = \Phi \in \{1,2,3\} \\ Y(t) &= C_i X(t) \end{aligned} \quad 3-33$$

where

$$\begin{aligned} A &= \begin{bmatrix} 0 & 0 & 1 & -1 & 0 & 0 \\ 0 & 0 & 0 & 1 & -1 & 0 \\ 0 & 0 & 0 & 0 & 0 & 0 \\ 0 & 0 & 0 & 0 & 0 & 0 \\ 0 & 0 & 0 & 0 & 0 & 0 \\ 0 & 0 & -1 & 0 & 0 & 0 \end{bmatrix}, A_1^\tau = \begin{bmatrix} 0 & 0 & 0 & 0 & 0 & 0 \\ 0 & 0 & 0 & 0 & 0 & 0 \\ 0 & 0 & 0 & 0 & 0 & 0 \\ 0 & 0 & 0 & -\lambda & 0 & 0 \\ \gamma_3 & \gamma_3 & \gamma_2 & 0 & \gamma_1 & 0 \\ 0 & 0 & 0 & 0 & 0 & 0 \end{bmatrix}, \\ A_2^\tau &= \begin{bmatrix} 0 & 0 & 0 & 0 & 0 & 0 \\ 0 & 0 & 0 & 0 & 0 & 0 \\ 0 & 0 & 0 & 0 & 0 & 0 \\ 0 & 0 & 0 & -\lambda & 0 & 0 \\ 0 & \gamma_3 & 0 & \gamma_2 & \gamma_1 & 0 \\ 0 & 0 & 0 & 0 & 0 & 0 \end{bmatrix}, A_3^\tau = \begin{bmatrix} 0 & 0 & 0 & 0 & 0 & 0 \\ 0 & 0 & 0 & 0 & 0 & 0 \\ 0 & 0 & 0 & 0 & 0 & 0 \\ \gamma_3 & 0 & \gamma_2 & \gamma_1 & 0 & 0 \\ 0 & \gamma_3 & 0 & \gamma_2 & \gamma_1 & 0 \\ 0 & 0 & 0 & 0 & 0 & 0 \end{bmatrix}, B = \begin{bmatrix} 0 \\ 0 \\ 1 \\ 0 \\ 0 \\ 0 \end{bmatrix}, \\ D_1(t) &= \begin{bmatrix} 0 \\ 0 \\ 0 \\ \lambda v_2^d + \varepsilon_2(t) \\ \gamma_4 \\ v_{L1}(t) \end{bmatrix}, D_2(t) = \begin{bmatrix} 0 \\ 0 \\ 0 \\ \lambda v_2^d + \varepsilon_2(t) \\ \gamma_4' \\ v_{L1}(t) \end{bmatrix}, D_3(t) = \begin{bmatrix} 0 \\ 0 \\ 0 \\ \gamma_4 \\ \gamma_4 \\ v_{L1}(t) \end{bmatrix}, \\ C_1 = C_2 &= \begin{bmatrix} 1 & 0 & 0 & 0 & 0 & 0 \\ 0 & 0 & 1 & 0 & 0 & 0 \end{bmatrix}, C_3 = [0 \ 0 \ 1 \ 0 \ 0 \ 0]. \end{aligned} \quad 3-34$$

Similar to the first type, in the first phase, the control goal is to ensure that V2 reaches the merging area between the vehicles in the mainstream. Therefore, the control goal is

$$Y_1^d(t) = \begin{bmatrix} \Delta x_{1,3}(j)/2 \\ v_2(t) \end{bmatrix} \quad 3-35$$

In the second phase, V1 provides the desired acceptable lead gap for V2, and accordingly, we have

$$Y_2^d(t) = \begin{bmatrix} g_{d,lead} \\ v_2(t) \end{bmatrix} \quad 3-36$$

In the third phase, V2 has merged and the only goal is that V1 moves at the desired mainstream free-flow speed. Therefore, we have

$$Y_3^d = v_{main}^d \quad 3-37$$

### 3.1.6 Type VI: Conventional-CAV-Conventional

In this scenario, V1 (the lead vehicle) and V3 (the lag vehicle) are conventional vehicles and V2 (merging vehicle) is a CAV (Figure 3-13). Similar to the first scenario, it is assumed that V3 is following V1 using the car-following model defined by equation 3-1, while V1 moves using the free-flow model described by equation 3-18. To consider the safe distance of V2 from the immediate vehicle ahead, VL2 is taken into account in the triplet modeling as a real-time disturbance. To facilitate the merging maneuver, a two-phase strategy is developed (Figure 3-14).

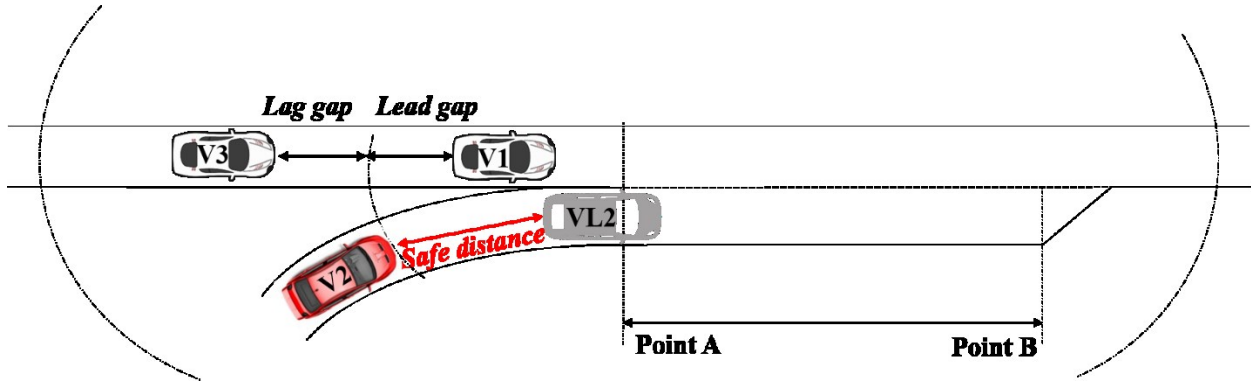


Figure 3-13. Sketch of triplet type VI

#### 3.1.6.1 Phase 1 (merging vehicle approaches the acceleration lane)

The best strategy for V2 is to reach the point A between V1-V3 at the same speed as V3. By doing so, V3 can perceive V2 and cooperate to provide enough lag gap. In this phase, V2 reaches point A between V1 and V3 at the same speed as V3.

#### 3.1.6.2 Phase 2 (merging vehicle on the acceleration lane)

V3 agrees to cooperate, and accordingly, it follows V2 (using the car-following model described by equation 3-1) with different model parameters) with a distance larger than usual (i.e., desired acceptable lag gap). At the same time, V2 provides enough lead gap from V1. Eventually, V2 faces the desired acceptable lead and lag gaps and merges.

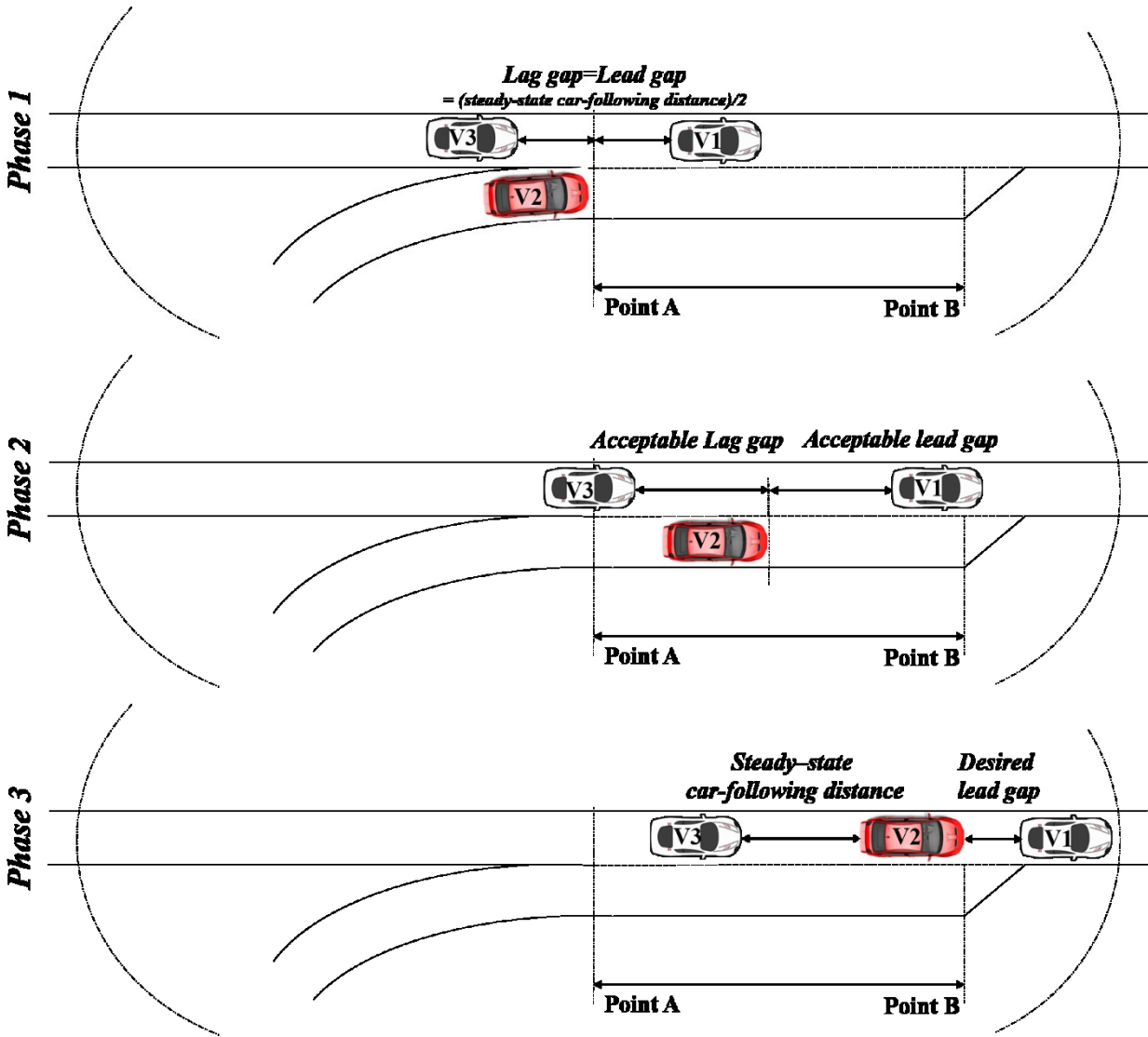


Figure 3-14. Movement phases of triplet type VI

### 3.1.6.3 Phase 3 (merging vehicle completes the maneuver)

After V2 undertakes the merging maneuver, it follows V1 with a certain distance (smaller than the desired acceptable lead gap). The movements of V1 and V3 can be modeled using the conventional car-following model (i.e., equation 3-1) and free-follow model (i.e., equation 3-18), respectively.

### 3.1.6.4 The general model and control targets of triplet type VI

Considering  $X = [\Delta x_{1,2}(t) \ \Delta x_{2,3}(t) \ v_1(t) \ v_2(t) \ v_3(t) \ \Delta x_{L,2,2}(t)]^T$  as the state-space vector,  $U(t) = a_2(t)$  as the input vector, and  $Y(t) = [\Delta x_{1,2}(t) \ v_2(t)]^T$  as the system output, the system model will be

$$\begin{aligned} \dot{X}(t) &= AX(t) + A_i^\tau X(t - \tau) + BU(t) + D_i(t), \quad i = \Phi \in \{1,2,3\} \\ Y(t) &= CX(t) \end{aligned} \quad 3-38$$

where

$$\begin{aligned} A &= \begin{bmatrix} 0 & 0 & 1 & -1 & 0 & 0 \\ 0 & 0 & 0 & 1 & -1 & 0 \\ 0 & 0 & 0 & 0 & 0 & 0 \\ 0 & 0 & 0 & 0 & 0 & 0 \\ 0 & 0 & 0 & 0 & 0 & 0 \\ 0 & 0 & 0 & -1 & 0 & 0 \end{bmatrix}, \quad A_1^\tau = \begin{bmatrix} 0 & 0 & 0 & 0 & 0 & 0 \\ 0 & 0 & 0 & 0 & 0 & 0 \\ 0 & 0 & -\lambda & 0 & 0 & 0 \\ 0 & 0 & 0 & 0 & 0 & 0 \\ \gamma_3 & \gamma_3 & \gamma_2 & 0 & \gamma_1 & 0 \\ 0 & 0 & 0 & 0 & 0 & 0 \end{bmatrix}, \\ A_2^\tau &= A_3^\tau = \begin{bmatrix} 0 & 0 & 0 & 0 & 0 & 0 \\ 0 & 0 & 0 & 0 & 0 & 0 \\ 0 & 0 & -\lambda & 0 & 0 & 0 \\ 0 & 0 & 0 & 0 & 0 & 0 \\ 0 & \gamma_3 & 0 & \gamma_2 & \gamma_1 & 0 \\ 0 & 0 & 0 & 0 & 0 & 0 \end{bmatrix}, \quad B = \begin{bmatrix} 0 \\ 0 \\ 0 \\ 1 \\ 0 \\ 0 \end{bmatrix}, \quad D_1(t) = D_3(t) = \begin{bmatrix} 0 \\ 0 \\ \lambda v_1^d + \varepsilon_2(t) \\ 0 \\ \gamma_4 \\ v_{L2}(t) \end{bmatrix}, \\ D_2(t) &= \begin{bmatrix} 0 \\ 0 \\ \lambda v_1^d + \varepsilon_2(t) \\ 0 \\ \gamma_4' \\ v_{L2}(t) \end{bmatrix}, \quad C = \begin{bmatrix} 1 & 0 & 0 & 0 & 0 & 0 \\ 0 & 0 & 0 & 1 & 0 & 0 \end{bmatrix}. \end{aligned} \quad 3-39$$

Similar to the first and fifth triplet types, the merging vehicle (V2) has to reach the merging area between the mainstream vehicles at the same speed in the phase 1.

$$Y_1^d(t) = \begin{bmatrix} \Delta x_{1,3}(t)/2 \\ v_1(t) \end{bmatrix} \quad 3-40$$

In phase 2, V2 provides enough lead gap from V1 while moving at the same speed.

$$Y_2^d(t) = \begin{bmatrix} g_{d,lead} \\ v_1(t) \end{bmatrix} \quad 3-41$$

In phase 3, V2 has merged and follows V1 with a smaller distance.

$$Y_3^d(t) = \begin{bmatrix} g_{s1,2} \\ v_1(t) \end{bmatrix} \quad 3-42$$

### 3.2 Model Predictive Control Design

The system models discussed in Section 3 are subjected to many changes, which may be caused by inaccurate prediction of conventional vehicle behaviors and motions, unexpected disturbances due to human-driven vehicles, delays caused by human-driven vehicles' reaction time, and further unexpected uncertainties. A model predictive control (MPC) scheme is employed to tackle the

uncertainties and delays in the system model while optimizing the defined cost functions and calculating the optimal control inputs for CAVs. Note that for each movement phase, the controller works independent of other movement phases. Generally, in each movement phase, by predicting the future values of state variables in a specific prediction horizon, MPC proposes the optimal control action for the current time to minimize a cost function [44], [95].

As described in the previous section, the system model for the six types of interacting vehicle triplets, in each phase of merging maneuver, are developed in the general form of

$$\begin{aligned} \dot{X}(t) &= AX(t) + A_\tau X(t - \tau) + BU(t) + D(t) \\ Y(t) &= CX(t) \end{aligned} \tag{3-43}$$

where the coefficient matrices may differ depending on the triplet type and the phase of movement, according to equations 3-9, 3-14, 3-28, 3-33, and 3-38. For example,  $A_\tau$  is zero in triplet type II, and  $D(t)$  is time-variant in all the triplet types except the first one. The general control goal is that the system output tracks different targets in each phase of merging maneuvers. Therefore, in this section, for the general model described by equation 3-43, a MPC is designed to obtain the optimal input trajectories for CAVs by minimizing a proposed general objective function. To be practically applicable, the system model and all computations are considered in discrete-time form.

### 3.2.1 Prediction model

To discretize the model described by equation 3-43, let  $t = j\Delta t$ , where  $j$  is the incremental time step. Therefore, we have

$$\begin{aligned} X(j+1) &= (I + \Delta t A)X(j) + \Delta t A_\tau X(j-k) + \Delta t BU(j) + \Delta t D(j) \\ Y(j) &= CX(j) \end{aligned} \tag{3-44}$$

where  $k = \text{round}(\tau/\Delta t)$ . For notation simplicity, let  $I + \Delta t A = A'$ ,  $\Delta t A_\tau = A'_\tau$ ,  $\Delta t B = B'$ , and  $\Delta t D(j) = D'(j)$ . Accordingly, we have

$$X(j+1) = A'X(j) + A'_\tau X(j-k) + B'U(j) + D'(j) \tag{3-45}$$

For triplet type I, we assume that  $D'(j)$  is constant over the prediction horizon, as it is a constant vector during all the movement phases. For the rest of triplets,  $D'(j)$  is related to the velocities of conventional vehicles (in the free-flow mode) which contain some uncertainties (i.e., a zero-mean normally distributed error  $\varepsilon_{1or2}$ ). In this case, the worst-case value for  $D'(j)$  is

considered over the prediction horizon, namely  $D'(j)$  is calculated using  $\pm 2\sigma_n$  instead of the uncertain value of  $\varepsilon_{1\text{or}2}$ . For instance, in the first phase of scenario IV, the worst-case scenario is that V1 and V2 move at a slower speed than expected, hence they create smaller gaps than anticipated. Therefore, by assuming the minimum speed values of V1 and V2 in  $D'(j)$  (using  $-2\sigma_n$  over the prediction horizon, we calculate the optimal control input. These assumptions allow us to formulate the prediction model as follows:

$$\begin{aligned} \hat{X}(j + l_x + 1 | j) &= A' \hat{X}(j + l_x | j) + A'_\tau \hat{X}(j - k + l_x | j) + B' U(j + l_x | j) + D'(j), \\ l_x &= 1, 2, 3, \dots, p_x \end{aligned} \quad 3-46$$

where  $p_x$  is the maximum value of the state prediction, i.e., the state prediction horizon. By defining the control increments over the control horizon ( $p_u$ ) and the vector of predicted outputs over prediction horizon ( $p_x$ ) as below, we have

$$\hat{Y}_j = \begin{bmatrix} \hat{Y}(j + 1 | j) \\ \vdots \\ \hat{Y}(j + p_x | j) \end{bmatrix}, \quad \mathbf{U}_j = \begin{bmatrix} U(j) \\ \vdots \\ U(j + p_u) \end{bmatrix} \quad 3-47$$

We also define a memory vector  $\bar{X}_j^k$  as follows:

$$\bar{X}_j^k = \begin{bmatrix} \hat{X}(j - k | j) \\ \vdots \\ \hat{X}(j - 1 | j) \end{bmatrix} \quad 3-48$$

where  $\hat{X}(j - k | j)$  to  $\hat{X}(j - 1 | j)$  represent a memory of the system caused by the reaction time of the conventional vehicle(s). By applying equation 3-46 recursively to the initial condition, the elements of the predicted output vector can be obtained, and the predictive model is

$$\hat{Y}_j = \mathbf{G}_1 X(j) + \mathbf{G}_2 \bar{X}_j^k + \mathbf{F}_1 \mathbf{U}_j + \mathbf{F}_2 D'(j) \quad 3-49$$

where the coefficient matrices  $\mathbf{G}_1$ ,  $\mathbf{G}_2$ ,  $\mathbf{F}_1$ , and  $\mathbf{F}_2$  are obtained in Appendix II. The target of MPC is that the system tracks the desired output ( $Y^d$ ) in each phase of each triplet type. Therefore, the quadratic objective function below is defined to track the outputs over the predicted horizon:

$$\begin{aligned} J(j) &= \frac{1}{2} \sum_{l_x=1}^{p_x} [\hat{Y}(j + l_x | j) - Y^d(j + l_x | j)]^T Q_{l_x} [\hat{Y}(j + l_x | j) - Y^d(j + l_x | j)] \\ &\quad + \frac{1}{2} \sum_{l_u=0}^{p_u} U(j + l_u)^T R_{l_u} U(j + l_u) \end{aligned} \quad 3-50$$

In this objective function, the first term represents the error between the actual and desired output, which is the main target of our control strategy. The second term is defined to avoid obtaining unrealistic large inputs values (acceleration).  $Q_{l_x}$  and  $R_{l_u}$  are symmetric positive semi-definite matrices. By simplifying the cost function using the prediction vectors, we have

$$J(j) = \frac{1}{2}(\hat{Y}_j - Y_d)^T Q(\hat{Y}_j - Y_d) + \frac{1}{2}U_j^T R U_j \quad 3-51$$

where  $Q$  and  $R$  are diagonal block matrices with  $Q_{l_x}$  and  $R_{l_u}$  on the main diagonal blocks. Note that adjusting  $Q$  and  $R$  help to adjust the convergence speed of these optimization process.

### 3.2.2 System constraints

The constraints are defined to address the safe distance between vehicles, the speed limits in different lanes, the maximum/minimum allowed acceleration, and the maximum/ minimum allowed jerk (i.e., the first derivative of acceleration). These constraints are defined assuming that the system is under normal operation condition, rather than the conditions including severe accelerations by the conventional vehicles which may lead to emergency braking by CAVs.

When the system switches from one phase to the next one, the system model and the desired control target may change accordingly. Consequently, high values of control input(s) and discontinuous derivative of the control input(s) may be created, which cause discomfort acceleration and jerk values for the passengers/driver. Therefore, we have considered different constraints on acceleration values and corresponding slew rate to limit the undesired responses when switching between different phases occurs. The constraints over the acceleration values are as below.

$$\underline{U} \leq U(j) \leq \bar{U} \quad 3-52$$

Generally, the upper-bar and lower-bar notations represent the lower and upper bounds of the variables, respectively. Furthermore, the slew rate constraint over the control inputs is

$$\underline{\Delta U} \leq \frac{(U(j) - U(j-1))}{\Delta t} \leq \bar{\Delta U} \quad 3-53$$

where  $\underline{\Delta U}$  and  $\bar{\Delta U}$  show the vector of lower and upper bounds for jerk, respectively. The limits over the speeds are as follows:

$$\underline{V} \leq [v_1(j) \quad v_2(j) \quad v_3(j)]^T \leq \bar{V} \quad 3-54$$



where  $\underline{V}$  and  $\overline{V}$  represent the vector of lower and upper bounds for speeds of vehicles, respectively. For the safe distance and not passing in a lane, we have

$$[\Delta x_{1,2}(j) \quad \Delta x_{2,3}(j) \quad \Delta x_{1,3}(j) \quad \Delta x_{L1,1}(j) \quad \Delta x_{L2,2}(j)]^T \geq \underline{\Delta X} \quad 3-55$$

where  $\underline{\Delta X}$  is the lower bound vector over the distances between vehicles. Note that all constraints are subject to change depending on the phase of the movement. For instance, the lag vehicle is not allowed to pass the lead vehicle in all the phases. At the same time, the merging vehicle can pass the lead and lag vehicles before merging, while it cannot pass them after accomplishing the merging maneuver. Furthermore,  $\Delta x_{L1,1}(j)$  and  $\Delta x_{L2,2}(j)$  are the distance of V1 and V2 (if they are CAVs) from their immediate vehicles ahead (if there is any), respectively. Therefore, they are also subject to change depending on different movement phases of different triplet types. Note that VL1 and VL2 may change as in actual traffic flow, they might accomplish merging maneuvers before the vehicles in the triplet and the order of vehicle changes.

### 3.2.3 Optimization solver

As all the constraint are convertible to the linear constraint over the control input, objective (i.e., equation 3-50) is a quadratic function imposed to linear constraints. Accordingly, we can use any quadratic programming (QP) techniques to obtain the optimal control input. As the suggested quadratic cost function is convex (proven in Appendix III), the solution found by QP methods (in each instant) is global optimum solution. In this study, in each phase of movement, the active-set method (as a QP method) are utilized to obtain the optimal control input for MPC problem (with known gradient value) in presence of the constraints [44], [95].

## 3.3 Simulations for Different Triplets of Vehicles

To evaluate the proposed modeling framework and the controllers, the simulations are implemented in MATLAB using a set of hypothetical merging scenarios for the aforementioned six types of triplets.

It is assumed that a higher level of traffic control determines the time of triplets' formation, when controllers trigger. For simulations, we assumed that controllers triggered 1 km before the lead vehicle of the triplet reaches the merging area (point  $A$ ), however in next chapter, we will show that the merging algorithms work efficiently even if the triplet formation happens 0.5 km before point  $A$ . Based on the previously developed car-following models [57], [70], [71], [97], in

this study, we assume that, for all the conventional vehicles, the reaction time equals 0.5 s,  $\alpha_1 = 0.5$ ,  $\alpha_2 = 0.125$ ,  $\beta_1 = 20$ , and  $\beta_2 = 1$ . Moreover, for the free-flow model, we assume  $\lambda=0.309$ , and  $\varepsilon = \mathcal{N}(0, \sigma)$  are a zero-mean normally distributed error with  $\sigma$  of 1.13. The car-following threshold distance is assumed to be 100 m. The desired speed on the mainstream and the merging lane are considered to be 100 km/h and 80 km/h, respectively. The acceptable lead and lag gaps are assumed to be 50 m; the desired steady-state distances (i.e., distances after merging) are assumed to be 30 m (between a lag CAV and a lead conventional vehicle) and 10 m (between CAVs); the length of the acceleration lane is 400 m; the origin is the beginning of the acceleration lane (point *A*); conventional vehicles can perceive the merging vehicles from 50 m before the origin. Additionally, the constraints are listed in Table 3-2. Note that the sampling time interval,  $p_x$ ,  $p_u$ , and  $p_d$  are considered to be 0.2 s, 50 steps (i.e., 10 s), 49 steps (i.e., 9.8 s), and 49 steps (i.e., 9.8 s), respectively. These values are chosen to make sure the computational time is reasonable for real-time application of the controllers, however, higher values can be use if a higher computational power is available. The coefficient matrices  $\mathbf{R}$  and  $\mathbf{Q}$  are chosen as diagonal matrices with the constant values of  $r$  and  $q$  on main diagonal. The values of  $r$  and  $q$  are fine-tuned by a try-and-error process. To solve the MPC optimization problem, the active-set method (with known gradient value) is utilized using *fmincon* solver in MATLAB. For the prediction horizon, the worst-case values of  $D'(j)$  are considered in (45). In this regard, the values of  $D'(j)$  is calculated using  $\pm 2\sigma_n$  instead of the uncertain value of  $\varepsilon_n$ . Although there is a 99.7 % probability that the value of a zero-mean normally distributed variable is within the boundary of  $\pm 3\sigma_n$ , as the boundary is too wide, we may risk the controller to be too conservative. Hence, we use a less conservative boundary (i.e.,  $\pm 2\sigma_n$ ) to calculate the worst-case values of  $D'(j)$ , as there is a 95.4 % probability that the aforementioned variable is within the boundary.

Note that VL1 and VL2 are also considered with the initial distances of 70 m ahead of V1 and V2 (if any of them are CAVs) to make sure that the generated optimal control sequences comply with the safe distance constraints.

To model the behavior of the conventional lag vehicle, when it cooperates to provide the acceptable lag gap for the merging vehicle, the car-following model is taken into account (e.g., the second movement phase of triplet type I, i.e., equation 3-6). In this case, we assumed  $\beta_1 = 40$  to model the larger distance allowed by the lag vehicle.

**Table 3-2- List of constraints**

Constraint type	Acceptable interval
Acceleration	$[-1.5, +1.5] m/s^2$
Speed on mainstream lane	$[40, 120] km/h$
Speed on merging lane	$[0, 120] km/h$
Safe distance between CAVs	2 m
Safe distance that CAVs should keep from conventional vehicles	5 m
Slew rate of control input in each iteration	$[-0.2, +0.2] m/s^3$
The vehicles are not allowed to overpass each other.	-

The simulations starting from reasonable initial values are conducted in MATLAB to demonstrate the effectiveness of the merging algorithms in Figure 3-15 to Figure 3-20. The vertical dot-dashed lines separate the movement phases.

### 3.3.1 *Triple type I: CAV-CAV-Conventional*

The simulation results of the proposed merging algorithm for triplet type I (Figure 3-15) show that, in the first phase, V1 and V2 cooperate to reach the merging area such that V2 locates in the middle of V1 and V3, that is,  $\Delta x_{1,2}(t) = \Delta x_{2,3}(t) = 23$  m. They also track the desired speed of the mainstream (i.e., 100 km/h) to avoid disturbing the mainstream flow. Phase 2 starts at  $t = 39.4$  s, when V3 (the conventional vehicle) perceives the merging vehicle and accept to cooperate by providing a larger lag distance while V1 and V2 cooperate to have acceptable lead gap (i.e., 50 m). When the accepted lead and lag gaps are provided, the merging is accomplished at  $t = 46$  s and phase 3 starts. In phase 3, V1 keeps the desired mainstream lane speed (i.e., 100 km/h); V2 keeps the desired steady-state distance (i.e., 10 m) from V1; and V3 keeps the conventional steady-state distance (i.e., 47 m), which we cannot control it. The cost function and CAVs' acceleration values for triplet type I are also illustrated in Figure 3-15. The cost function changes at the beginning of each scenario, as the system model and control goals change. Applying the optimal control inputs within the allowed boundary gradually minimizes the cost function without causing any constraints violation in the speed and gaps values.

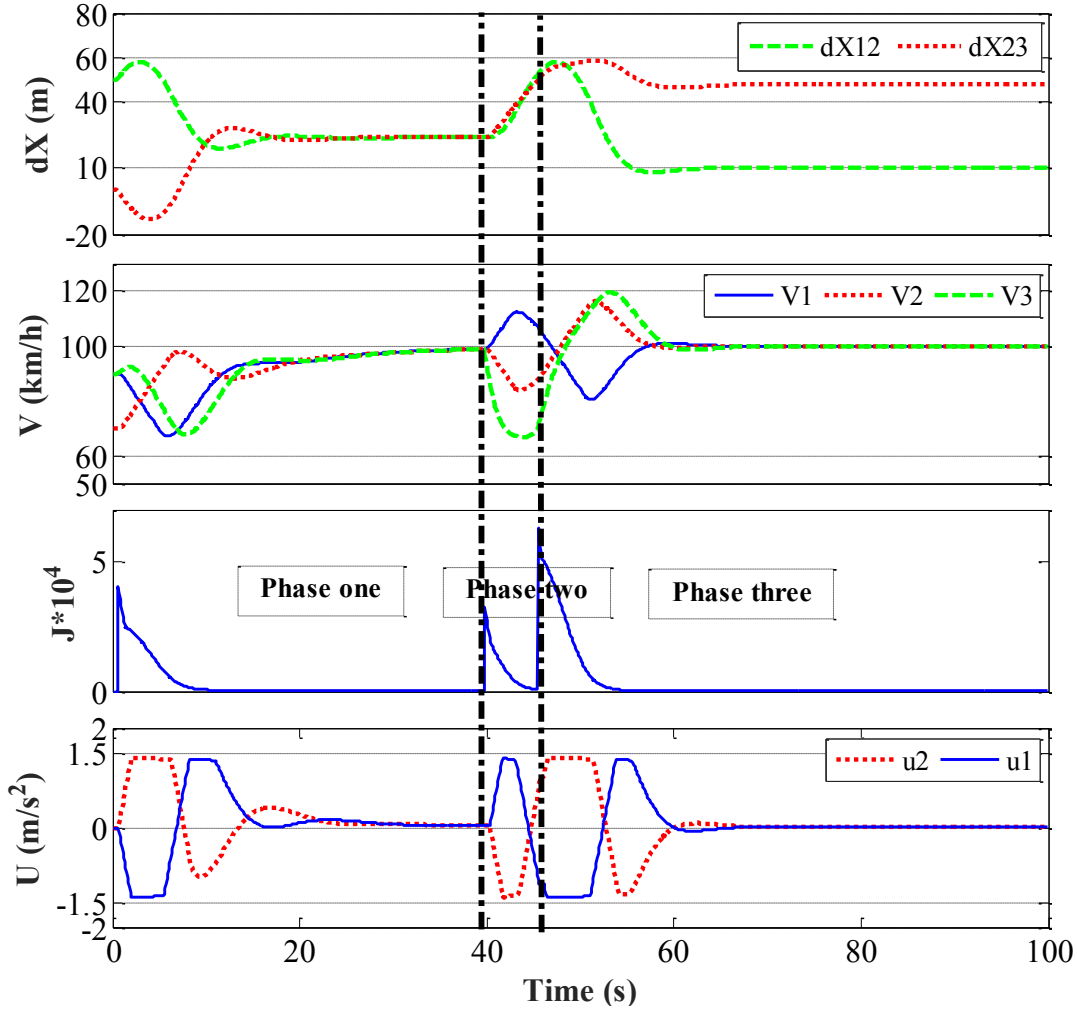


Figure 3-15. The result of merging scenario related to triplet type I

### 3.3.2 Triplet type II: Conventional-CAV-CAV

The two-phase merging algorithm of the triplet type II is depicted in Figure 3-16. It is shown that in the first phase, the CAVs ( $V_2$  and  $V_3$ ) cooperate to create acceptable lead and lag gaps (i.e., 50 m). This goal is achieved at  $t = 35$  s, and accordingly,  $V_2$  merges when it reaches point  $A$  at  $t = 47$  s. In phase 2,  $V_3$  follows  $V_2$  with 10 m distance (i.e., the steady-state distance between CAVs), and  $V_2$  follows  $V_1$  with 30 m distance (i.e., the steady-state distance between a lead conventional vehicle and a lag CAV). Note that since the values of lead and lag gaps are directly related to the uncertain movement of the conventional lead vehicle ( $V_1$ ), the system tracks the control goals with some uncertainties. For example,  $\Delta x_{1,2}(t)$  has a maximum  $\pm 1.25$  m error in tracing the desired lead and lag gaps in movement phase 1 and 2.

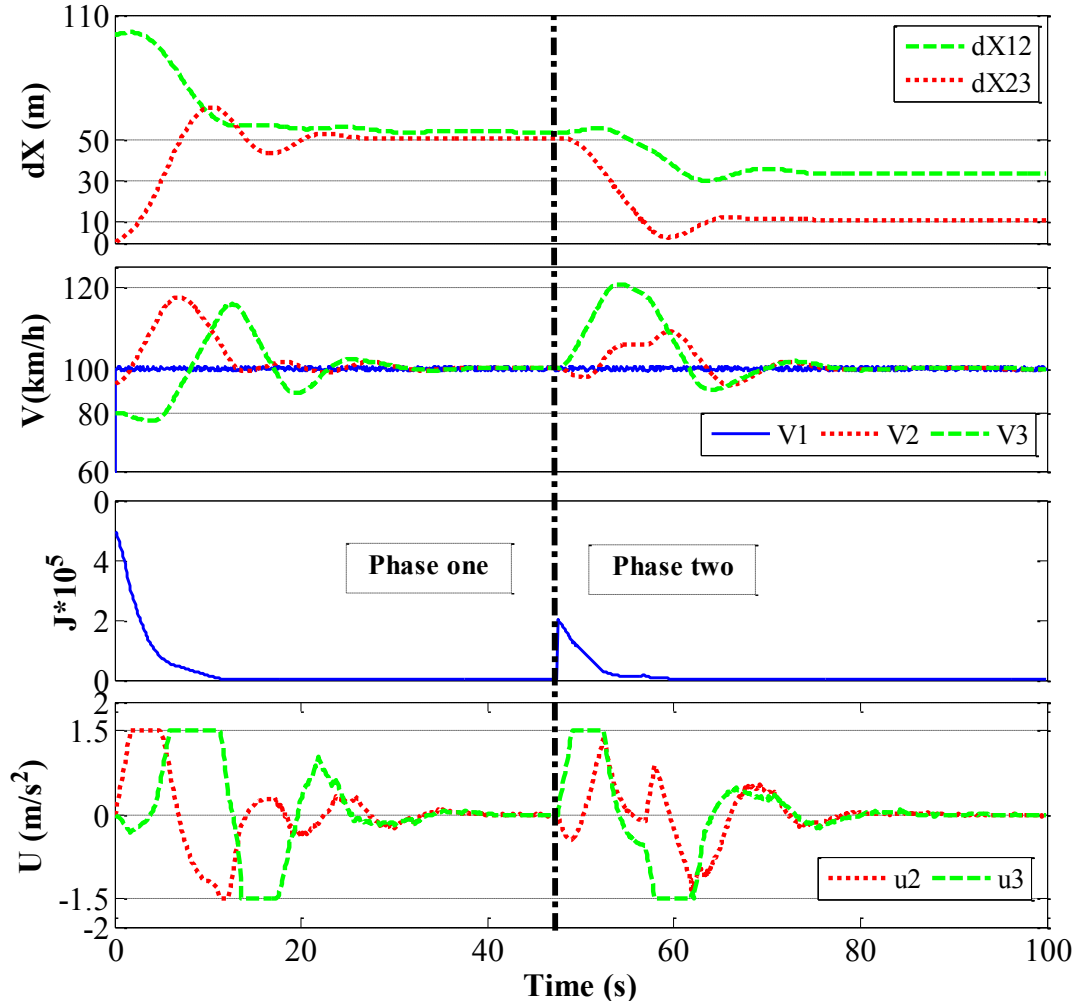


Figure 3-16. The result of merging scenario related to triplet type II

### 3.3.3 Triplet type III: CAV-Conventional-CAV

The two-phase merging algorithm of triplet type III is also simulated (Figure 3-17). In the first movement phase, V1 and V3 cooperate to have 50 m distance from the conventional merging vehicle (V2). Accordingly, the speed of CAVs (V1 and V3) will be the same as the speed of V2 (i. e., 80 km/h) after 20 s. Therefore, when V2 reaches point *A* at  $t = 39$  s, it merges between the two CAVs. In the second movement phase, V1 starts accelerating to reach the desired mainstream free-flow speed (i.e., 100 km/h). At the same time, V2 follows V1 with steady-state distance of 46 m and V3 follows V2 with the steady-state distance of 30 m. Note that in the first phase, the controller was able to reach its goals in 20 s, which makes the mainstream vehicles move at a speed 20 km/h lower than their own desired free-flow speed between  $t = 20$  s to  $t = 39$  s (i.e., it disturbs

the mainstream flow). Therefore, in this case, the controller can be engaged even when vehicles are closer than 1 km to point  $A$ .

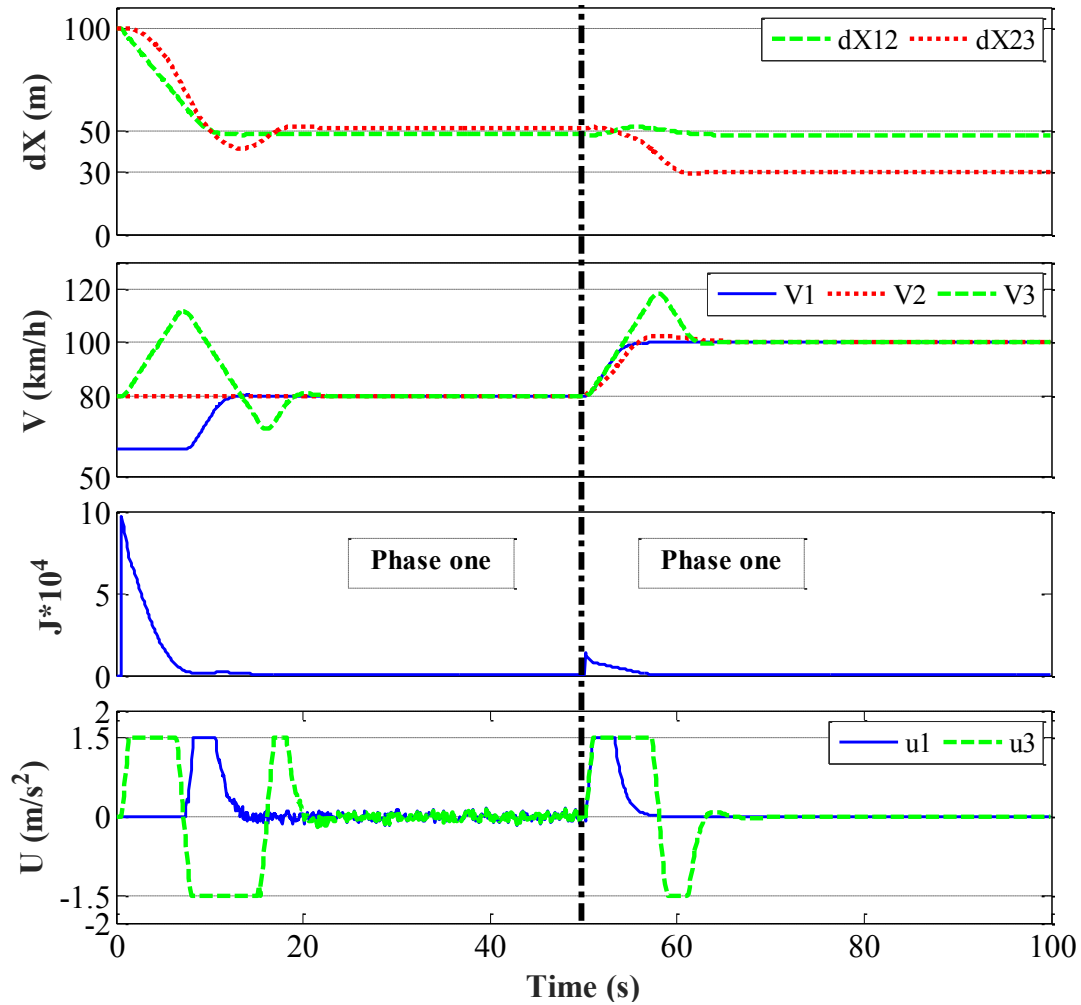


Figure 3-17. The result of merging scenario related to triplet type III

### 3.3.4 Triplet type IV: Conventional-Conventional-CAV

The simulation results of merging maneuver for triplet type IV is illustrated in Figure 3-18. In the first phase, the CAV ( $V_3$ ) keeps the desired distance of acceptable *lead+lag* gaps from  $V_1$  (i.e.,  $\Delta x_{1,3}(t) = 100$  m). At  $t = 28$  s,  $V_3$  is 100 m close to the point  $A$  and all the control goals are satisfied, and accordingly, it enters the second phase. In the second phase,  $V_3$  changes its leader to  $V_2$  and starts following it with the distance of desired acceptable lag gap (i.e., 50 m). At  $t = 43$  s,  $V_2$  reaches point  $A$  while the acceptable lead and lag gaps for it is provided, and accordingly,

it merges. In the third phase, V3 moves with 30 m steady-state distance from V2 and V2 is following its new leader (V1) with the steady-state distance of 43 m.

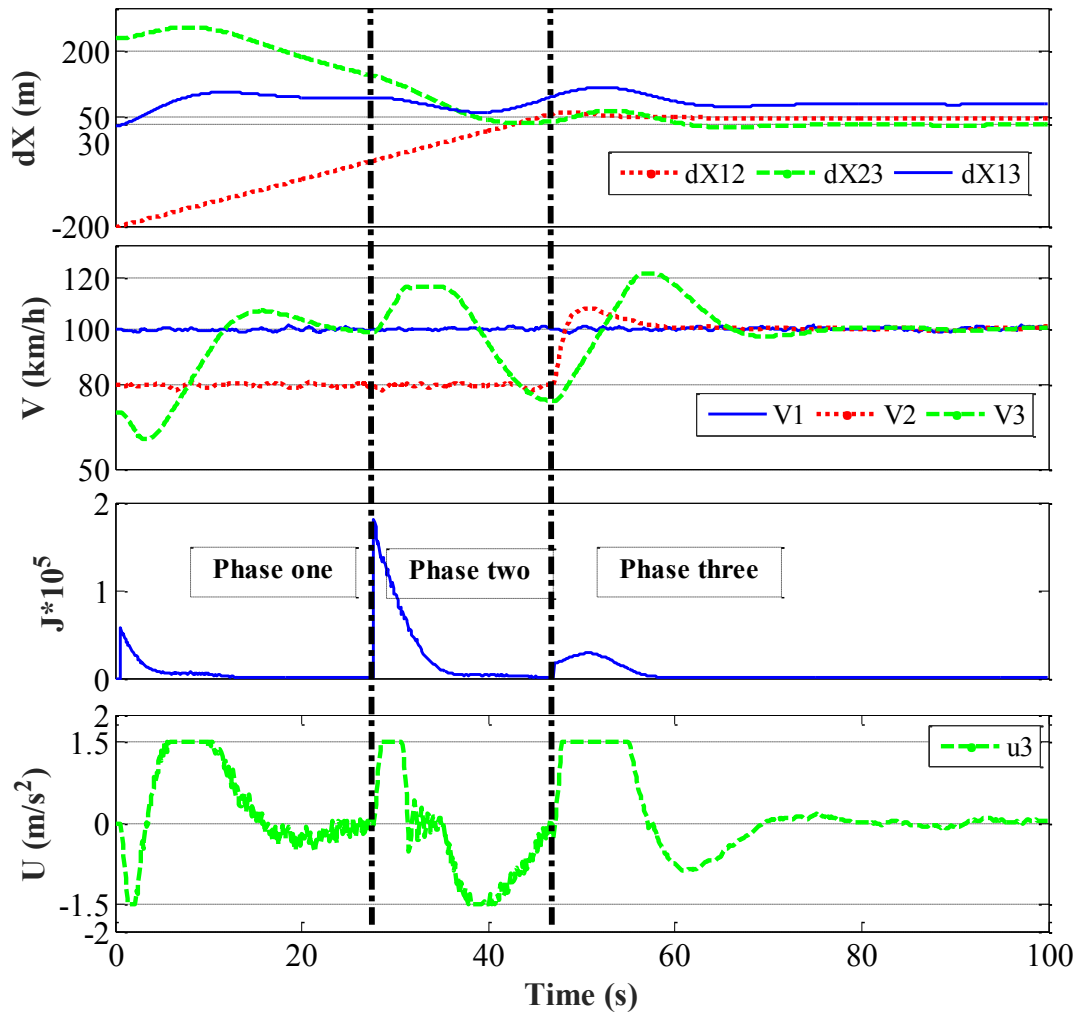


Figure 3-18. The result of merging scenario related to triplet type IV

### 3.3.5 Triplet type V: CAV-Conventional-Conventional

The three-phase merging scenario of triplet type V is illustrated in Figure 3-19, where only the lead vehicle (V1) is CAV. In the first movement phase, V1 decelerates to assure V2 reaches point A between V1-V3. However, the lower bound constraint on speed does not allow V1 to move at a speed lower than 60 km/h. Accordingly, V3 (the conventional lag vehicle) also decelerates after 0.5 s delay (because of its reaction time). As the lead gap reaches the constant value of 50 m at  $t = 32$  s, V1 and accordingly V3 move at the same speed as V2.

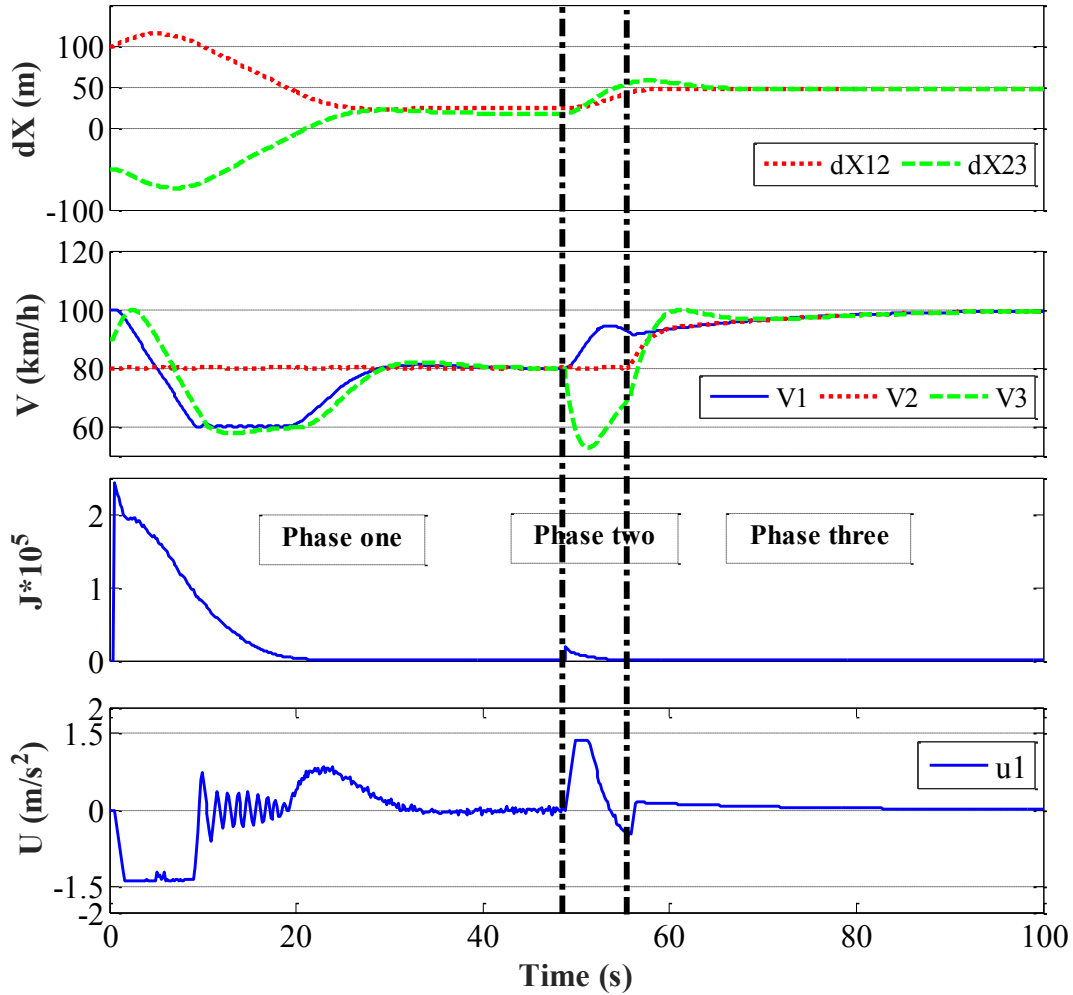


Figure 3-19. The result of merging scenario related to triplet type V

In phase 2, starting at  $t = 48$  s, when V2 reaches point  $A$ , V3 can perceive V2 and cooperate to provide enough lag gap. At the same time, V1 accelerates to provide the acceptable lead gap (50 m). Providing acceptable lead and lag gaps for V2 leads to completing the merging maneuver. In phase 3, V1 accelerates to reach the desire mainstream free-flow speed. Accordingly, V2 and V3 will move on the car-following mode. Note that in phase 2, we cannot control the speed violation of V3 (lower than 60 km/h), as the conventional vehicles cannot be controlled directly.

### 3.3.6 Triplet type VI: Conventional-CAV-Conventional

The three-phase merging algorithm related to triplet type VI is demonstrated in Figure 3-20, where only the merging vehicle (V2) is CAV.



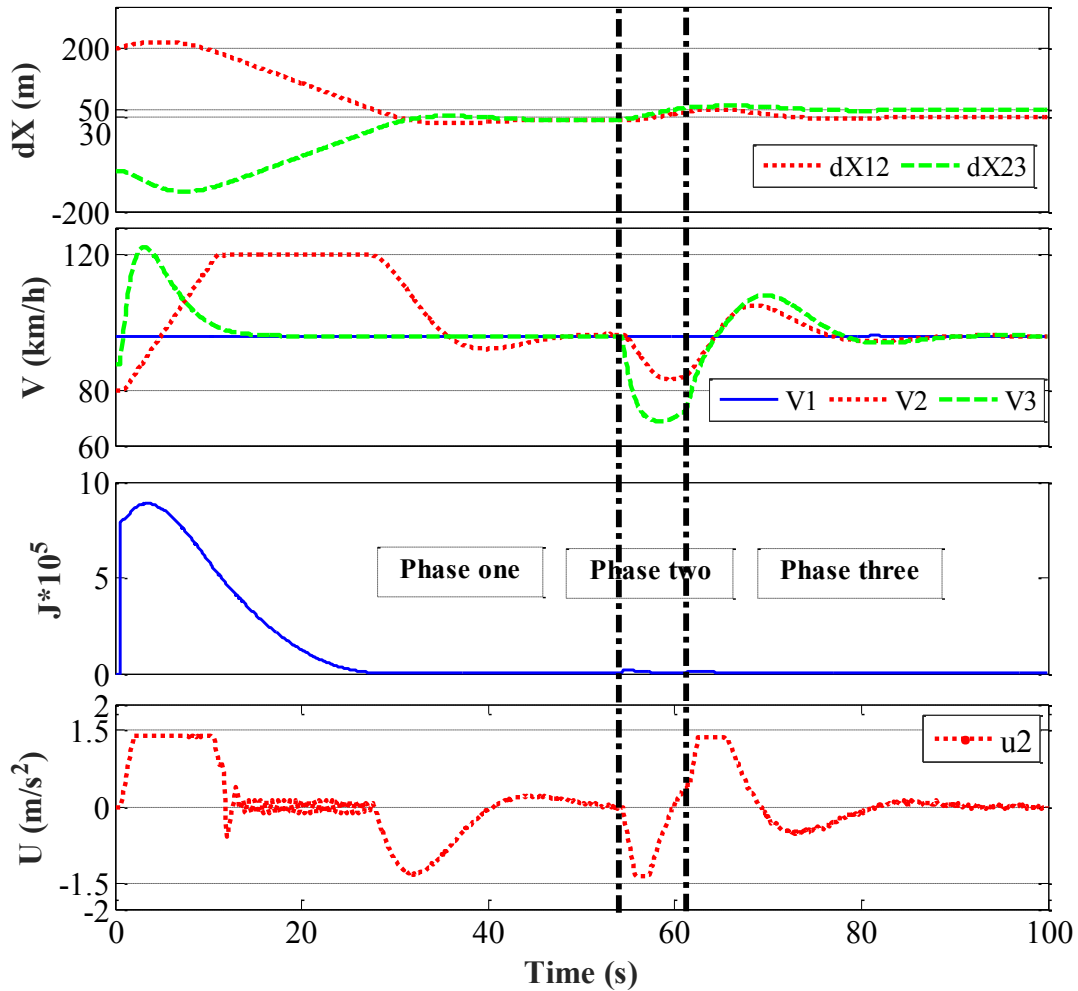


Figure 3-20. The result of merging scenario related to triplet type VI

In the first phase, V2 manages to reach point *A* between the two vehicles on the mainstream lane ( $\Delta x_{1,2}(t) = \Delta x_{2,3}(t) = 23$  m) at the same speed as V3 and V2. Providing these conditions at  $t = 52$  s, allows V3 to perceive V2 and cooperate with it. In the second phase, the acceptable lag gap is provided by V3 and the acceptable lead gap is achieved by controlling (decelerating) the CAV (V2), and hence, the merging is completed at  $t = 62$  s. In the third phase, vehicles move with their steady-state distances.

It is worth noting that since the uncertainty of the free-flow models is simulated by a uniformly-distributed error (using *rand* function in MATLAB), the controllers get affected by a negligible oscillation. However, the constraint over the jerk (the control input changes per second) guarantees that the oscillations of control inputs do not discomfort the driver/passengers. Furthermore, in some cases (Figure 3-19 and Figure 3-20), the CAV controller goal is to keep the

speed value within the allowed boundary, and at the same time, the CAV targets to obtain a smaller distance from other vehicles. Consequently, the controller has to repeatedly accelerate and decelerate (in small orders) to capture both goals. Applying constraint on jerk helps the controllers to assure that the acceleration values are still comfortable for the driver/passengers.

### 3.3.7 *Triplet type II with small headways*

The controllers are also effective when the acceptable lead and lag gaps are smaller than 50 m. As an example, in Figure 3-21, triplet type II is simulated assuming 5 m as the acceptable lead and lag gaps, as well as 3 m and 1 m as steady-state distances between conventional vehicles-CAV and CAV-CAV, respectively. The results show that the controller can still work efficiently (i.e., trace the targets accurately) with the smaller headway targets without requiring readjustment of the controller parameters.

### 3.3.8 *Initial Conditions*

To investigate that the proposed methodology can efficiently work independent of system initial conditions in certain boundaries, we test each of the six types of triplets using 25,000 samples of initial conditions. To choose the initial condition samples, first, we randomly select 250 samples between -1,000 and -500 as the starting position of V1 (i.e.,  $x_1(0)$ ). Then, for each sample of  $x_1(0)$ , we calculate the maximum and minimum values for both  $\Delta x_{1,2}(0)$  and  $\Delta x_{2,3}(0)$  such that V2 reaches the merging area (point A) within 50 m further than V1 and 50 m before V3 respectively, if all the vehicles travel at their desired speed (Figure 3-22). For each sample of  $x_1(0)$ , we randomly choose 100 samples between the minimum and maximum of  $\Delta x_{1,2}(0)$  and  $\Delta x_{2,3}(0)$  along with random samples for the velocities within the boundaries of desired speed  $\pm 15$  km/h. Therefore, we will have 25,000 samples of the initial values for the positions and velocities of the vehicles (Figure 3-23) by which we test the proposed merging algorithms. Moreover, VL1 and VL2 are considered with the initial distances of between 60 m to 120 m ahead of V1 and V2 respectively, if they are CAVs. Note that *rand* command in MATLAB is employed for uniformly sampling in the aforementioned sampling procedure.

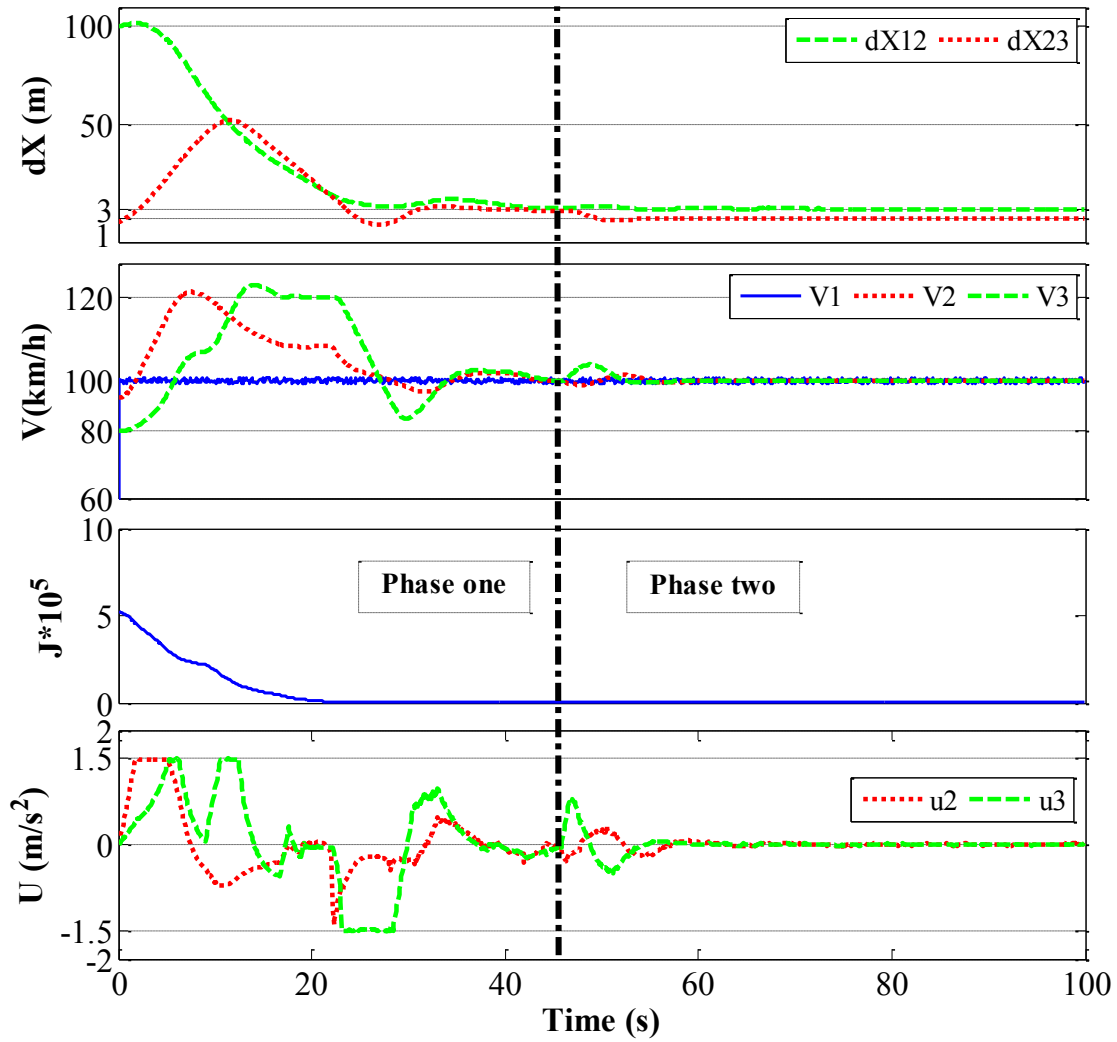


Figure 3-21. The result of merging scenario related to triplet type II, assuming smaller headways

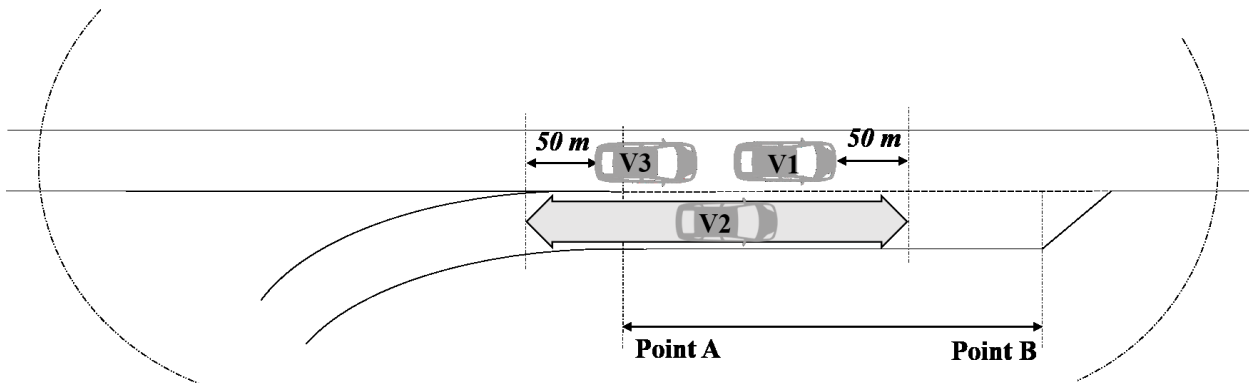


Figure 3-22. The hypothetical location of V2 with respect to V1 and V3

For all the tested initial condition values for the six triplet types, the merging vehicle (V2) was able to smoothly merge between the vehicles on the mainstream vehicles (V1 and V3) while

satisfying all the prescribed constraints. Moreover, MPC and the system model did not require readjusting the parameters for these simulation tests. Therefore, we conclude that the proposed methodology is able to work efficiently independent of the initial values for the reasonable initial conditions (i.e., within a predefined buffer) illustrated in Figure 3-22 and Figure 3-23.

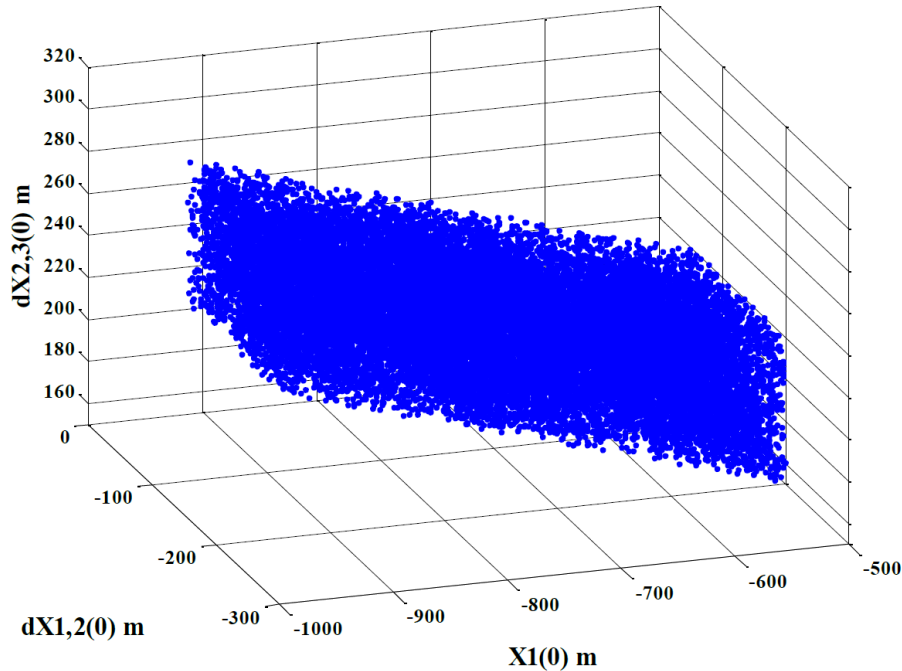


Figure 3-23. 25,000 samples of initial conditions of vehicles locations to test the merging algorithms

### 3.4 Concluding Remarks

This chapter proposes different cooperative merging algorithms for different triplets of vehicles composed of both conventional vehicles and CAVs. Considering a MIMO system model for each triplet allows capturing the uncertainties related to the conventional vehicles. Via cooperative consecutive movement phases for each triplet, the engaged CAVs manage to gain the cooperation of the conventional lag vehicle in the merging process when one is detected. Using the MPC scheme in each phase and applying the active-set method, optimal trajectories and commands for CAVs, engaged in the triplet, are calculated. The simulation results show that the proposed methodology leads to cooperative optimal merging maneuvers while satisfying the system constraints related to safety and comfort. By testing the algorithms for 25,000 different initial conditions within certain boundaries, it is also shown that the proposed merging algorithms work efficiently without a need to readjust the parameters of the controllers. This shows that we can

fine-tune the controllers for different boundaries of the initial values that are required by the triplet sequences determination method in the higher level of traffic control framework.

In the following chapter, all the proposed merging algorithms for different types of triplets of vehicles aggregated in a hierarchical traffic control framework for mixed traffic in the merging area. The methodology for triplets' formation and triplets' interactions are also discussed.

## Chapter 4: **MERGING UNDER CONTINUOUS TRAFFIC FLOW**

In this chapter, we present a triplets' formation algorithm to employ the cooperative merging algorithms developed in the previous chapter in continuous traffic flow. Moreover, different triplets' interactions will be discussed to determine a practical approach to model the conditions when two adjacent triplets interact with each other by sharing one vehicle. Handling the triplets' interactions and formations are the tasks for the higher level of the proposed traffic control framework. To simulate the continuous traffic flow under cooperative or non-cooperative (i.e., normal operation) operation conditions, different modes of behaviors and the transition conditions between them are also presented.

### **4.1 Merging Sequence and Triplets Formation Algorithm**

The higher level of proposed traffic control framework (Figure 4-1) is responsible for triplets' formation, which translates into determining the type of triplets and the time of formation for each merger. In this study, triplets' formation is based on two criteria, which are the prediction of vehicles' arrival time at the merging area and the priority rules in selecting different triplets.

The higher level of the framework has access to the locations and speeds of all the vehicles in the control zone using V2I communications and video surveillance. When a merging vehicle enters the control zone, the higher level of the framework predicts the arrival time of the merging vehicle to the merging area (point *A*) based on its current speed and location. Based on the predicted arrival time, the locations of the mainstream vehicles are also predicted to see where they will be located when the merger arrives at point *A*. Accordingly, the set of mainstream vehicles are determined that will meet the merging vehicle within a certain buffer (e.g.,  $\pm 50$  m, similar to the previous chapter). Therefore, the higher level of framework faces different choices for triplet formation. According to the control flexibility and the system uncertainties, different triplets will have different priorities to be chosen.

In this regard, the triplets with a higher number of CAVs are more flexible in providing acceptable lead and lag gaps for the merger, which makes them more of interests to be formed. Moreover, merging between two vehicles with a lag CAV (e.g., triplets type II and IV) is more preferred than merging between two vehicles with lag conventional vehicle (e.g., triplets type I

and VI), as in the latter case, the merging vehicle has to gain the cooperation of the lag conventional vehicle for providing an acceptable lag gap.

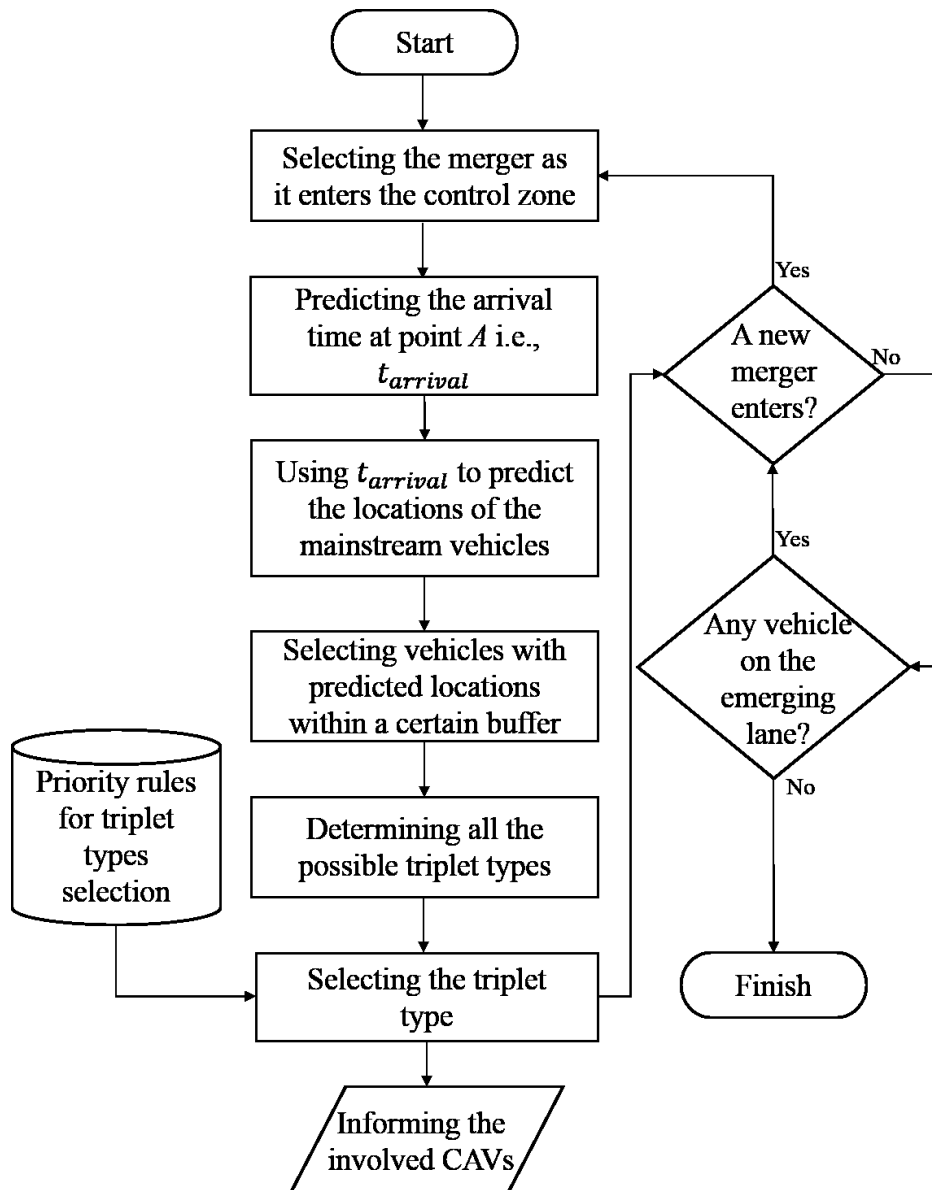


Figure 4-1. The higher level of control framework

While, in practice, an aggressive driver might deny to cooperate to create a lag gap for the merging vehicle, even though the assumptions of our suggested merging algorithm are met by the merger (i.e., reaching the merging area between the lag and lead vehicles, and moving at the same speed of mainstream vehicles). Therefore, the triplets with a lag CAV vehicle have priority to be formed

over the triplets with a lag conventional vehicle. Based on these arguments, the higher level of traffic control framework assigns priority to form different triplets based on the order below:

- 1- Triplets with two CAVs including a lag CAV: type II and III
- 2- Triplets with two CAVs and a lag conventional vehicle: type I
- 3- Triplets with only one CAV as the lag vehicle: type IV
- 4- Triplets with only one CAV as the merging vehicle: VI
- 5- Triplets with only one CAV as the lead vehicle: V

Note that among triplets type II and III, the earlier case has higher propriety as there are CAVs on both merging and mainstream lanes, which enables us to manage the available gaps on both lanes such that the sufficient lead and lag gaps are created.

#### 4.2 Triplets' Interactions

Generally, a light traffic condition on the merging lane leads to the large distance headways between the vehicles on the ramp (e.g., Figure 4-2), which allows the triplets of vehicles to accomplish the merging maneuver independently as they are formed far from each other. However, in the case of moderate or heavy traffic conditions on the merging lane, the consecutive triplets of vehicles may share a vehicle (e.g., Figure 4-3 and Figure 4-4).

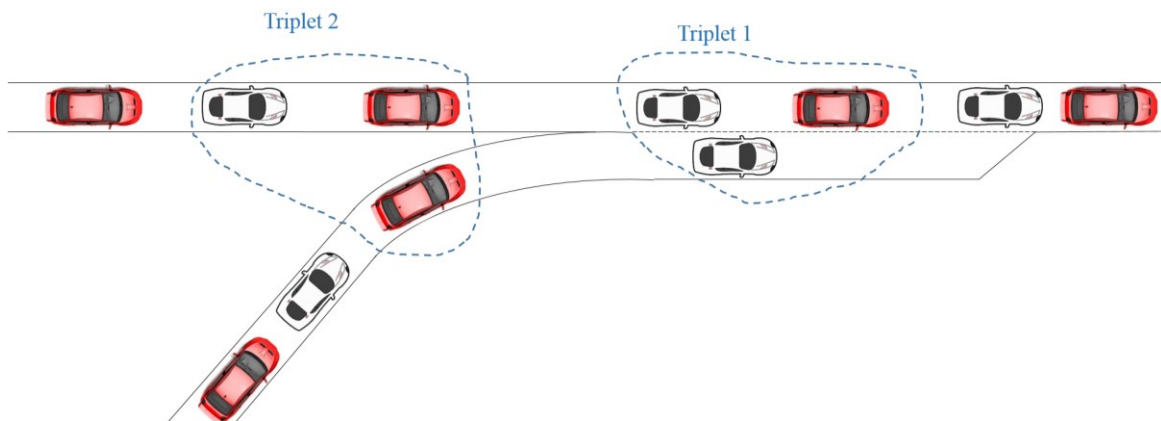


Figure 4-2. The light traffic leads to independency between triplets

As is shown in Figure 4-3, if the shared vehicle is a conventional vehicle (i.e., the cases in which the downstream triplet is one of the types I, V, VI, and VIII and the upstream triplet is one of types II, IV, VI, and VIII), the downstream triplet does not impact movement of the upstream triplet, and only a safe distance constraints in the merging lane is required. Therefore, controllers corresponding to each triplet can perform independently. On the other hand, if a CAV is shared



between two consecutive triplets of vehicles, i.e., when the downstream triplet is one of types II, III, IV, and VII, and the upstream triplet is of types I, III, V, and VII, (e.g., Figure 4-4), there is a concern that “according to which triplet the shared vehicle should generate the optimal control input.”

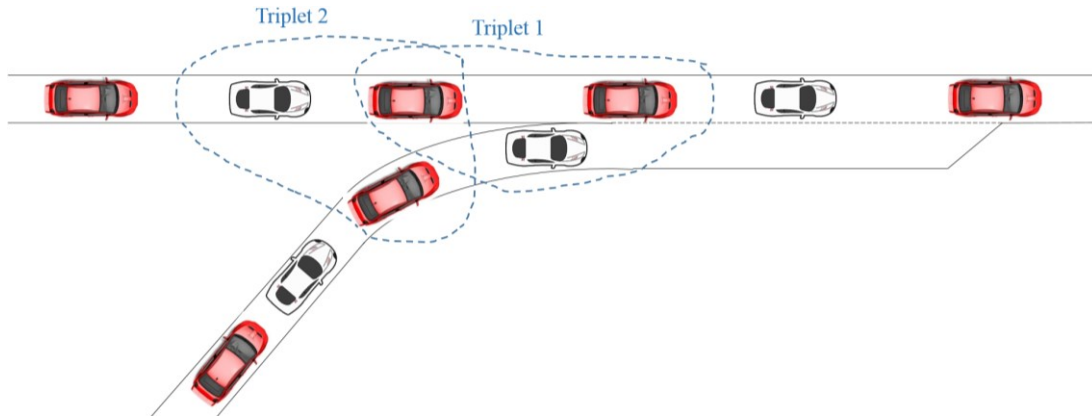


Figure 4-3. A shared conventional vehicle between two consecutive triplets

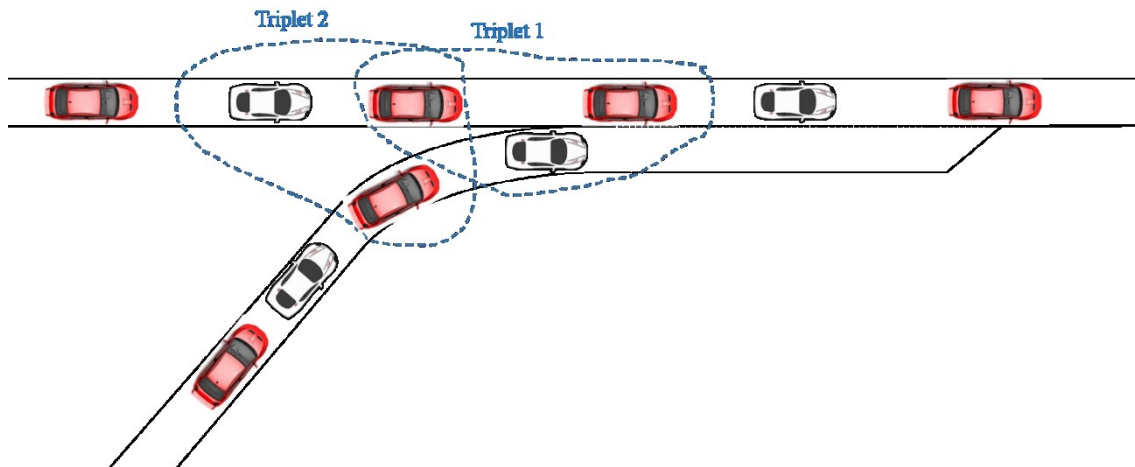



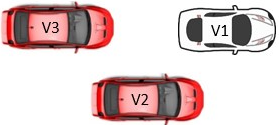
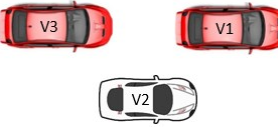
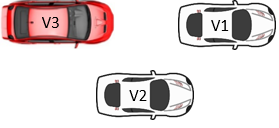
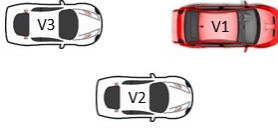


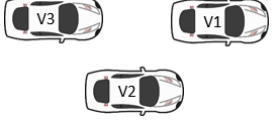
Figure 4-4. A shared CAV between two consecutive triplets

In this case, two approaches are proposed to calculate the optimal commands for the engaged CAVs. One approach is to model both triplets by a single united MIMO system and solve the problem cooperatively. Another approach is to consider the shared vehicle as a conventional vehicle from the upstream triplet’s point of view and calculate the control input for the shared vehicle in the downstream triplet. However, in the earlier approach, since the dimension of the optimizations problem increases, a higher computational power will be required, which mitigates the real-time application of the proposed framework. In the following, we elaborate on all the cases

which include a shared CAV between two consecutive triplets (i.e., upstream and downstream triplets) to see which approach is preferred.

Note that we also define two more triplet types where all three vehicles are CAV (triplet type VII) or conventional (triplet type VIII) to investigate their interactions with the six of types triplets the suggested in the previous chapter. Table 4-1 summarizes all types of triplets, where V1, V2, and V3 are the lead, lag, and merging vehicles, respectively; vehicles in red represent CAVs and vehicles in black and white show conventional vehicles—the gray vehicles with the question mark also represents either CAV or conventional vehicle through the text.

**Table 4-1- The symbolic layouts of different triplets of vehicles;**

Triplet Type I	Triplet Type II
	
Triplet Type III	Triplet Type IV
	
Triplet Type V	Triplet Type VI
	
Triplet Type VII	Triplet Type VIII
	

#### 4.2.1 *Upstream triplet is type I*

In the case where the upstream triplet is type I and the downstream triplet is one of types II, III, IV, and VII, as is shown in Figure 4-5. One approach is to consider both triplets' models (i.e. subsystems) as a single united MIMO model and solve the control problem for both at the same time cooperatively. Another approach is to consider the upstream triplet as a triplet type VI, where

the lead vehicle is conventional vehicle. Therefore, the controller of the downstream triplet calculates the optimal commands for the shared vehicle, while the upstream triplet only uses the position and speed of the shared vehicle as a disturbance in its model, i.e., upstream triplet takes V1 as a conventional vehicle.

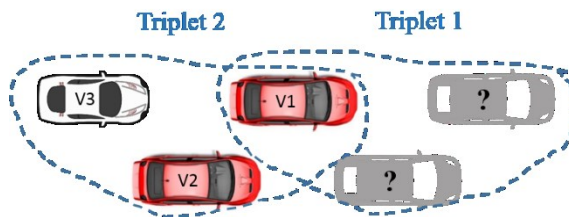


Figure 4-5. Sketch of two interacting triplets when the following one is type I

#### 4.2.2 *Upstream triplet is type V*

In this case as is shown in Figure 4-6, the downstream triplet can be one of types II, III, IV, and VII. As only one vehicle (i.e., lead vehicle) is CAV in the upstream triplet (i.e., type V), if we take it as a part of the downstream triplet, the upstream triplet will be disjointed, as there is no control over it. Moreover, we can model both triplets in a single united MIMO system and solve the control problem cooperatively. However, it may lead to a myopic control problem, as the goal for V1 in upstream triplet is different than the goal in triplet one. Especially, if the downstream vehicle has only one CAV (i.e., V1), the shared vehicle cannot satisfy two control goals at the same time. Therefore, in this case, we cannot form the upstream triplet, as the framework cannot not guarantee a safe and optimal merging algorithm.

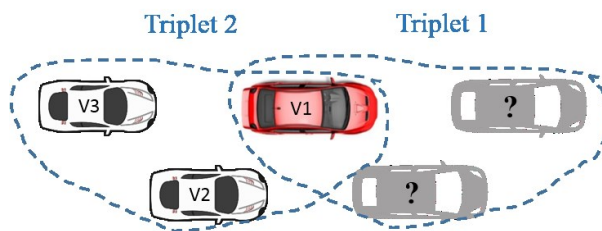


Figure 4-6. Sketch of two interacting triplets when the upstream triplet is type V

#### 4.2.3 *Upstream triplet is type III*

In this case (Figure 4-7), the downstream triplet can be one of types II, III, IV, and VII. One approach is to solve the problem using a cooperative control scheme by taking all the vehicles' model in a single united system. However, the lag vehicle in the upstream triplet is a CAV which might be shared with another upstream triplet. This may lead the cooperative control problem to

grow in dimension, and lead to a non-practical real-time solution. On the other hand, if the control command of the shared vehicle is calculated in the downstream triplet, the upstream triplet can consider its lead vehicle (V1) as a conventional vehicle and solve the control problem independently of the downstream triplet, i.e., to consider the upstream triplet as a type IV.

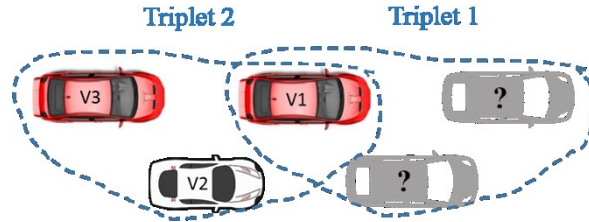


Figure 4-7. Sketch of two interacting triplets when the upstream one is type III

#### 4.2.4 *Upstream triplet is type VII*

In this case, all the vehicles of the upstream triplet are CAVs as is shown in Figure 4-8. The control goal is to create acceptable lead and lag gaps for the merging vehicle. In order to create sufficient lead and lag gaps, it is enough to have two CAVs on both lanes to control the locations of the vehicles on both lanes. Therefore, we will consider the upstream triplet as a type II, and the lead vehicle (V1) will be taken as an external disturbance. In other words, the control input of V1 is calculated in the downstream triplet and is sent to the upstream triplet using V2V communication. In general, all the triplets with type VII can be converted to a triplet type with one conventional vehicle based on the priority rule in selecting the triplets discussed in the previous subsection.

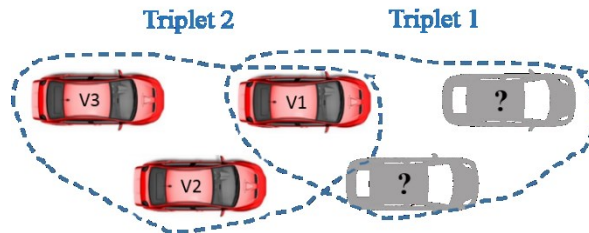


Figure 4-8. Sketch of two interacting triplets when the following one is type VII

### 4.3 Normally and Cooperatively Operated Traffic Conditions

In this subsection, we introduce different driving modes for conventional vehicles (i.e., car-following and free flow modes) and CAVs (cruise control and adaptive cruise control modes). An emergency stop mode is also defined to simulate the conditions that vehicles have to stop. The goal of this chapter is to evaluate the proposed cooperative traffic control framework (using triplets of vehicles) in comparison to the normally operated traffic condition (i.e., non-cooperative

condition). Therefore, the entire behaviors of conventional vehicles and CAVs are described under both normally and cooperatively operated conditions using different modes of driving.

#### 4.3.1 *Driving modes*

As we mentioned in chapter 2, in continuous traffic flow, conventional vehicles can have two modes of driving, i.e., car-following and free-flow modes (as mentioned in equations 2-1 and 2-5, respectively). We also introduce another driving mode, namely emergency brake mode, required for the merging conventional vehicles to stop at the end of the acceleration lane if needed. In other words, if a conventional vehicle, traveling on the acceleration lane, does not find sufficient lead and lag gaps to merge, it has to stop at the end of the acceleration lane while idling and waiting to merge. We used the car-following equation 2-1 to develop the emergency stop mode for conventional vehicles:

$$a(t) = \gamma_1 v(t - \tau) + \gamma_3 (Acc_{Length} - x(t - \tau)) + \gamma_4 \quad 4-1$$

where  $Acc_{Length}$  is the location of the end of the acceleration lane. This model shows that the vehicle follows a dummy stopped vehicle at the end of the acceleration lane.

Under normally operated traffic condition, we define two different modes of driving, which are cruise control (CC) and adaptive cruise control (ACC) modes. A CAV travels by CC mode to maintain the desired lane speed if it does not detect any vehicle in front within a certain distance (i.e., the space headway threshold). If a CAV senses a vehicle in front, closer than the space headway threshold, it will follow it by an ACC mode. CC and ACC modes are defined as follows using models described in equations 2-1 and 2-5, respectively.

$$a_n(t) = \lambda' [v_n^d - v_n(t)] \quad 4-2$$

$$a_n(t) = \gamma'_1 v_n(t) + \gamma'_2 v_{n-1}(t) + \gamma'_3 \Delta x_{n-1,n}(t) + \gamma'_4 \quad 4-3$$

where  $a_n$  represents the acceleration value for the  $n$ th CAV. Similar to the conventional vehicles, a merging CAV should be able to stop at the end of the acceleration lane if it cannot merge under normally or cooperatively operation traffic conditions. Therefore, an emergency stop mode is developed as below.

$$a(t) = \gamma'_1 v(t) + \gamma'_3 (Acc_{Length} - x(t)) + \gamma'_4 \quad 4-4$$

These models are similar to the conventional vehicles driving models, but without delay (i.e., zero reaction time) and uncertainty (i.e., zero tracking error). Moreover, the coefficients of the equations (i.e.,  $\lambda'$  and  $\gamma'$ 's) are adjusted such that CAVs can follow its leading vehicle closer, and can react faster, comparing to the conventional vehicles.

#### 4.3.2 *Vehicles behavior under normal operation condition*

The driving behavior of the vehicles under normal operation traffic condition (non-cooperative modes) is described in a flowchart shown in Figure 4-9. Based on this flowchart, the vehicles on the mainstream lane can only have two driving modes of car-following/ACC and free-flow/CC depending on their distance from the vehicle ahead. For the vehicles on the merging lane, we assumed that they will merge by order of arrival (i.e., first-arrived, first-merged). Therefore, if a vehicle on the merging lane perceives a vehicle in front, it will only check the distance headway to choose between car-following/ACC and free-flow/CC modes. While, if there is no vehicle in front, the merging vehicle will monitor the adjacent mainstream lane for sufficient lead and lag gaps (i.e., distance from the lead and lag vehicles) when it enters the acceleration lane. If it finds sufficient lead and lag gaps, it will merge. However, if it cannot find enough gap to merge, and it is close to the end of the acceleration lane (e.g., 50 meters), the emergency stop mode will be activated. The merging vehicle keeps waiting for an acceptable lead and lag gaps to merge, and when it merges, it will choose to travel on free-flow/CC mode or car-following/ACC mode depending on the distance from the lead vehicle.

Note that the acceptable lead and lag gaps are the gaps larger than the critical lead and lag gaps, which are described in equations 2-8 and 2-9, respectively, for the conventional vehicle during non-emergency stop modes. For CAVs, we consider a fixed critical lead and lag gaps values which are smaller comparing to the values corresponding to the conventional vehicles. During the emergency brake, the vehicle can still merge if it finds enough gap. However, the gap acceptance models described in equations 2-8 and 2-9 are not suitable as they result in a very large critical gaps values (from the order of 10,000 meters) for a stopped merging vehicle. Therefore, we also propose the model below for calculating the values of the critical gaps during the emergency stop mode.

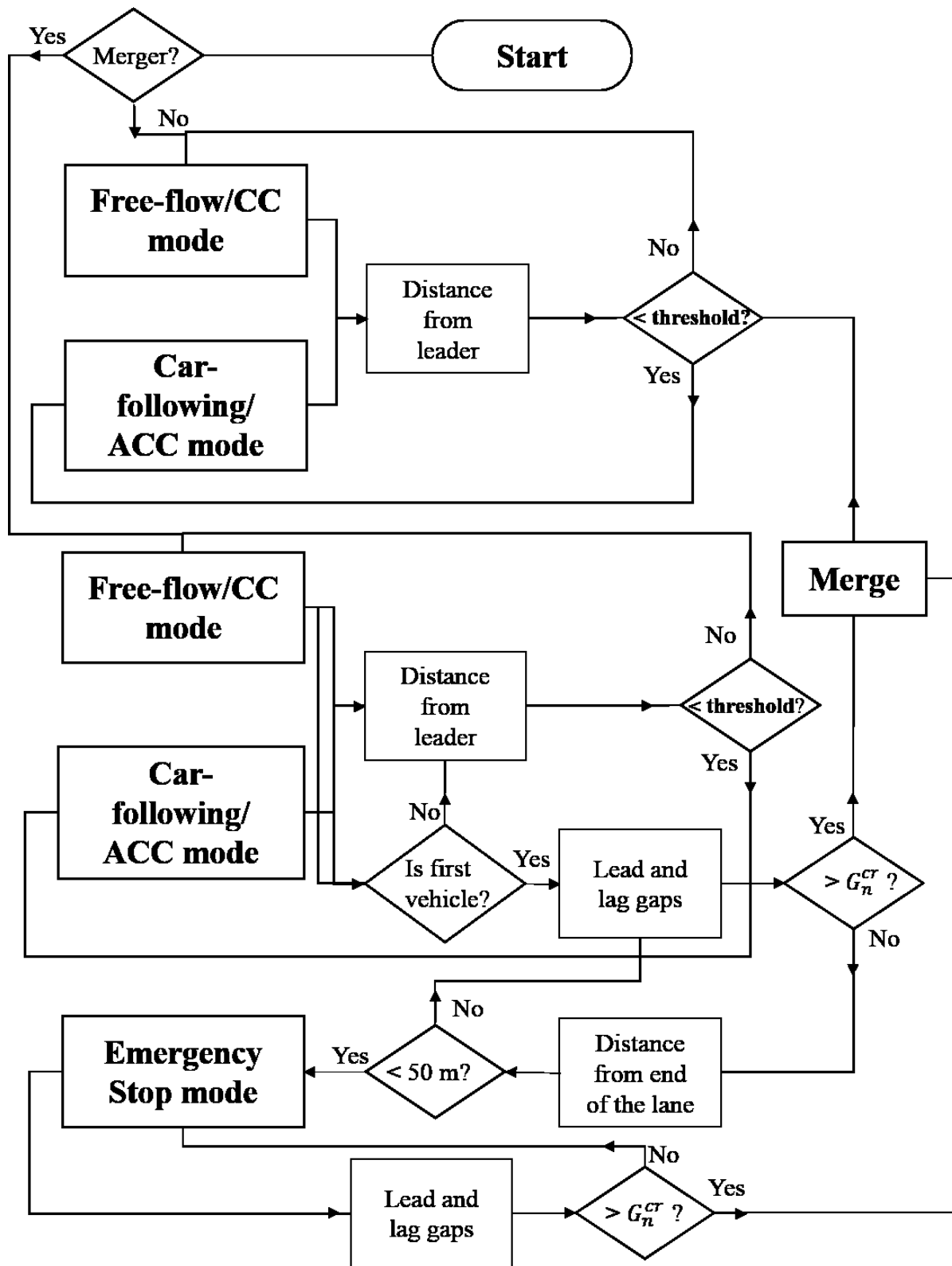


Figure 4-9. Flowchart for driving behaviors of vehicles under normal operation condition

$$G_n^{cr,lead/lag}(t) = G_{n,min}^{lead/lag} + \delta_n \Delta v_n^{lead/lag} \quad 4-5$$

where  $G_{n,min}^{lead/lag}$  represents the minimum acceptable lead or lag gaps,  $\Delta v_n^{lead/lag}$  is the speed difference between the lead/lag vehicle and the merging vehicle, and  $\delta_n$  is a coefficient to model the impact of the speed difference on the values of the critical gaps. Note that the model can be readjusted for different vehicle types (conventional and CAVs).

Moreover, the distance threshold to switch from the free-flow/CC mode to the car-following/ACC mode can be chosen randomly for different conventional drivers, while it is a fixed value for CAVs depending on the maximum range of its detector.

### 4.3.3 *Vehicles behavior under cooperative operation condition*

The cooperative operation condition refers to the condition where the suggested cooperative traffic control framework controls CAVs in the control zone in the merging area. The higher level of proposed framework monitors all the vehicles within the control zone. When a vehicle enters a control zone, the higher level of the traffic control framework investigates all the possible triplets' types that the merging vehicle can be a part of and assigns it to the triplet (if possible). As a triplet is formed, the higher level of the framework informs all the CAVs engaged to the triplet to activate the cooperative mode, as is described in a flowchart shown in Figure 4-10. In this flowchart, the non-cooperative driving mode refers to modes related to the normal operation condition (i.e., free-flow/CC and car-following/ACC modes), and cooperative driving mode is related to CAVs engaged in different triplet types. All the CAVs, which are not part of a triplet, as well as all the conventional vehicles move under normal operation traffic condition, as is described in Figure 4-9.

Note that, if there is more than one CAV in a triplet, the higher level of the framework will assign the control computation responsibility to only one of CAVs. Therefore, the optimal trajectories are calculated in the onboard processor of one of CAVs and then are sent to the other CAV(s) engaged in the triplet using V2V communication. The necessary information related to surrounding vehicles is also transferred by V2V or I2V communications. MPC is employed to calculate the optimal solution in each movement phase. Accomplishing each movement phase allows the triplet to switch to the next triplet, resulting in the accomplishment of the merging maneuver at the end of all the movement phases. As the vehicle merges, the triplet is disjointed and the engaged CAVs travel on the normal operation condition.



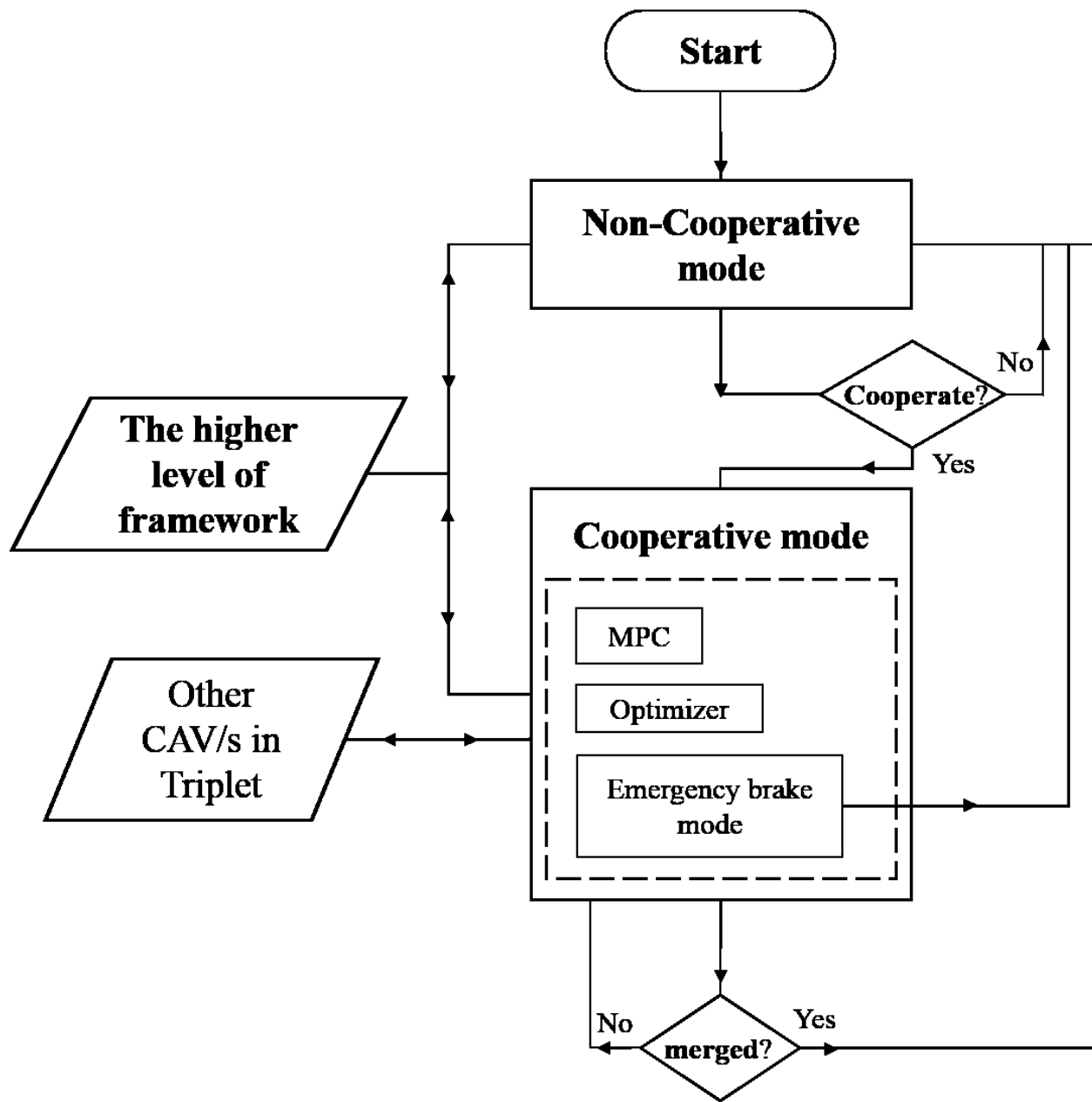


Figure 4-10. Flowchart for driving behaviors of CAVs able to cooperate for merging

Although the higher level of the traffic control framework forms the triplets such that the merging is guaranteed, the cooperative merging may fail because of uncertainties related to human-driven vehicles (i.e., conventional vehicles). Accordingly, if the merging vehicle (a conventional or CAV) cannot merge before a certain distance to the end of the acceleration lane (e.g., 50 meters), the emergency stop mode becomes activated and the triplet will be disjointed and CAVs will travel using non-cooperative driving modes.

#### 4.4 Simulations for Continuous Mixed-Traffic Flow

In order to evaluate the proposed cooperative traffic control framework, a simulator is developed in MATLAB, capable of simulating continuous mixed traffic flow in merging areas (as is shown in Figure 4-11, where red and blue colored vehicles are CAVs and conventional vehicles; the triangle shows the formed triplets and bold colors represent the activation of the triplet). Using our proposed cooperative framework, many simulation scenarios with different total flows, penetration rates of CAVs, and rates of ramp flow/ mainstream flow are conducted, and then, the results are compared to the results of non-cooperative (normal operation) traffic condition. For each simulation different random seeds are tested and the average of the results are calculated to account for the system's stochastic properties, caused by randomness in vehicle headways (i.e., time intervals that vehicles enter the system), initializing the type of vehicles (i.e., conventional vehicle or CAV), conventional vehicles' driving behavior (i.e., free-flow speed tracking randomness, different critical lead and lag gaps acceptance, and different threshold values to switch between driving modes for different drivers). To evaluate the effectiveness of the proposed traffic control framework in terms of operation, safety, and robustness, we consider three indicators, which are the travel time of the vehicles, the number of stopped vehicles at the end of the acceleration lane, as well as the number of failed triplets, respectively.

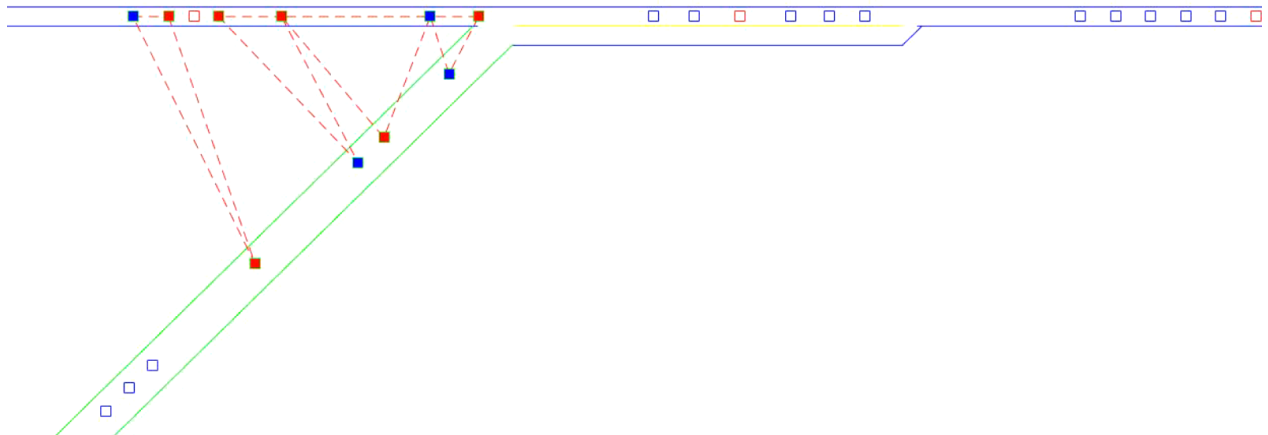


Figure 4-11. Developed simulator in MATLAB

The higher level of traffic control is responsible for triplets' formation using a certain buffer to predict the possible triplets that a merging vehicle may face. The controllers start working 500 meters before the merging vehicle reaches the merging area. We considered that the prediction buffer is  $\pm 75$  meters, and similar to chapter 3, many initial values are tested to fine-tune the

controllers. For generating the type of vehicles (i.e., conventional vehicle or CAV) in the highway, we used sampling from a binominal distribution by  $binornd(1, r)$  command in MATLAB, where  $r$  is the ratio of the number of CAVs to the number of conventional vehicles. For CAVs, the critical lead and lag gaps are considered as 20 and 30 meters, respectively, under CC and ACC modes, while twice these values are considered under emergency stop mode. For conventional vehicles, the critical lead and lag gaps are considered randomly using the models in equations 2-8 and 2-9, respectively, except for when the vehicles are in emergency stop mode, where we considered the model below.

$$G_n^{cr,lead}(t) = 30 + \Delta v_n^{lead} \quad 4-6$$

$$G_n^{cr,lag}(t) = 50 + 2\Delta v_n^{lag} \quad 4-7$$

The equations 4-6 and 4-7, are developed such that the lead and lag gaps are twice larger comparing to non-emergency stop modes when the speed difference between the merging vehicle and the mainstream vehicles is 15 km/h. Note that the control output targets are also modified based on the worst-case values of defined critical lead and lag gaps values, similar to chapter 3.

Moreover, it is assumed that CAVs can detect the leading vehicle closer than 150 meters and the threshold to switch from CC to ACC is 100 meters. For the conventional vehicles, we assumed that the threshold to switch from free-flow mode to car-following mode is a uniformly distributed random value between 80 and 90 meters, depending on different drivers. Note that all the other configurations of the system models are the same as chapter 3.

Some failure conditions are assumed for the triplets to be disjointed, avoiding disruption in the traffic flow, which are as follows:

- 1- Merging vehicle switches to emergency stop mode or it speeds drops to less than 10 km/h.
- 2- In triplet type III, a vehicle other than the triplet's merging vehicle merges between the lead and lag gap.
- 3- In triplet types I, IV, V, and VI, the conditions to switch from the first to the second movement phase are not provided and the merging vehicle is closer than 200 meters to the end of the acceleration lane.
- 4- In triplet types I, IV, V, and VI, the conditions to switch from the second to the third movement phase are not provided and the merging vehicle is closer than 100 meters to the end of the acceleration lane.

- 5- In triplet types II and III the conditions to switch from the first to the second movement phase are not provided and the merging vehicle is closer than 100 meters to the end of the acceleration lane.

To compare the performance of the proposed cooperative traffic control framework with the non-cooperative traffic condition, we simulate a merging area same as chapter 3 and consider 3 different total traffic flows (1,000, 1,500, and 2,000 veh/h) with 3 different ratios of ramp flow to mainstream flow (20%, 40%, and 50%) along with 5 different penetration rates of CAVs (10%, 20%, 40%, 60%, and 80%). These values are distinguished based on a try-and-error procedure to find some thresholds from which the traffic flow behavior (i.e., the average length of the formed platoons, the average travel time, and the number of stopped merging vehicles) starts changing. We run each scenario for 10 times with different random seeds for both cooperative and non-cooperative traffic conditions and the detailed results are collected in Table 4-2 for all 450 different scenarios. Note that 70 vehicles are considered on ramp lane, while the number of vehicles may change on the mainstream depending on different average headway. The average travel time is calculated for both lanes for vehicles which travel between the locations -700 m and +700m, i.e., the segment of the road that the control framework can have impact on the traffic.

Generally, when the penetration rate of CAV increases, the length of available gaps between vehicles increase, providing more opportunity for the merging vehicles to merge. This behavior can be explained by CAVs' ability to detect vehicles in a longer distance than conventional vehicles and to form more platoons and longer gaps. Moreover, as CAVs on the merging lane can accept smaller lead and lag gaps to merge, less merging vehicles will have to stop at the end of acceleration lane comparing to the traffic conditions with a lower penetration rate of CAVs.

The results show that when there is light traffic condition on both lanes (e.g., total flow equals 1,000 veh/h), the majority of the vehicles travel using the free flow driving mode on both lanes. Under this condition, sufficient gaps on the mainstream lane for the merging vehicles are created such that most of the vehicles can merge without stopping at the end of acceleration lane. Accordingly, the traffic control framework can be used mainly for improving the comfort of CAVs' occupants by providing smooth motion trajectories while having a little impact on the safety and travel time. For example, when we have a total flow of 1,000 veh/h, with 50% CAVs, and 50% of the traffic demand on the ramp (shown in Figure 4-12), less than three vehicles (2.6%)

were found stopping at the end of the merging lane out of a total of 70 simulated vehicles on the ramp. The deployment of the proposed traffic control framework for this scenario improves the traffic operations by reducing the average number of stopped vehicles to 0.8, which is a negligible value under normal operations. Even by increasing the flow rate of the mainstream lane to merging lane, the number of stopped vehicles does not significantly increase. Note that throughout the simulation results of this section, blue and red lines are related to conventional and CAVs, respectively; the origin for the location of the vehicles is the intersection of lines extended from the merging and mainstream lanes, i.e., point *A* in previous chapter; and the left and right directions of the merging areas are negative and positive signed values of the locations, respectively.

**Table 4-2- Results of 450 different scenarios for cooperative (shown by “Coop.”) and non-cooperative (shown by “Non-Coop.”) traffic conditions**

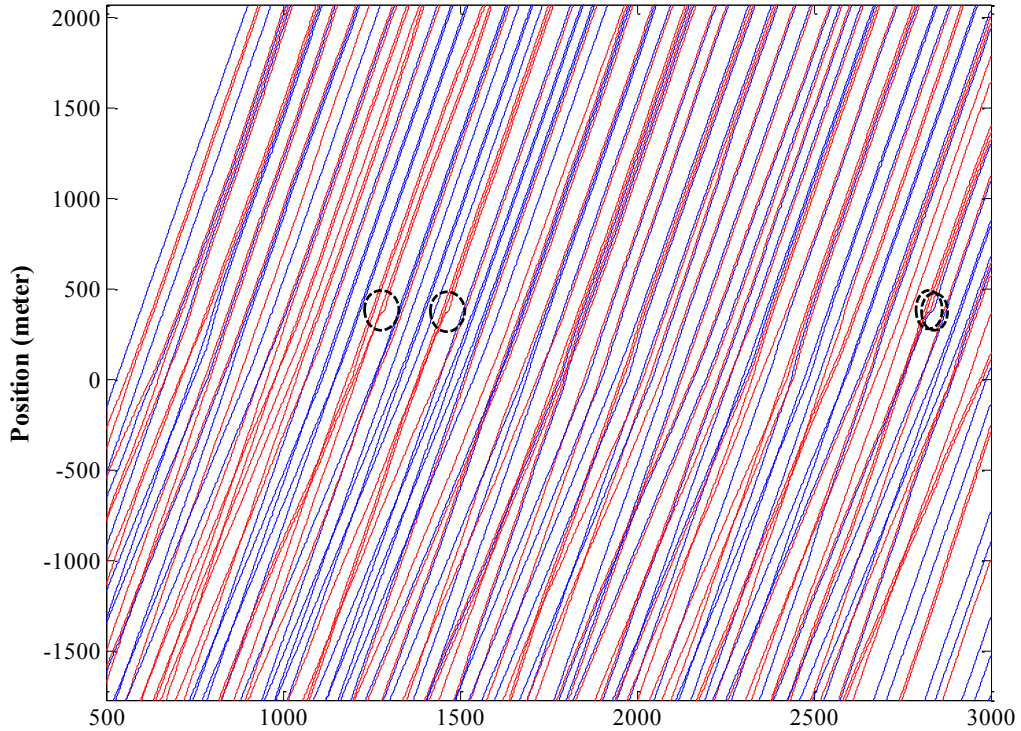
Total Flow (vehicle/h)	Ramp/ Mainstream Flow Ratio	CAVs/ Conventional Vehicles Ratio	Average Travel Time (s)				Average Stopped Vehicles (out of 70 vehicles)		Average Failed triplets
			Ramp		Mainstream		Coop.	Non- Coop.	Coop.
			Coop.	Non- Coop.	Coop.	Non- Coop.			
1,000	20%	10%	55.8	58.2	50.0	50.0	2.7	4.6	0.0
		20%	54.7	57.5	49.8	50.5	1.3	3.6	0.0
		50%	53.5	55.3	49.9	50.1	1.1	1.3	0.0
		60%	52.3	54.9	50.1	49.9	0.0	0.1	0.0
		80%	52.2	54.8	50.0	49.6	0.0	0.0	0.0
	35%	10%	54.8	56.1	50.1	50.0	2.1	7.3	0.0
		20%	53.2	55.8	49.8	49.8	2.3	3.8	0.0
		50%	53.5	55.2	50.4	50.0	2.4	5.1	0.0
		60%	53.1	54.0	50.0	50.1	0.0	1.1	0.0
		80%	53.1	53.8	49.9	49.7	0.0	0.0	0.0
	50%	10%	55.6	57.3	50.0	51.1	5.4	14.0	0.0
		20%	54.5	57.0	50.3	50.2	1.1	9.1	0.0
		50%	54.4	56.6	50.6	49.9	0.8	2.6	0.0
		60%	54.5	56.1	49.9	49.6	0.0	0.9	0.0
		80%	54.1	55.2	50.1	49.7	0.0	0.3	0.0

Total Flow (vehicle/h)	Ramp/ Mainstream Flow Ratio	CAVs/ Conventional Vehicles Ratio	Average Travel Time (s)				Average Stopped Vehicles (out of 70 vehicles)		Average Failed triplets
			Ramp		Mainstream		Coop.	Non- Coop.	Coop.
			Coop.	Non- Coop.	Coop.	Non- Coop.			
1500	20%	10%	55.0	59.8	50.0	50.5	8.8	15.4	0.0
		20%	54.2	58.0	50.6	50.3	4.3	13.8	0.0
		50%	53.5	57.2	50.5	50.2	1.8	10.8	0.0
		60%	53.4	56.9	50.6	50.4	0.6	10.0	0.0
		80%	53.0	56.0	50.6	50.3	0.1	9.4	0.0
	35%	10%	56.8	62.3	49.9	50.2	18.2	30.1	0.0
		20%	53.3	59.7	49.1	49.9	4.6	23.5	0.0
		50%	52.6	57.3	50.4	50.0	2.8	18.0	0.0
		60%	52.5	56.0	49.6	49.5	2.5	11.2	0.1
		80%	52.7	55.2	49.5	49.7	2.0	8.4	0.2
	50%	10%	57.3	76.7	49.8	50.4	17.0	37.7	0.1
		20%	54.5	67.4	49.4	49.9	7.4	19.9	0.1
		50%	53.0	56.6	49.8	49.7	3.1	9.5	0.2
		60%	52.8	55.7	49.7	49.6	1.9	4.1	0.3
		80%	52.6	55.0	48.7	49.7	1.1	3.8	0.4
2000	20%	10%	65.3	86.1	50.2	52.6	23.6	47.4	1.0
		20%	64.3	84.1	52.3	51.2	18.2	42.7	1.3
		50%	61.1	83.6	55.3	53.4	11.8	40.2	2.8
		60%	68.1	74.7	62.3	49.9	18.2	31.4	8.5
		80%	59.2	67.8	80.3	49.9	22.4	26.6	10.1
	35%	10%	137.6	200.3	51.2	50.5	48.2	69.1	3.4
		20%	81.3	120.2	51.3	50.9	36.1	52.2	5.3
		50%	55.4	60.2	50.4	50.0	12.4	38.5	5.5
		60%	55.4	68.3	50.9	50.2	9.7	35.1	6.0
		80%	55.5	60.1	51.8	50.0	7.2	32.6	6.8
	50%	10%	120.6	183.5	54.0	50.5	38.0	67.5	1.5
		20%	78.7	128.7	52.3	50.1	29.9	64.9	2.2
		50%	65.3	111.8	49.3	49.6	25.3	61.4	3.1
		60%	63.9	102.9	49.9	49.9	26.5	57.3	6.7
		80%	62.7	98.8	48.8	48.6	29.2	54.1	7.6

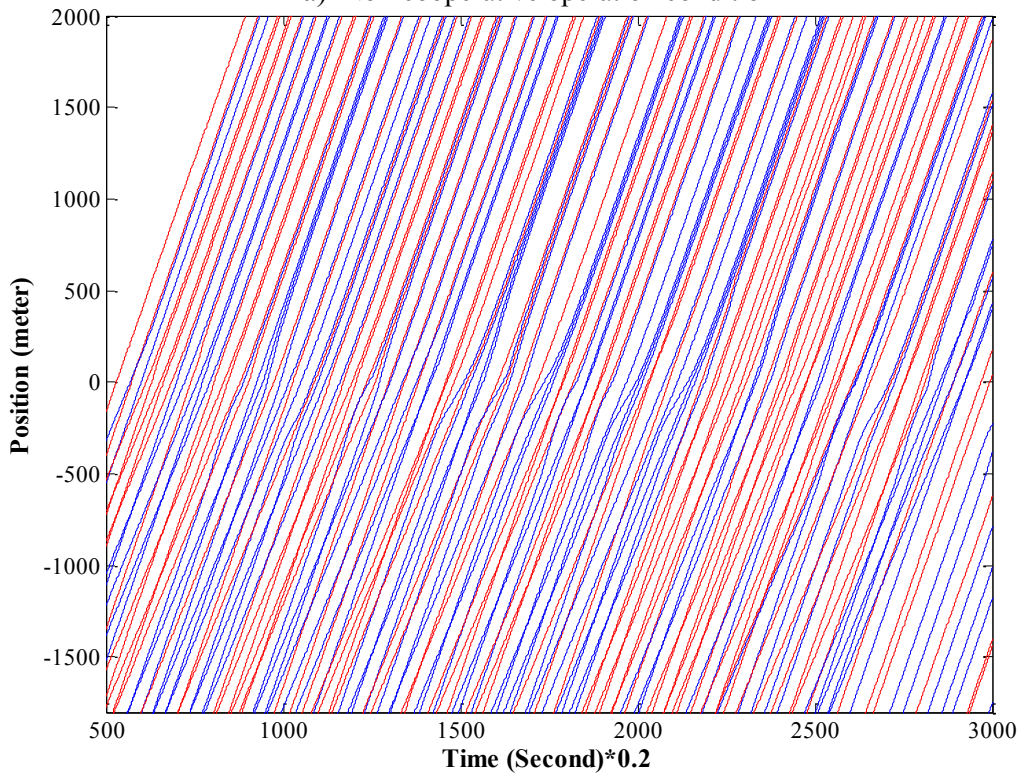
As the total traffic flow increases on both lanes, more merging vehicles may have to stop at the end of the acceleration lane, which requires a traffic control framework. For example, the simulation traffic scenario of 1,500 veh/h total flow, 50% CAVs, and 50% of the traffic demand on the ramp (shown in Figure 4-13), an average of 9.5 vehicles cannot find enough gaps to merge, leading to their stopping at the end of acceleration lane, increasing the average travel time for merging vehicles. However, applying the proposed methodology, we are able to decrease the stopped vehicles to 3.1 vehicles and decrease the merging vehicles' travel time by 3.6 s. Note that in this case, the stopped vehicles are those that could not be part of a triplet to accomplish the merging maneuver. In this traffic flow scenario, decreasing the penetration rate of CAVs leads to an increase in the number of stopped vehicles, as is expected. The results (in Figure 4-14) show that by only a 10% penetration rate of CAVs, applying the proposed framework can mitigate the stopped vehicles from 37.7 to 17.0 vehicles while improving the travel time by 25.3%. Applying the proposed traffic control framework in a traffic condition with the total flow of 1,500 veh/h, the improvement in mitigating the number of stopped merging vehicles and decreasing the travel time of the merging vehicles are shown in Figure 4-15. In this section, the reduction in the value of a parameter (e.g., travel time and the number of stopped merging vehicles) in cooperative traffic condition with respect to the non-cooperative traffic condition is calculated using equation below:

$$Reduction (\%) = \frac{(P_{non-coop} - P_{coop})}{P_{non-coop}} \times 100 \quad 4-8$$

where  $P_{non-coop}$  and  $P_{coop}$  are the value of the parameter under the non-cooperative and cooperative traffic operation, respectively.



a) Non-cooperative operation condition



b) Cooperative operation condition

Figure 4-12. Effectiveness of the proposed framework in the light traffic flow of 1,000 veh/h with 50% CAVs and 50% ramp flow ratio.



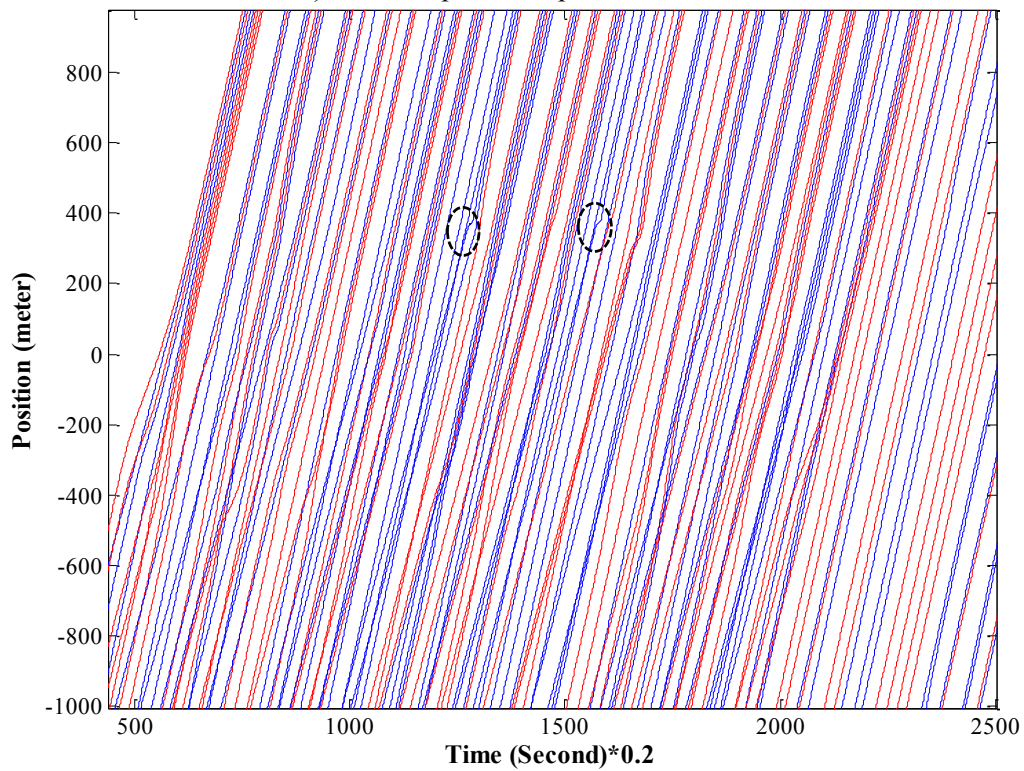
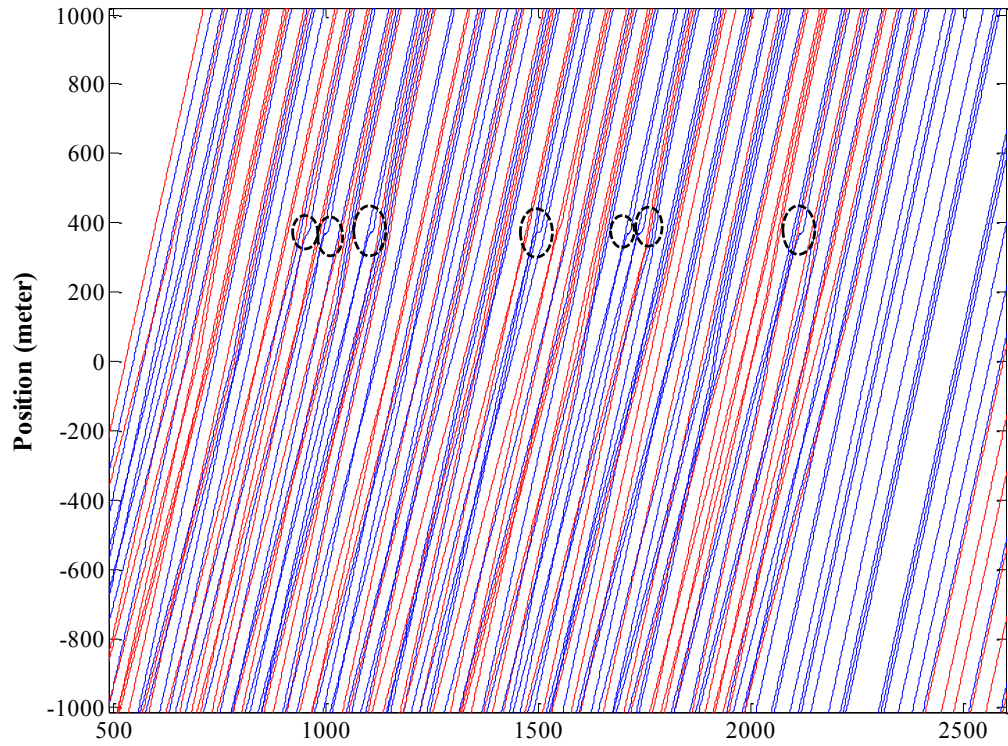
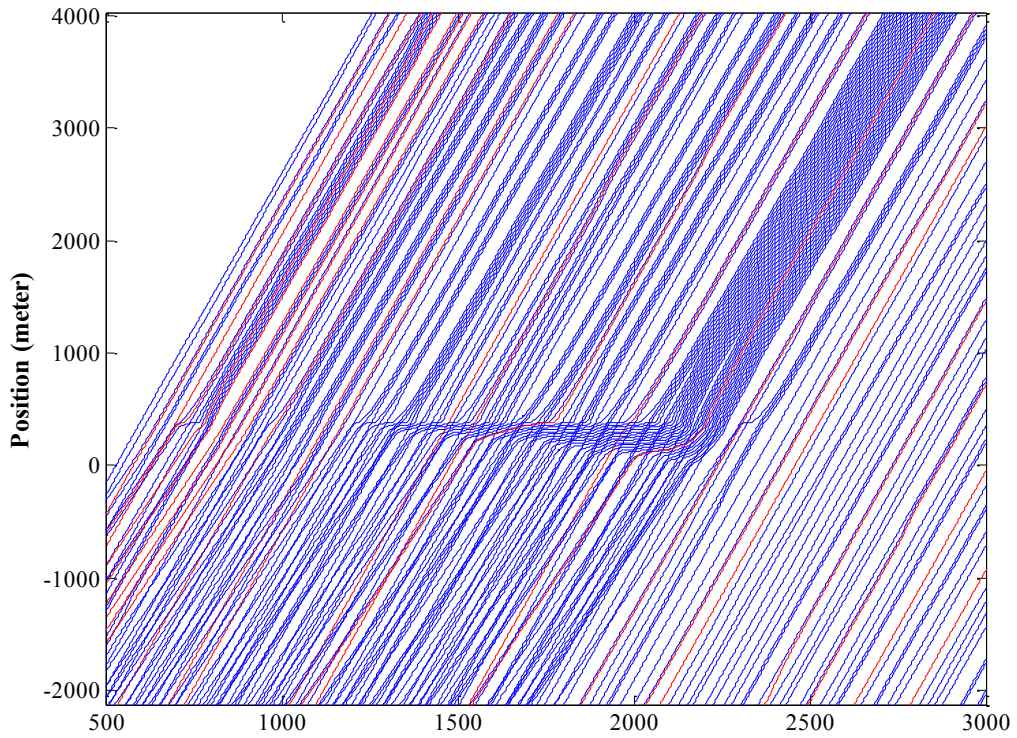
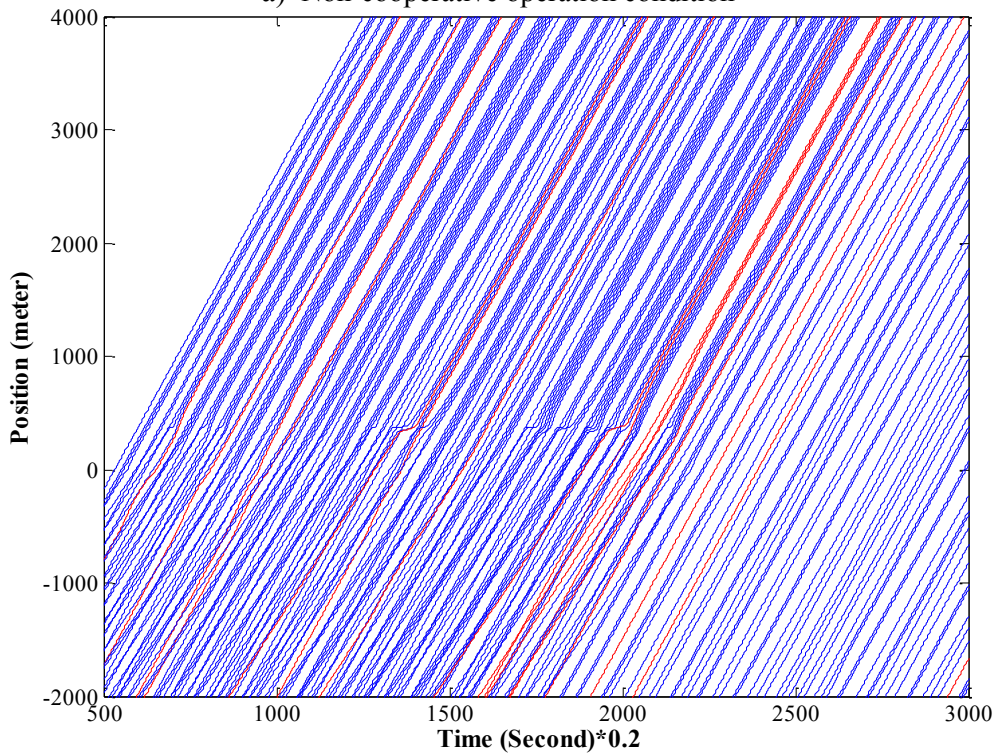


Figure 4-13. Effectiveness of the proposed framework in moderate traffic flow of 1,500 veh/h with 50% CAVs and 50% ramp flow ratio.

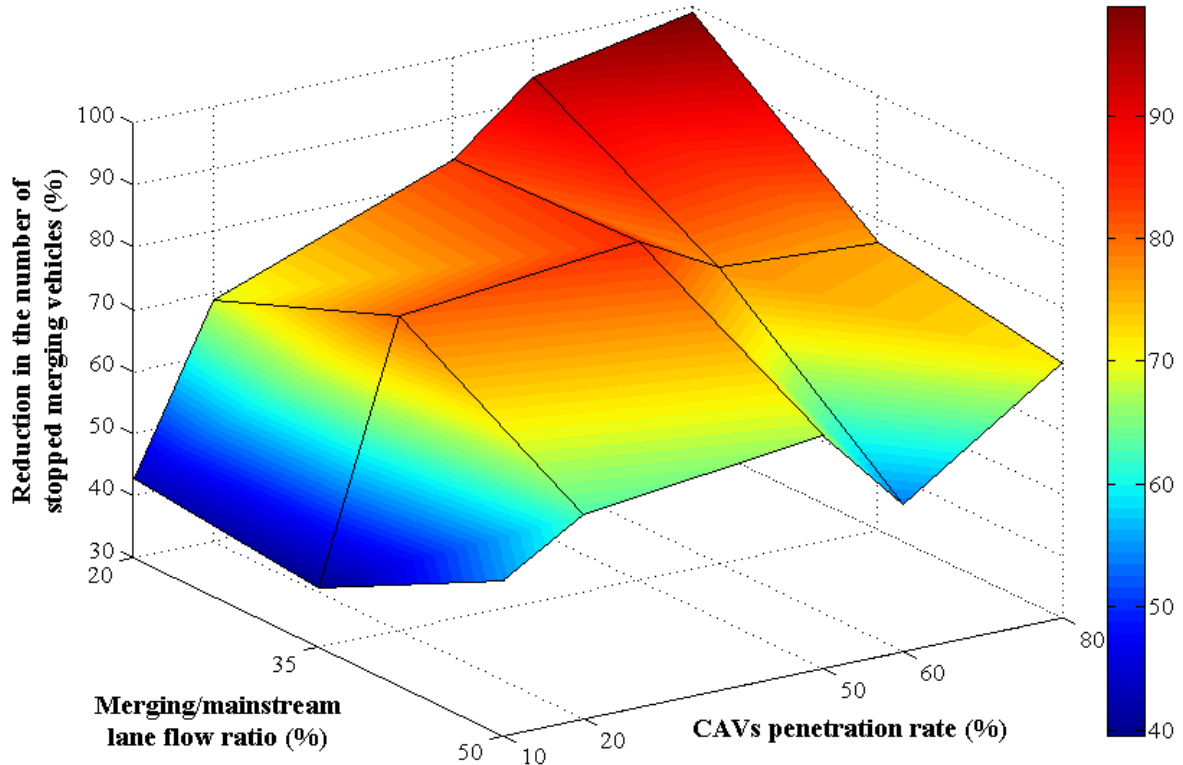


a) Non-cooperative operation condition

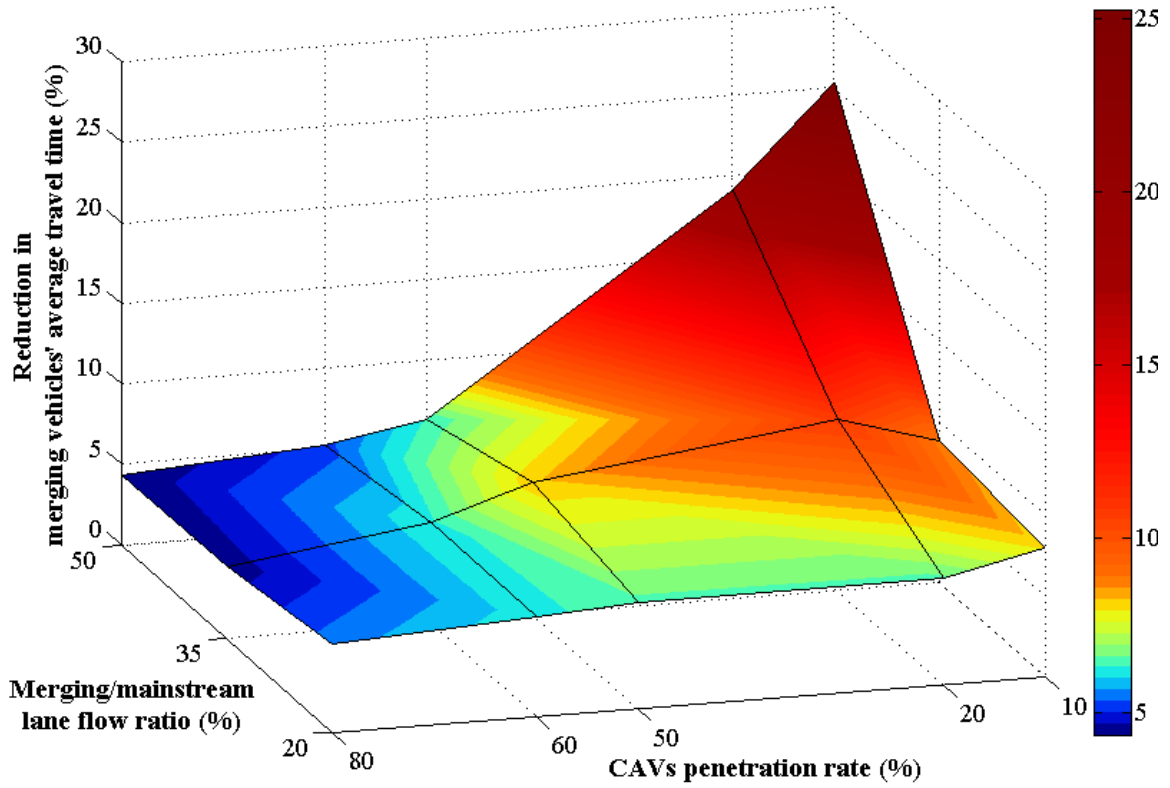


b) Cooperative operation condition

Figure 4-14. Effectiveness of the proposed framework in the moderate traffic flow of 1,500 veh/h with 10% CAVs and 50% ramp flow ratio.



a) Effects on the number of stopped merging vehicles



b) Effects on the travel time of the merging vehicles

Figure 4-15. The effectiveness of the proposed framework to improve the traffic safety and operation assuming a total traffic demand of 1,500 veh/h.

The results also show that under the heavy traffic flow condition (e.g., total flow equals 2,000 veh/h), the merging vehicles can rarely find enough gap to merge, leading to congestion on the ramp lane. For example, when the total flow is 2,000 veh/h and the ratio of ramp flow to mainstream flow is 20%, with 50% CAVs penetration rate, the proposed framework can improve the merging vehicles travel time by 27% while mitigating the number of stopped vehicles from 40.2 to 11.8 vehicles. However, there are still some vehicles trapped at the end of the acceleration lane and are not able to merge for a long time, as is shown in Figure 4-16. These trapped vehicles are either part of a failed triplet or a vehicle that does not belong to any triplet. Moreover, since the gaps for the merging vehicles are created by the triplets, i.e., there is no gap left on the mainstream, it slightly impacts the travel time of the mainstream vehicles (3.5 % increasing).

In the traffic condition of 2,000 veh/h the total traffic flow with merging flow rate of 20%, when we increase the penetration rate of CAVs to more than 50%, although larger gaps will be formed between platoons of vehicles on the mainstream lane, longer platoons of CAVs will be also formed. As a result, when a merging vehicle meets a platoon (i.e., fully congested traffic, as the platoons are too long), forming a triplet leads to a shockwave in the traffic and may result in full stop of upstream vehicles on the mainstream lane. Accordingly, the number of failed-triplets and the travel time of the mainstream vehicles increase drastically. Furthermore, when there are very long platoons on the merging lane (e.g., 50% ramp flow rate and more than 50% CAVs penetration rate), the shockwave appears on the merging lane, which causes failure in predicting the correct arrival time of vehicles by the higher level of traffic control framework. The performance of the framework, when the total flow is 2,000 veh/h, is presented in Figure 4-17 in terms of the number of stopped vehicles at the end of acceleration lane as well as the improvement/deterioration in the travel time of mainstream and merging lanes—the negative values shows the deterioration of a parameter.

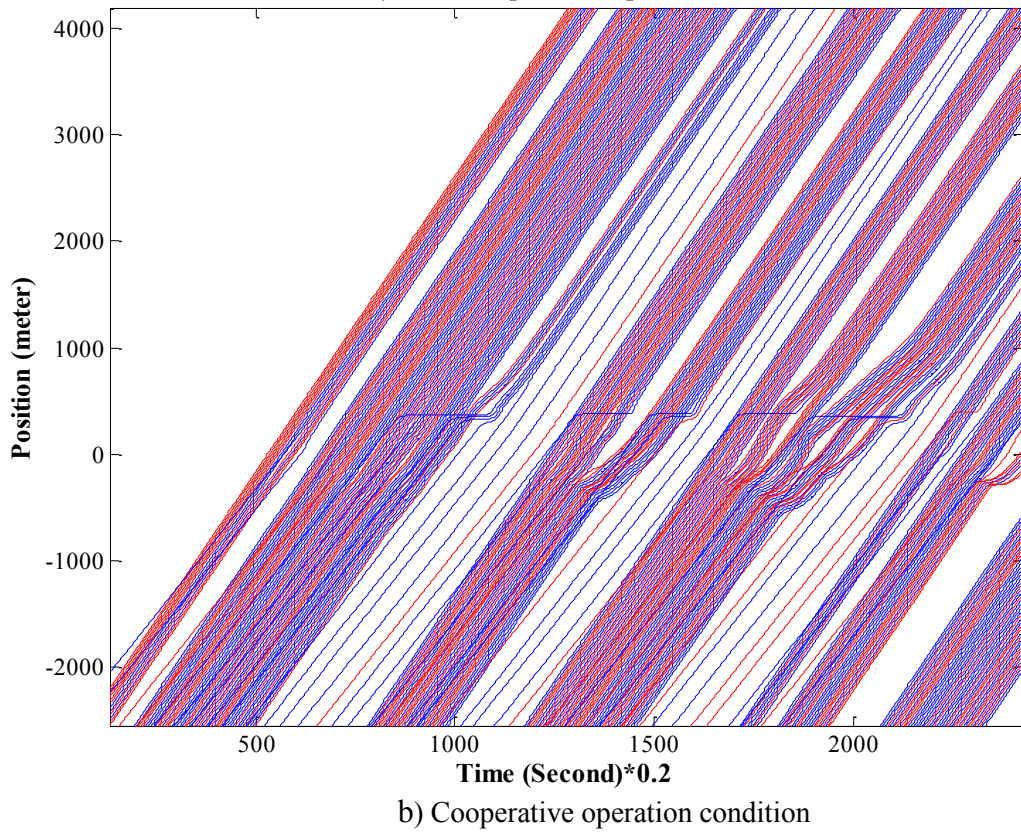
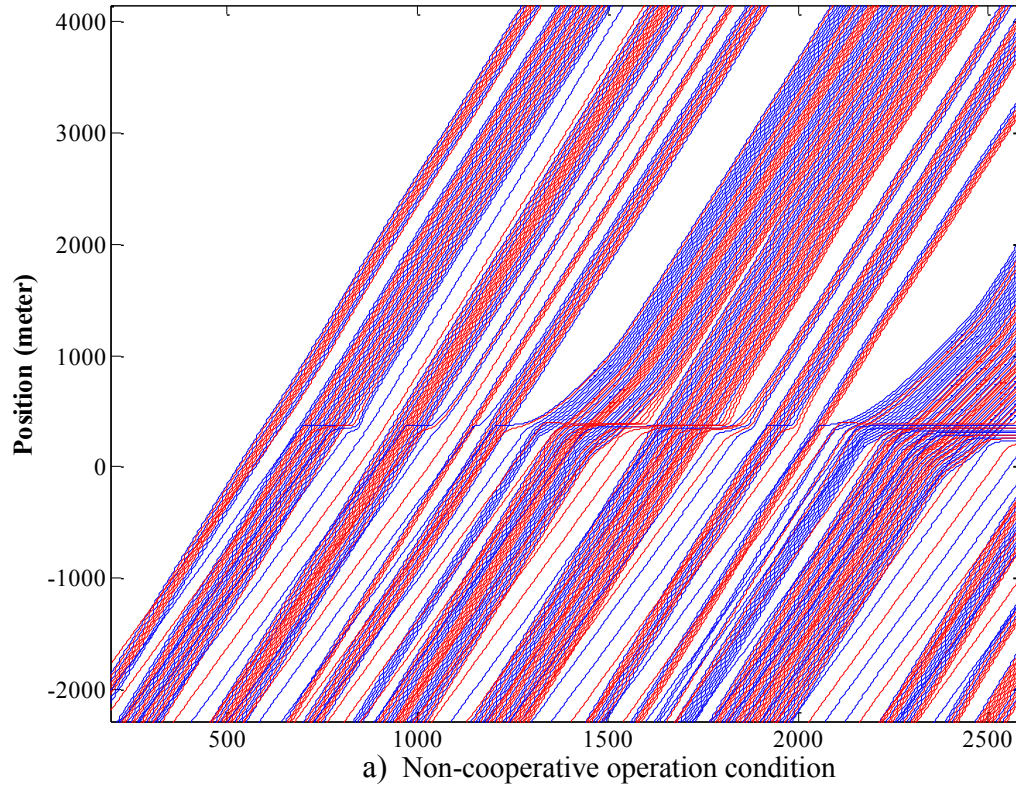
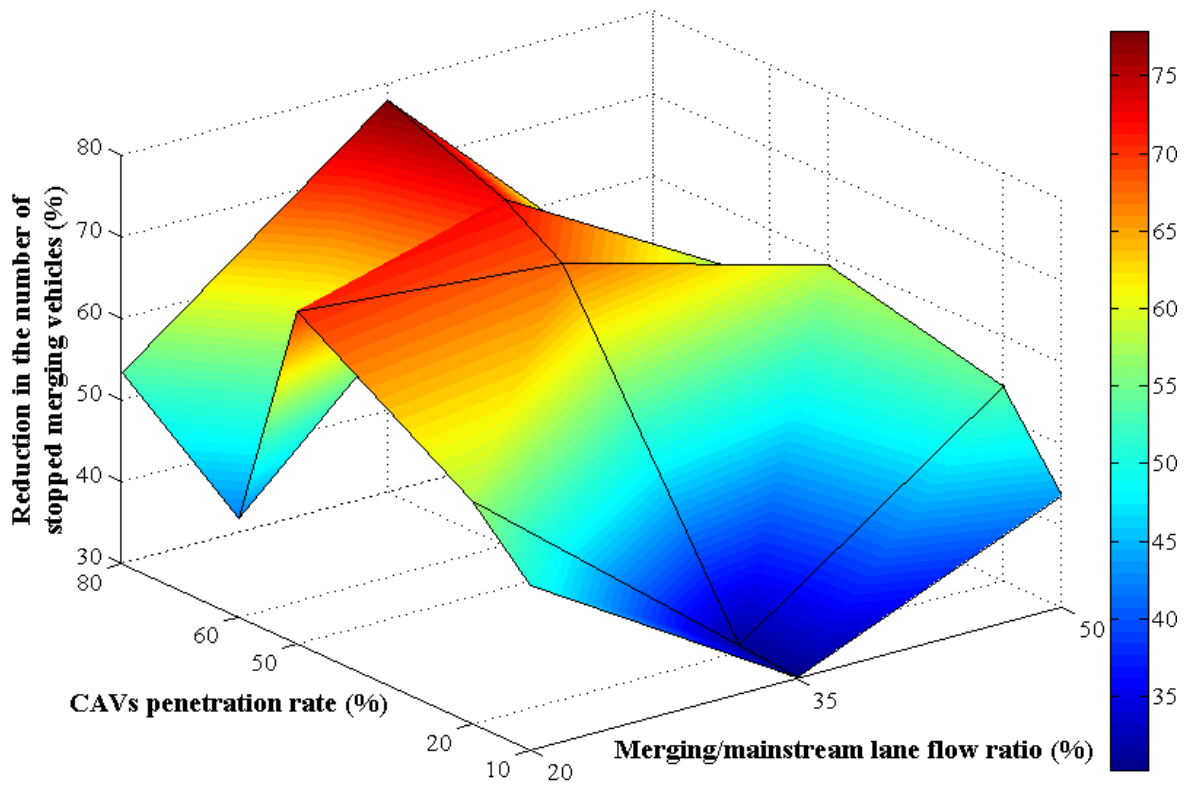
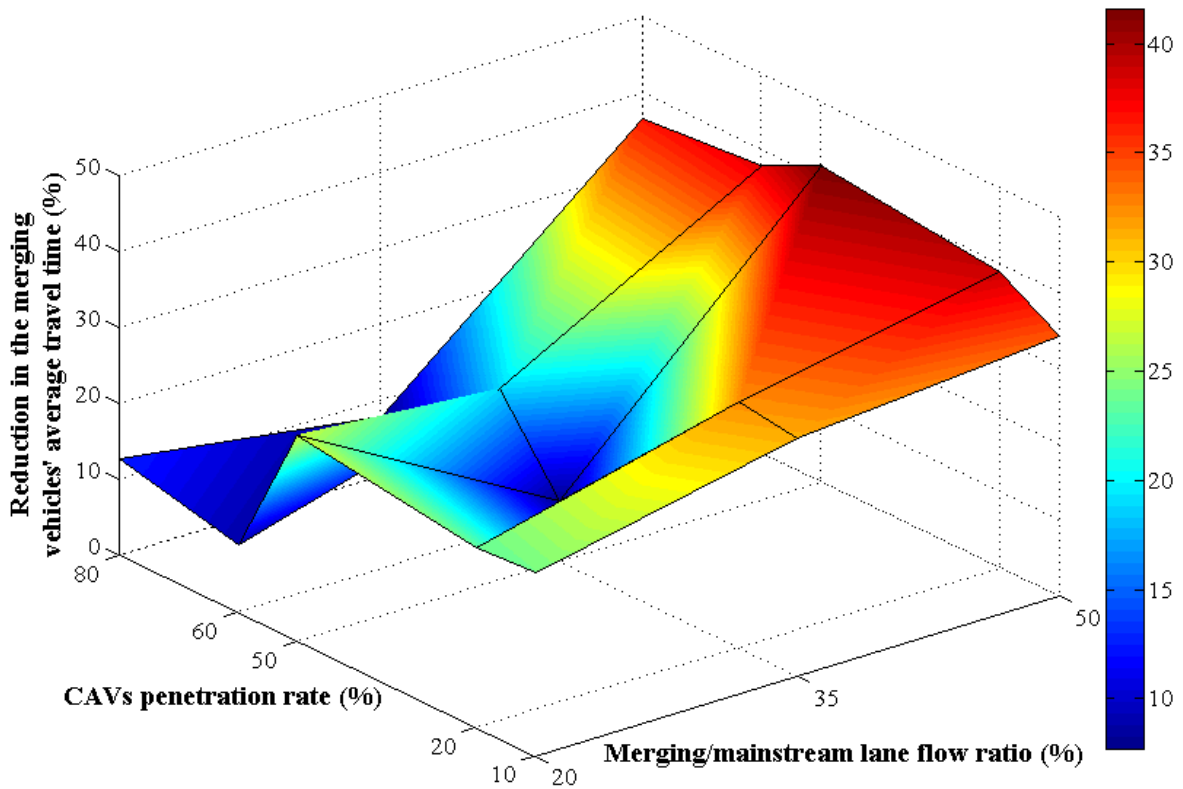


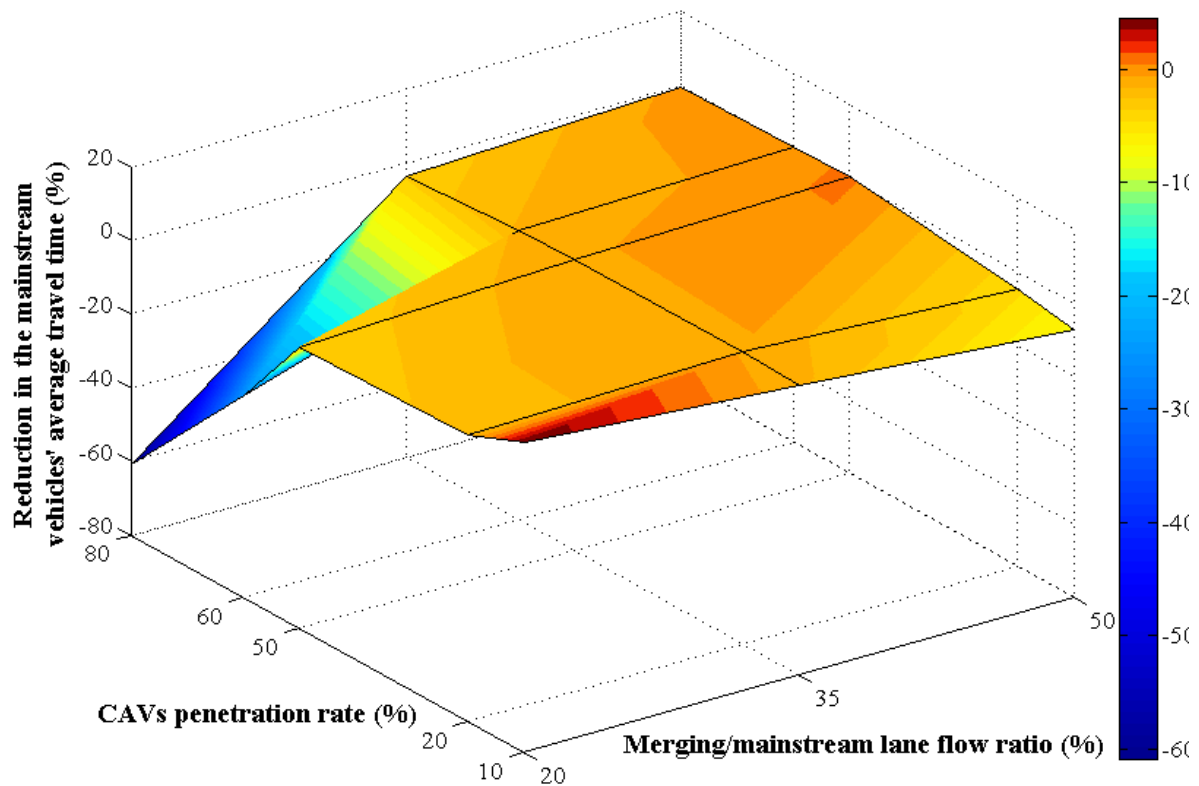
Figure 4-16. Effectiveness of the proposed framework in the moderate traffic flow of 2,000 veh/h with 50% CAVs and 20% ramp flow ratio.



a) Effects on the number of stopped merging vehicles



b) Effects on travel time on the merging lane



c) Effects on travel time on the mainstream lane

Figure 4-17. The effectiveness of the proposed framework to improve the traffic safety and operation assuming a total traffic demand of 2,000 veh/h.

#### 4.5 Concluding Remarks

This chapter proposes a methodology for triplets' formation technique that can be successfully integrated into the higher level of the proposed traffic control framework. In this regard, the higher level of the framework predicts the arrival time of each merging vehicle and assigns it to a triplet of vehicles (if possible) to cooperatively accomplish the merging maneuver. Priority rules to select a triplet are also defined for the case where the merging vehicle faces different choices of triplets. To evaluate the entire framework, a simulator is developed in MATLAB, and many different scenarios of the traffic flow conditions and CAVs penetration rates are investigated. The results show that the proposed framework is able to improve the traffic safety (i.e., number of stopped vehicles at the end of acceleration lane) and operation (the travel time of the merging vehicles) under a variety of traffic flow conditions without disturbing the mainstream lane traffic. However, under the very heavy traffic, when there are very long platoons of vehicles on the mainstream or on the merging lane, creating gaps by triplets in the platoons leads to shockwave in traffic flow and negatively effecting the travel time of the mainstream vehicles. Moreover, it is shown that the

proposed framework is robust (i.e., very limited number of failed triplets) under many traffic conditions, while only under very heavy traffic on the mainstream lane (i.e., very long platoons), the created shockwave impacts the prediction of vehicles arrival time by the higher level of the framework, leading to failure of some triplets.



## Chapter 5: CONCLUSIONS AND THE FUTURE DIRECTION

### 5.1 Summary

This thesis proposes a two-level hierarchical cooperative traffic control framework for the mixed traffic vehicular flow in the merging areas. The higher level of the traffic control framework is responsible for triplets' formation, which is based on the type of triplet and prediction of the arrival time of the merging and mainstream vehicles. The higher level of the framework also monitors the control zone and sends the necessary information to CAVs engaged in the triplets. The lower level of the framework comprises different cooperative merging algorithms for different types of triplets. When a triplet is formed by the higher level, the CAVs engaged in the triplet get informed to cooperate together to accomplish the merging maneuver. For each triplet, a MIMO system model is considered such that the uncertainties related to the conventional vehicles are captured, as well as a cooperative merging algorithm is developed in consecutive movement phases. In each movement phase, the desired control targets for CAVs are defined to provide sufficient lead and lag gaps for the merging vehicle, to gain the cooperation of the conventional lag vehicle in the merging process when one is detected, and to provide a condition that the conventional merging vehicle accepts smaller lead and lag gaps when one is detected. Using MPC scheme in each phase and applying the active-set method, optimal trajectories and commands (i.e., acceleration values) for CAVs, engaged in the triplet, are calculated to prepare the model for transition to the next movement phases. Some practical constraints are also considered to guarantee smooth motion trajectories (i.e., derivable position and speed values along with limited changes in acceleration values). Similarly, constraints are defined to ensure safe and comfort maneuvers (i.e., avoiding rear-end collisions, as well as satisfying the speed, acceleration, and jerk limits) for the interacting vehicles in each triplet. When the system switches from one movement phase to the next one, the system model and the desired control target may change accordingly, resulting in high values of control input(s) and discontinuous derivative of the control input(s). Considering the aforementioned constraints also mitigates the consequences of switching between different phases of movement (e.g., sharp acceleration changes).

All the merging algorithms for different triplets of vehicles are tested through many simulations considering different initial values. The simulation results show that the proposed cooperative merging algorithms leads to optimal merging maneuvers while satisfying the system

constraints related to safety and comfort. Moreover, the proposed merging algorithms work efficiently as they generate smooth motion trajectories, and they limit occurrence of “failed merging” instances (i.e. the stopping of the merging vehicle at the end of acceleration lane) without a need to readjust the parameters of the controllers.

To evaluate the performance of the entire cooperative traffic control framework, a simulator was developed in MATLAB able to simulate different traffic conditions in the merging area. We ran the simulator for different scenarios (i.e. different combinations of traffic flow, penetration rates of CAVs, and rates of ramp flow/ mainstream flow for different random seeds). The results show that the proposed framework is able to improve traffic safety (i.e., decrease the number of stopped vehicles at the end of acceleration lane) and operation (decrease the travel time of the merging vehicles) under a variety of traffic flow conditions without disturbing the mainstream lane traffic. It is also shown that the proposed framework is robust since only limited number of triplets fail to accomplish the merging maneuver. However, under the very heavy traffic, which includes very long platoons of vehicles, the triplets of vehicles may be disjointed without accomplishing the merging maneuver.

## **5.2 Research Contributions**

This thesis is developed to advance mixed traffic control, especially in the merging areas. The proposed cooperative traffic control framework can improve the traffic conditions of the mixed traffic environment with respect to traffic safety and operations. The developed microscopic simulator can be exploited by transportation researchers and practitioners to evaluate the existing transportation infrastructures under different traffic conditions with different penetration rates of CAVs. It can also help the transportation community to evaluate future transportation plans aiming at the gradual replacement of conventional vehicles with CAVs. Moreover, the proposed framework is expandable to different types of vehicle maneuvers such as lane-changing on highways, left and right turning movements at intersections, as well as egress maneuvers of vehicles exiting the freeways.

## **5.3 Future Work**

The proposed method can be improved by considering a multi-stage triplets' formation. In some cases, especially during congested traffic conditions, because of an inaccurate prediction of the arrival time of the vehicles or unpredicted actions of downstream triplets, the triplet fails early

before accomplishing any movement phase. Therefore, considering a second step in planning the triplets' formation can revise the decision made at the beginning of the control zone and lead to disjoint and reform new triplets, which leads to more effective performance. Another multi-stage traffic control framework is to consider a pre-control zone area to create random gaps between vehicles, especially in a very congested traffic condition on mainstream lane, so that the triplets can be formed easily in the next step.

The developed MATLAB-based simulator as a basic proof-of-concept testing tool can be expanded to include different models for CAVs with different cooperation features in multi-lane highways, urban area intersections, and roundabouts.

Furthermore, due to the stochastic nature of the conventional vehicles driving behavior, the proposed framework requires calibration of various parameters in order to accurately capture the real-world vehicular interactions. Moreover, human-driving vehicles' behavior may differ when they are in the proximity of CAV. It is anticipated that actual observations of the real-world implementation of this framework might be more difficult to collect. Therefore, the validation and calibration process can be undertaken by conducting a survey among the drivers of different categories (e.g. age, genders, experience, etc.) to evaluate their behavior in similar scenarios. Similarly, a driving simulator can be employed to observe the driving behavior of drivers from different categories in our proposed mixed traffic control framework. As a result, validation and calibration of the entire framework could be done using the data collected from these two methods.

## Chapter 6: APPENDICES

### 6.1 Appendix I

**Theorem:** If the merging vehicle, the leader vehicle, and the lag vehicle move at the same speed, the merging vehicle will accept the smallest adjacent gap to merge.

**Proof:** To have a smaller adjacent gap, it is required to have smaller lead and lag gaps. Assume that the speed of the merging vehicle is smaller than the speed of lead vehicle. Therefore, we have:

$$\Delta v_n^{lead} \geq 0 \tag{6-1}$$

According to equation 2-8, we have:

$$G_n^{cr,lead}(t) = \exp(0.508 + \varepsilon_n^{lead}(t)) \tag{6-2}$$

Now, if the merging vehicle moves at a speed higher than the lead vehicle,

$$\Delta v_n^{lead} < 0 \tag{6-3}$$

and accordingly, we have

$$G_n^{cr,lead}(t) = \exp(0.508 + |0.420\Delta v_n^{lead}| + \varepsilon_n^{lead}(t)) \tag{6-4}$$

Since  $\exp(0.508 + |0.420\Delta v_n^{lead}| + \varepsilon_n^{lead}(t)) > \exp(0.508 + \varepsilon_n^{lead}(t))$ , we can conclude that if the merging vehicle travels slower than the lead vehicle, it will accept a smaller lead gap.

With a similar argument for the critical lag gap, we can conclude that if the merging vehicle moves faster than lag vehicle ( $\Delta v_n^{lag} \leq 0$ ), the merging vehicle will accept a smaller lag gap.

All in all, if  $\Delta v_n^{lag} \leq 0$  and  $\Delta v_n^{lead} \geq 0$ , we will have the smallest acceptable lead and lag gaps. However, generally, the vehicles in the mainstream move at a speed close to the desired mainstream speed. Accordingly, in the condition where the lead vehicle speed and the lag vehicle speed are equal, the smallest acceptable lead and lag gaps can be achieved only if the merging vehicle also moves at a same speed.

## 6.2 Appendix II

By applying the system model (given in equation 3-46) equation recursively to the initial condition, the elements of the predicted output vector can be obtained as below:

$$\hat{Y}(j+1|j) = CA'X(j) + CA'_\tau X(j-k) + CB'U(j) + CD'(j)$$

$$\hat{Y}(j+2|j) = CA'^2 X(j) + CA'A'_\tau X(j-k) + CA'_\tau X(j-k+1) + CA'B'U(j) + CB'U(j+1) + C(A' + I)D'(j)$$

$$\hat{Y}(j+3|j) = CA'^3 X(j) + \left[ CA'^2 A'_\tau X(j-k) + CA'A'_\tau X(j-k+1) + CA'_\tau X(j-k+2) \right] + \left[ CA'^2 B'U(j) + CA'B'U(j+1) + CB'U(j+2) \right] + C(A'^2 + A' + I)D'(j)$$

⋮

$$\begin{aligned} \hat{Y}(j+k+1|j) &= (CA'^{k+1} + CA'_\tau)X(j) + \left[ CA'^k A'_\tau X(j-k) + \dots + CA'A'_\tau X(j-1) \right] \\ &+ \left[ CA'^k B'U(j) + CA'^{k-1} B'U(j+1) + \dots + CB'U(j+k) \right] + C(A'^k + A'^{k-1} + \dots \\ &+ I)D'(j) \end{aligned}$$

$$\begin{aligned} \hat{Y}(j+k+2|j) &= (CA'^{k+2} + CA'A'_\tau + CA'_\tau A')X(j) \\ &+ \left[ (CA'^{k+1} A'_\tau + CA'_\tau A'_\tau)X(j-k) + \dots + CA'^2 A'_\tau X(j-1) \right] \\ &+ \left[ (CA'^{k+1} B' + CA'_\tau B')U(j) + CA'^k B'U(j+1) + \dots + CB'U(j+k+1) \right] + C(A'^{k+1} \\ &+ A'^k + \dots + I + A'_\tau)D'(j) \end{aligned}$$

$$\begin{aligned} \hat{Y}(j+k+3|j) &= (CA'^{k+3} + CA'^2 A'_\tau + CA'A'_\tau A' + CA'_\tau A'^2)X(j) \\ &+ \left[ (CA'^{k+2} A'_\tau + CA'A'_\tau A'_\tau + CA'_\tau A'A'_\tau)X(j-k) \right. \\ &+ \left. (CA'^{k+1} A'_\tau + CA'_\tau A'_\tau)X(j-k+1) + \dots + CA'^3 A'_\tau X(j-1) \right] \\ &+ \left[ (CA'^{k+2} B' + CA'A'_\tau B' + CA'_\tau A'B')U(j) + (CA'^{k+1} B' + CA'_\tau B')U(j+1) + \dots \right. \\ &+ \left. CB'U(j+k+2) \right] + C(A'^{k+2} + \dots + I + A'A'_\tau + A'_\tau(A' + I))D'(j) \end{aligned}$$

$$\begin{aligned}
\hat{Y}(j+k+4|j) &= \left( CA'^{k+4} + CA'^3 A'_\tau + CA'^2 A'_\tau A' + CA' A'_\tau A'^2 + CA'_\tau A'^3 \right) X(j) \\
&+ \left[ \left( CA'^{k+3} A'_\tau + CA'^2 A'_\tau A'_\tau + CA' A'_\tau A'_\tau A' + CA'_\tau A'^2 A'_\tau \right) X(j-k) \right. \\
&+ \left( CA'^{k+2} A'_\tau + CA' A'_\tau A'_\tau + CA'_\tau A'_\tau A' \right) X(j-k+1) \\
&+ \left. \left( CA'^{k+1} A'_\tau + CA'_\tau A'_\tau \right) X(j-k+2) + \dots + CA'^4 A'_\tau X(j-1) \right] \\
&+ \left[ \left( CA'^{k+3} B' + CA'^2 A'_\tau B' + CA' A'_\tau A'_\tau B' + CA'_\tau A'^2 B' \right) U(j) + \left( CA'^{k+2} B' + CA' A'_\tau B' \right. \right. \\
&+ \left. \left. CA'_\tau A'_\tau B' \right) U(j+1) + \left( CA'^{k+1} B' + CA'_\tau B' \right) U(j+2) + \dots + CB' U(j+k+3) \right] \\
&+ C \left( A'^{k+3} D' + A'^{k+2} D' + \dots + D' \right) + CA'^2 A'_\tau D'(j) + CA' A'_\tau [(A' + I) D' + CA'_\tau (A'^2 \\
&+ A' + I) D'(j) \\
&\quad \vdots \\
\hat{Y}(j+p_x|j) &= (CA'^{p_x} + \dots) X(j) \\
&+ \left[ \left( CA'^{p_x-1} A'_\tau + \dots \right) X(j-k) + \dots + \left( CA'^{p_x-k} A'_\tau + \dots \right) X(j-1) \right] \\
&+ \left[ \left( CA'^{p_x-1} B' + \dots \right) U(j) + \dots + \left( CB' + \dots \right) U(j+p_x-1) \right] + C(A'^{p_x-1} + \dots + I \\
&+ \dots) D'(j)
\end{aligned}$$

These equations can be aggregated in the prediction model as follows (given in equation 3-49):

$$\hat{Y}_j = G_1 X(j) + G_2 \bar{X}_j^{k_3} + F_1 U_j + F_2 D'(j)$$

where

$$G_1 = \begin{bmatrix} CA' \\ CA'^2 \\ \vdots \\ CA'^{k_3} \\ CA'^{k_3+1} + CA'_\tau \\ CA'^{k_3+2} + CA' A'_\tau + CA'_\tau A' \\ CA'^{k_3+3} + CA'^2 A'_\tau + CA' A'_\tau A' + CA'_\tau A'^2 \\ CA'^{k_3+4} + CA'^3 A'_\tau + CA'^2 A'_\tau A' + CA' A'_\tau A'^2 + CA'_\tau A'^3 \\ \vdots \\ CA'^{p_x} + \dots \end{bmatrix}$$

$$\mathbf{G}_2 = \begin{bmatrix}
CA'_\tau & 0 & 0 & \dots & 0 \\
CA'A'_\tau & CA'_\tau & 0 & \dots & 0 \\
CA'^2A'_\tau & CA'A'_\tau & & & \\
\vdots & \vdots & & & \\
CA'^{k_3}A'_\tau & \vdots & & & CA'A'_\tau \\
CA'^{k_3+1}A'_\tau + CA'_\tau A'_\tau & \vdots & & & CA'^2A'_\tau \\
CA'^{k_3+2}A'_\tau + CA'A'_\tau A'_\tau + CA'_\tau A'A'_\tau & CA'^{k_3+1}A'_\tau + CA'_\tau A'_\tau & & & CA'^3A'_\tau \\
\vdots & CA'^{k_3+2}A'_\tau + CA'A'_\tau A'_\tau + CA'_\tau A'A'_\tau & & & \vdots \\
(CA'^{p_x-1}A'_\tau + \dots) & \dots & & & (CA'^{p_x-k_3}A'_\tau + \dots)
\end{bmatrix}$$

$$\mathbf{F}_1 = \begin{bmatrix}
CB' & 0 & 0 & \dots & 0 \\
CA'B' & CB' & 0 & \dots & 0 \\
CA'^2B' & CA'B' & & & \\
\vdots & \vdots & & & \\
CA'^{k_3}B' & \vdots & & & CB' \\
CA'^{k_3+1}B' + CA'_\tau B' & CA'^{k_3}B' & & & CB' \\
CA'^{k_3+2}B' + CA'A'_\tau B' + CA'_\tau A'B' & CA'^{k_3+1}B' + CA'_\tau B' & & & \\
\vdots & CA'^{k_3+2}B' + CA'A'_\tau B' + CA'_\tau A'B' & & & \vdots \\
(CA'^{p_x-1}B' + \dots) & \dots & & & (CB' + \dots)
\end{bmatrix}$$

$$\mathbf{F}_2 = \begin{bmatrix}
C \\
C(A' + I) \\
C(A'^2 + A' + I) \\
\vdots \\
C(A'^{k_3} + A'^{k_3-1} + \dots + I) \\
C(A'^{k_3+1} + A'^{k_3} + \dots + I) + C(A'_\tau) \\
C(A'^{k_3+2} + \dots + I) + C(A'A'_\tau + A'_\tau(A' + I)) \\
C(A'^{k_3+3} + A'^{k_3+2} + \dots + I) + C(A'^2A'_\tau + A'A'_\tau(A' + I) + A'_\tau(A'^2 + A' + I)) \\
\vdots \\
C(A'^{p_x-1} + \dots + I + \dots)
\end{bmatrix}$$

### 6.3 Appendix III

In this section, we prove that the cost function for MPC is convex. Therefore, if the employed QP optimization algorithm find an optimal solution, it is a globally optimum solution.

#### 6.3.1 Method one

In each phase of movement, the objective is a quadratic function as

$$J(j) = \frac{1}{2}(\hat{Y}_j - Y_d)^T Q(\hat{Y}_j - Y_d) + \frac{1}{2}U_j^T R U_j \quad 6-5$$

If we prove that a quadratic function is convex, the summation of them is also convex. To prove that  $f(x) = x^T Q x$  is convex, it is sufficient to prove that:

$$f(\lambda x + (1 - \lambda)y) \leq \lambda f(x) + (1 - \lambda)f(y) \text{ for all } \lambda \in [0, 1] \quad 6-6$$

Therefore,

$$(\lambda x + (1 - \lambda)y)^T Q (\lambda x + (1 - \lambda)y) \leq \lambda x^T Q x + (1 - \lambda)y^T Q y \quad 6-7$$

Simplifying and rearranging the non-equality above will lead us to

$$(x - y)^T Q (x - y) \geq 0 \quad 6-8$$

Which is true for the positive semi-definite  $Q$ . Therefore, the cost function is also convex, as it is the summation of two quadratic functions.

### 6.3.2 *Method two*

Another way to prove the convexity of a function is to show the second derivative of it (the Hessian  $\nabla^2 f(x)$ ) is positive semi-definite. In our case, we have to prove that

$$\frac{\partial^2 J(\mathbf{U}_j)}{\partial \mathbf{U}_j^2} \geq 0 \quad 6-9$$

We know that

$$J(j) = \frac{1}{2} (\hat{\mathbf{Y}}_j - \mathbf{Y}_d)^T \mathbf{Q} (\hat{\mathbf{Y}}_j - \mathbf{Y}_d) + \frac{1}{2} \mathbf{U}_j^T \mathbf{R} \mathbf{U}_j \quad 6-10$$

where

$$\hat{\mathbf{Y}}_j = \mathbf{G}_1 X(j) + \mathbf{G}_2 \bar{\mathbf{X}}_j^{k_3} + \mathbf{F}_1 \mathbf{U}_j + \mathbf{F}_2 D' \quad 6-11$$

The second derivative of the cost function with respect to the input is:

$$\frac{\partial^2 J(\mathbf{U}_j)}{\partial \mathbf{U}_j^2} = \mathbf{F}_1^T \mathbf{Q} \mathbf{F}_1 + \mathbf{R} \quad 6-12$$

Therefore, by assuming that  $\mathbf{R}$  and  $\mathbf{Q}$  are positive semi-definite, the cost function is convex. Since we can convert all the constraints to the linear constraints on the input, the cost function will be convex over the constraints.



## Chapter 7: REFERENCES

- [1] J. Rios-Torres and A. A. Malikopoulos, “A survey on the coordination of connected and automated vehicles at intersections and merging at highway on-ramps,” *IEEE Transactions on Intelligent Transportation Systems*, vol. 18, no. 5, pp. 1066–1077, 2017.
- [2] Standing Senate Committee report 2018, “Transport and Communications (TRCM Automated Vehicles 2018),” 2018.
- [3] R. Bishop, “A Survey of intelligent Vehicle Application,” in *Proceedings of IEEE intelligent Vehicles Symposium*, 2000.
- [4] M. Kyriakidis, R. Happee, and J. C. F. de Winter, “Public opinion on automated driving: Results of an international questionnaire among 5000 respondents,” *Transportation research part F: traffic psychology and behaviour*, vol. 32, pp. 127–140, 2015.
- [5] G. Rempel and D. Michelson, “Connected and Automated Vehicle Activities in Canada,” in *TRB-TR News*, (317), 2018, no. 317, pp. 10–18.
- [6] C. Rödel, S. Stadler, A. Meschtscherjakov, and M. Tscheligi, “Towards autonomous cars: the effect of autonomy levels on acceptance and user experience,” in *Proceedings of the 6th International Conference on Automotive User Interfaces and Interactive Vehicular Applications*, 2014, pp. 1–8.
- [7] D. J. Fagnant and K. Kockelman, “Preparing a nation for autonomous vehicles: opportunities, barriers and policy recommendations,” *Transportation Research Part A: Policy and Practice*, vol. 77, pp. 167–181, 2015.
- [8] B. S. Kerner, “Effect of Automatic Driving on Probability of Breakdown in Traffic Networks,” in *Breakdown in Traffic Networks*, Springer, 2017, pp. 275–295.
- [9] A. Talebpour and H. S. Mahmassani, “Influence of connected and autonomous vehicles on traffic flow stability and throughput,” *Transportation Research Part C: Emerging Technologies*, vol. 71, pp. 143–163, 2016.
- [10] R. Bertini and S. Malik, “Observed dynamic traffic features on freeway section with merges and diverges,” *Transportation Research Record: Journal of the Transportation Research*

- Board*, no. 1867, pp. 25–35, 2004.
- [11] L. C. Davis, “Effect of cooperative merging on the synchronous flow phase of traffic,” *Physica A: Statistical Mechanics and its Applications*, vol. 361, no. 2, pp. 606–618, 2006.
- [12] H. Yi and T. E. Mulinazzi, “Urban freeway on-ramps: Invasive influences on main-line operations,” *Transportation Research Record*, vol. 2023, no. 1, pp. 112–119, 2007.
- [13] W. Cao, M. Mukai, T. Kawabe, H. Nishira, and N. Fujiki, “Cooperative vehicle path generation during merging using model predictive control with real-time optimization,” *Control Engineering Practice*, vol. 34, pp. 98–105, 2015.
- [14] National Highway Traffic Safety Administration, “NHTSA Preliminary statement of policy concerning automated vehicles,” 2013.
- [15] S. L. Poczter and L. M. Jankovic, “The Google Car: driving toward a better future?,” *Journal of Business Case Studies (Online)*, vol. 10, no. 1, p. 7, 2014.
- [16] P. Varaiya, “Smart cars on smart roads: problems of control,” *IEEE Transactions on automatic control*, vol. 38, no. 2, pp. 195–207, 1993.
- [17] W. J. Schakel and B. Van Arem, “Improving traffic flow efficiency by in-car advice on lane, speed, and headway,” *IEEE Transactions on Intelligent Transportation Systems*, vol. 15, no. 4, pp. 1597–1606, 2014.
- [18] C. Roncoli, M. Papageorgiou, and I. Papamichail, “Traffic flow optimisation in presence of vehicle automation and communication systems—Part II: Optimal control for multi-lane motorways,” *Transportation Research Part C: Emerging Technologies*, vol. 57, pp. 260–275, 2015.
- [19] S. Kato, S. Tsugawa, K. Tokuda, T. Matsui, and H. Fujii, “Vehicle control algorithms for cooperative driving with automated vehicles and intervehicle communications,” *IEEE Transactions on Intelligent Transportation Systems*, vol. 3, no. 3, pp. 155–161, 2002.
- [20] R. Rajamani, H.-S. Tan, B. K. Law, and W.-B. Zhang, “Demonstration of integrated longitudinal and lateral control for the operation of automated vehicles in platoons,” *IEEE Transactions on Control Systems Technology*, vol. 8, no. 4, pp. 695–708, 2000.

- [21] S. Tsugawa, S. Kato, T. Matsui, H. Naganawa, and H. Fujii, "An architecture for cooperative driving of automated vehicles," in *Intelligent Transportation Systems, 2000. Proceedings. 2000 IEEE*, 2000, pp. 422–427.
- [22] A. Bose and P. A. Ioannou, "Analysis of traffic flow with mixed manual and semiautomated vehicles," *IEEE Transactions on Intelligent Transportation Systems*, vol. 4, no. 4, pp. 173–188, 2003.
- [23] Y.-M. Yuan, R. Jiang, M.-B. Hu, Q.-S. Wu, and R. Wang, "Traffic flow characteristics in a mixed traffic system consisting of ACC vehicles and manual vehicles: A hybrid modelling approach," *Physica A: Statistical Mechanics and its Applications*, vol. 388, no. 12, pp. 2483–2491, 2009.
- [24] D. Ngoduy, "Application of gas-kinetic theory to modelling mixed traffic of manual and ACC vehicles," *Transportmetrica*, vol. 8, no. 1, pp. 43–60, 2012.
- [25] B. Van Arem, C. J. G. Van Driel, and R. Visser, "The impact of cooperative adaptive cruise control on traffic-flow characteristics," *IEEE Transactions on Intelligent Transportation Systems*, vol. 7, no. 4, pp. 429–436, 2006.
- [26] A. Uno, T. Sakaguchi, and S. Tsugawa, "A merging control algorithm based on inter-vehicle communication," in *Intelligent Transportation Systems, 1999. Proceedings. 1999 IEEE/IEEEJ/JSAI International Conference on*, 1999, pp. 783–787.
- [27] M. Antoniotti, A. Desphande, and A. Girault, "Microsimulation analysis of multiple merge junctions under autonomous ahs operation," in *Intelligent Transportation System, 1997. ITSC'97., IEEE Conference on*, 1997, pp. 147–152.
- [28] B. Ran, S. Leight, and B. Chang, "A microscopic simulation model for merging control on a dedicated-lane automated highway system," *Transportation Research Part C: Emerging Technologies*, vol. 7, no. 6, pp. 369–388, 1999.
- [29] X.-Y. Lu, H.-S. Tan, S. E. Shladover, and J. K. Hedrick, "Automated vehicle merging maneuver implementation for AHS," *Vehicle System Dynamics*, vol. 41, no. 2, pp. 85–107, 2004.
- [30] X.-Y. Lu and J. K. Hedrick, "Longitudinal control algorithm for automated vehicle

- merging,” *International Journal of Control*, vol. 76, no. 2, pp. 193–202, 2003.
- [31] H. Park, C. S. Bhamidipati, and B. L. Smith, “Development and evaluation of enhanced intellidrive-enabled lane changing advisory algorithm to address freeway merge conflict,” *Transportation research record*, vol. 2243, no. 1, pp. 146–157, 2011.
- [32] W. Daamen, B. van Arem, and I. Bouma, “Microscopic dynamic traffic management: Simulation of two typical situations,” in *Intelligent Transportation Systems (ITSC), 2011 14th International IEEE Conference on*, 2011, pp. 1898–1903.
- [33] S. Sivaraman, M. M. Trivedi, M. Toppelhofer, and T. Shannon, “Merge recommendations for driver assistance: A cross-modal, cost-sensitive approach,” in *Intelligent Vehicles Symposium (IV), 2013 IEEE*, 2013, pp. 411–416.
- [34] J. Wei, J. M. Dolan, and B. Litkouhi, “Autonomous vehicle social behavior for highway entrance ramp management,” in *Intelligent Vehicles Symposium (IV), 2013 IEEE*, 2013, pp. 201–207.
- [35] Y. Wang, E. Wenjuan, W. Tang, D. Tian, G. Lu, and G. Yu, “Automated on-ramp merging control algorithm based on Internet-connected vehicles,” *IET Intelligent Transport Systems*, vol. 7, no. 4, pp. 371–379, 2013.
- [36] T. Awal, L. Kulik, and K. Ramamohanrao, “Optimal traffic merging strategy for communication-and sensor-enabled vehicles,” in *Intelligent Transportation Systems- (ITSC), 2013 16th International IEEE Conference on*, 2013, pp. 1468–1474.
- [37] J. Wei, J. M. Dolan, and B. Litkouhi, “A prediction-and cost function-based algorithm for robust autonomous freeway driving,” in *Intelligent Vehicles Symposium (IV), 2010 IEEE*, 2010, pp. 512–517.
- [38] W. Levine and M. Athans, “On the optimal error regulation of a string of moving vehicles,” *IEEE Transactions on Automatic Control*, vol. 11, no. 3, pp. 355–361, 1966.
- [39] J. Rios-Torres and A. A. Malikopoulos, “Automated and cooperative vehicle merging at highway on-ramps,” *IEEE Transactions on Intelligent Transportation Systems*, vol. 18, no. 4, pp. 780–789, 2017.

- [40] Z. Wang, L. Kulik, and K. Ramamohanarao, “Proactive traffic merging strategies for sensor-enabled cars,” in *Automotive Informatics and Communicative Systems: Principles in Vehicular Networks and Data Exchange*, IGI Global, 2009, pp. 180–199.
- [41] R. Scarinci, B. Heydecker, and A. Hegyi, “Analysis of traffic performance of a merging assistant strategy using cooperative vehicles,” *IEEE Transactions on Intelligent Transportation Systems*, vol. 16, no. 4, pp. 2094–2103, 2015.
- [42] R. Scarinci, A. Hegyi, and B. G. Heydecker, “Cooperative ramp metering—A study of the practicality of a ramp metering development using intelligent vehicles,” in *45th Annual UTSG Universities’ Transport Study Group Conference*, 2013.
- [43] I. A. Ntousakis, I. K. Nikolos, and M. Papageorgiou, “Optimal vehicle trajectory planning in the context of cooperative merging on highways,” *Transportation research part C: emerging technologies*, vol. 71, pp. 464–488, 2016.
- [44] B. Moaveni and M. Karimi, “Subway Traffic Regulation Using Model-Based Predictive Control by Considering the Passengers Dynamic Effect,” *Arabian Journal for Science and Engineering*, vol. 42, no. 7, pp. 3021–3031, 2017.
- [45] L. Makarem and D. Gillet, “Model predictive coordination of autonomous vehicles crossing intersections,” in *Intelligent Transportation Systems-(ITSC), 2013 16th International IEEE Conference on*, 2013, pp. 1799–1804.
- [46] K.-D. Kim and P. R. Kumar, “An MPC-Based Approach to Provable System-Wide Safety and Liveness of Autonomous Ground Traffic.,” *IEEE Trans Automat Contr*, vol. 59, no. 12, pp. 3341–3356, 2014.
- [47] C. Letter and L. Eleftheriadou, “Efficient control of fully automated connected vehicles at freeway merge segments,” *Transportation Research Part C: Emerging Technologies*, vol. 80, pp. 190–205, 2017.
- [48] J. Rios-Torres, A. Malikopoulos, and P. Pisu, “Online optimal control of connected vehicles for efficient traffic flow at merging roads,” in *Intelligent Transportation Systems (ITSC), 2015 IEEE 18th International Conference on*, 2015, pp. 2432–2437.
- [49] J. Rios-Torres and A. A. Malikopoulos, “Impact of connected and automated vehicles on

- traffic flow,” in *Intelligent Transportation Systems (ITSC), 2017 IEEE 20th International Conference on*, 2017, pp. 1–6.
- [50] B. Ciuffo, V. Punzo, and M. Montanino, “Thirty years of Gipps’ car-following model: Applications, developments, and new features,” *Transportation Research Record: Journal of the Transportation Research Board*, no. 2315, pp. 89–99, 2012.
- [51] L. C. Davis, “Effect of adaptive cruise control systems on mixed traffic flow near an on-ramp,” *Physica A: Statistical Mechanics and its Applications*, vol. 379, no. 1, pp. 274–290, 2007.
- [52] R. Pueboobpaphan, F. Liu, and B. van Arem, “The impacts of a communication based merging assistant on traffic flows of manual and equipped vehicles at an on-ramp using traffic flow simulation,” in *Intelligent Transportation Systems (ITSC), 2010 13th International IEEE Conference on*, 2010, pp. 1468–1473.
- [53] M. Zhou, X. Qu, and S. Jin, “On the impact of cooperative autonomous vehicles in improving freeway merging: a modified intelligent driver model-based approach,” *IEEE Transactions on Intelligent Transportation Systems*, vol. 18, no. 6, pp. 1422–1428, 2017.
- [54] M. Treiber, A. Hennecke, and D. Helbing, “Congested traffic states in empirical observations and microscopic simulations,” *Physical review E*, vol. 62, no. 2, p. 1805, 2000.
- [55] L. Zhao, A. Malikopoulos, and J. Rios-Torres, “Optimal control of connected and automated vehicles at roundabouts: An investigation in a mixed-traffic environment,” *IFAC-PapersOnLine*, vol. 51, no. 9, pp. 73–78, 2018.
- [56] R. Scarinci and B. Heydecker, “Control concepts for facilitating motorway on-ramp merging using intelligent vehicles,” *Transport reviews*, vol. 34, no. 6, pp. 775–797, 2014.
- [57] K. I. Ahmed, “Modeling drivers’ acceleration and lane changing behavior,” Massachusetts Institute of Technology, Cambridge, MA., 1999.
- [58] D. C. Gazis, R. Herman, and R. B. Potts, “Car-following theory of steady-state traffic flow,” *Operations research*, vol. 7, no. 4, pp. 499–505, 1959.
- [59] D. C. Gazis, R. Herman, and R. W. Rothery, “Nonlinear follow-the-leader models of traffic

- flow,” *Operations research*, vol. 9, no. 4, pp. 545–567, 1961.
- [60] R. Herman, “Car-following and steady state flow,” in *Theory of Traffic Flow Symposium Proceedings*, 1959, pp. 1–13.
- [61] G. Lee, “A generalization of linear car-following theory,” *Operations Research*, vol. 14, no. 4, pp. 595–606, 1966.
- [62] S. Bexelius, “An extended model for car-following,” *Transportation Research*, vol. 2, no. 1, pp. 13–21, 1968.
- [63] H. N. Koutsopoulos and H. Farah, “Latent class model for car following behavior,” *Transportation research part B: methodological*, vol. 46, no. 5, pp. 563–578, 2012.
- [64] S. Hamdar, M. Treiber, H. Mahmassani, and A. Kesting, “Modeling driver behavior as sequential risk-taking task,” *Transportation Research Record: Journal of the Transportation Research Board*, no. 2088, pp. 208–217, 2008.
- [65] D. Kahneman and A. Tversky, “Prospect theory: An analysis of decision under risk,” in *Handbook of the fundamentals of financial decision making: Part I*, World Scientific, 2013, pp. 99–127.
- [66] A. Hanken and T. H. Rockwell, “A model of car following derived empirically by piecewise regression analysis,” in *Proceedings of the Third International Symposium on the Theory of Traffic Flow* Operations Research Society of America, 1967.
- [67] G. F. Newell, “Nonlinear effects in the dynamics of car following,” *Operations research*, vol. 9, no. 2, pp. 209–229, 1961.
- [68] M. Bando, K. Hasebe, A. Nakayama, A. Shibata, and Y. Sugiyama, “Dynamical model of traffic congestion and numerical simulation,” *Physical review E*, vol. 51, no. 2, p. 1035, 1995.
- [69] M. Bando, K. Hasebe, K. Nakanishi, and A. Nakayama, “Analysis of optimal velocity model with explicit delay,” *Physical Review E*, vol. 58, no. 5, p. 5429, 1998.
- [70] W. Helly, “Simulation of bottlenecks in single-lane traffic flow,” In *Proceedings of the Symposium on Theory of Traffic Flow Research Laboratories, General Motors*, pp. 207-

- 238). New York: Elsevier, 1959.
- [71] J. F. Gabard, J. J. Henry, J. Tuffal, and Y. David, "Traffic responsive or adaptive fixed time policies? A critical analysis with SITRA-B," in *Proceedings of the International Conference on Road Traffic Signalling. Institution of Electrical Engineers*, 1982, pp. 89–92.
- [72] W. Helly, "Simulation of bottlenecks in single-lane traffic flow," In *Proceedings of the Symposium on Theory of Traffic Flow Research Laboratories, General Motors*, p. 207±238). New York: Elsevier, 1959.
- [73] R. F. Benekohal and J. Treiterer, "CARSIM: Car-following model for simulation of traffic in normal and stop-and-go conditions," *Transportation research record*, no. 1194, 1988.
- [74] P. Hidas, "Modelling lane changing and merging in microscopic traffic simulation," *Transportation Research Part C: Emerging Technologies*, vol. 10, no. 5, pp. 351–371, 2002.
- [75] Q. Yang and H. N. Koutsopoulos, "A microscopic traffic simulator for evaluation of dynamic traffic management systems," *Transportation Research Part C: Emerging Technologies*, vol. 4, no. 3, pp. 113–129, 1996.
- [76] P. G. Gipps, "A behavioural car-following model for computer simulation," *Transportation Research Part B: Methodological*, vol. 15, no. 2, pp. 105–111, 1981.
- [77] Z. Zheng, "Recent developments and research needs in modeling lane changing," *Transportation Research Part B: Methodological*, vol. 60, pp. 16–32, 2014.
- [78] T. Toledo, "Integrated driving behavior modeling." Northeastern University, 2002.
- [79] D. J. Sun and L. Elefteriadou, "Lane- Changing Behavior on Urban Streets: An 'In-Vehicle' Field Experiment- Based Study," *Computer- Aided Civil and Infrastructure Engineering*, vol. 27, no. 7, pp. 525–542, 2012.
- [80] S. Wolfram, "Statistical mechanics of cellular automata," *Reviews of modern physics*, vol. 55, no. 3, p. 601, 1983.
- [81] C. F. Daganzo, "In traffic flow, cellular automata= kinematic waves," *Transportation*



- Research Part B: Methodological*, vol. 40, no. 5, pp. 396–403, 2006.
- [82] R. D. Worrall, A. G. Bullen, and Y. Gur, “An elementary stochastic model of lane-changing on a multilane highway,” *Highway Research Record*, no. 308, 1970.
- [83] K. Singh and B. Li, “Estimation of traffic densities for multilane roadways using a markov model approach,” *IEEE Transactions on industrial electronics*, vol. 59, no. 11, pp. 4369–4376, 2012.
- [84] P. G. Gipps, “A model for the structure of lane-changing decisions,” *Transportation Research Part B: Methodological*, vol. 20, no. 5, pp. 403–414, 1986.
- [85] R. Herman and G. Weiss, “Comments on the highway-crossing problem,” *Operations Research*, vol. 9, no. 6, pp. 828–840, 1961.
- [86] A. J. Miller, “Nine estimators of gap-acceptance parameters,” *Publication of: Traffic Flow and Transportation*, 1971.
- [87] D. R. Drew, L. R. LaMotte, J. H. Buhr, and J. A. Wattleworth, “Gap acceptance in the freeway merging process,” *Highway research record*, vol. 208, pp. 1–36, 1967.
- [88] B. S. Kerner and S. L. Klenov, “Deterministic microscopic three-phase traffic flow models,” *Journal of Physics A: mathematical and general*, vol. 39, no. 8, p. 1775, 2006.
- [89] M. Sarvi and M. Kuwahara, “Microsimulation of freeway ramp merging processes under congested traffic conditions,” *IEEE Transactions on Intelligent Transportation Systems*, vol. 8, no. 3, pp. 470–479, 2007.
- [90] M. J. Cassidy and S. Ahn, “Driver turn-taking behavior in congested freeway merges,” *Transportation Research Record*, vol. 1934, no. 1, pp. 140–147, 2005.
- [91] Z. Wang, L. Kulik, and K. Ramamohanarao, “Robust traffic merging strategies for sensor-enabled cars using time geography,” in *Proceedings of the 17th ACM SIGSPATIAL International Conference on Advances in Geographic Information Systems*, 2009, pp. 362–371.
- [92] L. Li, F.-Y. Wang, and Y. Zhang, “Cooperative driving at lane closures,” in *2007 IEEE Intelligent Vehicles Symposium*, 2007, pp. 1156–1161.

- [93] I. A. Ntousakis, K. Porfyri, I. K. Nikolos, and M. Papageorgiou, “Assessing the impact of a cooperative merging system on highway traffic using a microscopic flow simulator,” in *ASME 2014 International Mechanical Engineering Congress and Exposition*, 2014, p. V012T15A024-V012T15A024.
- [94] S. Huang and T. H. Lee, *Applied predictive control*. Springer Science & Business Media, 2013.
- [95] E. F. Camacho and C. B. Alba, *Model predictive control*. Springer Science & Business Media, 2013.
- [96] A. Kondyli and L. Elefteriadou, “Driver behavior at freeway-ramp merging areas: focus group findings,” *Transportation Research Record: Journal of the Transportation Research Board*, no. 2124, pp. 157–166, 2009.
- [97] M. Brackstone and M. McDonald, “Car-following: a historical review,” *Transportation Research Part F: Traffic Psychology and Behaviour*, vol. 2, no. 4, pp. 181–196, 1999.